THE UNIVERSITY OF ALBERTA

SOME STUDIES ON 5-FLUOROURACIL-5-^{18}F AND 5-FLUORO-2'-
DEOXYURIDINE-5-^{18}F FOR POTENTIAL USE IN DIAGNOSTIC ONCOLOGY

by

$\textcircled{C}$ DOUGLAS NORMAN ABRAMS

A THESIS

SUBMITTED TO THE FACULTY OF GRADUATE STUDIES AND RESEARCH

IN PARTIAL FULFILMENT OF THE REQUIREMENTS FOR THE DEGREE

OF MASTER OF SCIENCE

IN

BIONUCLEONICS

FACULTY OF PHARMACY AND PHARMACEUTICAL SCIENCES
EDMONTON, ALBERTA

FALL 1977

DEDICATION

To Sharon

for guiding the way.

ABSTRACT

The ease of the radiofluorination of uracil and 2'-deoxyuridine as potential radiopharmaceuticals was examined. In addition, the tissue distribution of 5-fluorouracil-6-^{3}H and 5-fluoro-2'-deoxyuridine-6-^{3}H was investigated to determine the value of the ^{18}F labeled analogs as adjuvants in the evaluation of cancer therapy.

A synthetic procedure allowing the introduction of ^{19}F directly into the pyrimidine nucleus of either uracil or 2'-deoxyuridine was developed utilizing elemental fluorine. The desired product was isolated from the crude reaction mixture and purified by a modified high pressure liquid chromatographic technique. The synthetic and purification steps required between 60 and 90 minutes, allowing chemical yields of approximately 58 and 56% for FU-5-^{19}F and FUdR-5-^{19}F respectively.

The ^{18}F used throughout this project was produced on the Van de Graaff accelerator, located at the Nuclear Research Center, University of Alberta, utilizing the ^{20}Ne(d,α)^{18}F nuclear reaction.

Evaluation of the decay curve and gamma spectrum, as well as half-life determinations and chemical analysis indicated that the ^{18}F produced was isotopically pure. The physical half-life was measured to be 110.68 ± 0.85 minutes. Different methods for recovering the ^{18}F produced were developed and adapted to the synthesis of FUdR-5-^{18}F, including chemical and recoil techniques.

Comparative studies on the tissue distribution of the tritiated analogs, FU-6-^{3}H and FUdR-6-^{3}H, were performed. Two tumor models were utilized including the Lewis lung carcinoma and the Ehrlich

ascites carcinoma, as well as the appropriate controls. The results suggested that FUdR-6-^{3}H was incorporated into the gastrointestinal tract and tumor to a greater degree than FU-6-^{3}H in each model studied. FUdR-6-^{3}H was also observed to have greater tissue to muscle, blood, heart, and lung ratios than FU-6-^{3}H.

Examination of the excretion rates of the tritiated analogs from the various models indicated that both compounds were excreted more slowly from the Ehrlich model than from either the Lewis lung or control mice during the initial or rapid excretion phase. The data also indicated that FU-6-^{3}H was excreted more slowly than FUdR-6-^{3}H during the second or slow phase in each of the models studied. The effective half-lives of FUdR-5-^{18}F and FU-5-^{18}F were calculated to be approximately 0.92 hours for both compounds using the excretion data derived from the tritiated compounds.

ACKNOWLEDGEMENTS

TABLE OF CONTENTS

LIST OF TABLES

LIST OF FIGURES

LIST OF PHOTOGRAPHIC PLATES

I. INTRODUCTION

One of the many criteria for proper cancer treatment is the evaluation of the response of a given malignancy to a therapeutic regimen. This is also important in determining the efficacy of experimental procedures in animal models. A number of procedures have been investigated over the years. Older techniques such as Chromium-51 and Phosphorous-32 release tests are subject to loss of radioactivity through the intact cell membranes and the reutilization of the lost radioactivity by other cells[1]. In addition, these techniques must be performed in vitro and any biopsy is limited by tumor accessibility and frequency of sampling. These limitations also apply to microcytotoxicity assays. In vivo procedures such as tumor regrowth and autopsy are subject to obvious restrictions.

The observation that 5-iodo-2'-deoxyuridine (IUdR) is incorporated into cellular DNA and is not released until cell death and lysis has occurred was exploited by many workers as a method of measuring tumor cell viability[2-6]. After radioiodinated IUdR had been incorporated into the malignant cells, the loss of radioactivity from the tumor mass was used to determine the rate of cell death. This method was found to produce results within eight to ten days with a smaller error than the regrowth method which requires approximately thirty days[7].

The fluorinated pyrimidines have been known to localize in some tumor models, although via a different mechanism than the iodinated compounds[34]. If 5-fluoro-2'-deoxyuridine (FUdR) could be tagged with Fluorine-18 (^{18}F), an alternative procedure may be available for measuring the rate of tumor growth or suppression. Potential advantages of this procedure would be:

1. The measurement of active uptake of radioactivity into the tumor mass would be possible, while the IUdR method measures the passive release of radioactivity from the cells.

2. Repetitive scanning would be feasible due to the short physical half-life of ^{18}F which affords a negligible background count rate within twenty-four hours. Daily repetitions could perceivably yield results sooner than the eight to ten days now required with the IUdR technique.

3. Images obtained with a positron camera and ^{18}F may have higher sensitivity than those images obtained with a non-coincident photon emitting nuclide and allow a decrease in the amount of radioactivity needed per scan.

4. The short effective half-life of FUdR-5-^{18}F and the small radio-active dose administered to the patient would result in a low total radiation dose to the patient.

5. The fluorine moiety of FUdR-5-^{18}F is not lost during catabolism of the pyrimidine nucleus; therefore, problems with fluoride-^{18}F localizing in the skeletal tissues are minimized. This is important as the 5-iodo substituent is cleaved from IUdR metabolically and presents a hazard to the thyroid gland and increases the whole body background as the free iodide.

The objective of this project was to determine whether FUdR-5-^{18}F or 5-fluorouracil-5-^{18}F (FU-5-^{18}F) would exhibit sufficient tumor selectivity and incorporation within the limited time available with ^{18}F. This included the development of a rapid method for the synthesis and purification of FUdR-5-^{18}F and FU-5-^{18}F using the Van

de Graaff accelerator as the isotope source. The two radiopharma-
ceuticals were evaluated with respect to their ease of synthesis
and purification and the rate, extent and selectivity of their
incorporation into a tumor mass.

Two tumor models were investigated using the tritiated analogs
of FUdR and FU to determine the short term distribution patterns of
each compound. A direct electrophilic fluorination technique using
elemental fluorine was developed as a synthetic route to both radio-
pharmaceuticals. Separation and purification of the desired products
was accomplished through high pressure liquid chromatography.

II. LITERATURE SURVEY

A.   HALOGENATED PYRIMIDINES

A wide variety of research in the area of halogenated pyrimidine base and nucleoside analogs has resulted in a good understanding of the chemistry and biochemistry of these compounds. Many experimental techniques utilizing either radiobromine or iodine labeled 2-deoxy-uridine (2'-UdR) have been developed from this knowledge. These include tumor imaging[8-10], localization of metastases[1,11], DNA tracing[12], normal and tumor cell kinetics[3,5,6,13,14], measurement of cell death[2,4,7,15], induction of tumor and viral growth[16,17], X-ray sensi-tization[18], use as mutagens[19] and use as antineoplastics[20].

Two phases of cancer treatment of particular interest to the specialties of nuclear medicine and radiopharmacy are early detection of the disease and evaluation of the subsequent treatment response. As early as 1953, radioiodinated pyrimidines were investigated for use as tumor imaging agents. In that year, Prusoff et al.[21] prepared radioiodinated iodouracil, iodouridine and iodoorotic acid using [131]I. However, the authors concluded that none of these agents were signifi-cantly incorporated into the tumor tissue. It was not until 1961 that the potential use of radioiodinated 5-iodo-2'-deoxyuridine (IUdR-5-^{131}I) in tumor imaging was realized[22]. Its usefulness in whole body tumor imaging was evaluated in greater detail by Rotenberg[8] and Schumacher[9].

Radioiodinated IUdR has also been used to evaluate different therapeutic regimens in cancer treatment. One method involved in vitro or in vivo labeling of leukemic or ascitic cells with IUdR-5-[125]I [2-6]. The labeled cells were harvested and reinjected into a normal host. Since the radioactivity was released only from cells which have

undergone lysis, the efficacy of treatment was indicated by the rate
of loss of the radioactivity of the control group compared with the
treatment group. A second method utilized in vivo labeling of solid
tumors with IUdR-5-^{125}I and monitored the rate of loss of radioactivity
from the tumor site[7]. This technique was found to produce results
within eight to ten days, somewhat sooner than the thirty days required
by the regrowth method. This method was reported to have a smaller
error than the regrowth method.

All of these techniques are based on the fact that substitu-
tion of bromine or iodine for hydrogen on the C^5 of 2'-UdR results in
an analog of thymidine which is incorporated into the DNA helix. Sub-
stitution of fluorine at this position forms an analog of 2'-UdR which
exhibits profoundly different metabolic and biochemical properties
than the other halo derivatives (figure 1).

B.   FLUORINATED PYRIMIDINES

    1. History

The search for differences in tumor and normal cell metabolism as
a basis for chemotherapy resulted in the modification of normal cell
components to exploit these differences. Modification of compounds by
substitution of fluorine for hydrogen was known to induce significantly
altered biochemical and physiological responses to the fluorinated
analog with respect to the natural product. This is illustrated by
compounds such as fluoroacetate and para-fluorophenylalanine which are
highly toxic and by fluorinated steroids which exhibit greater anti-
inflammatory activity than the hydrogen analogs[23]. The observation
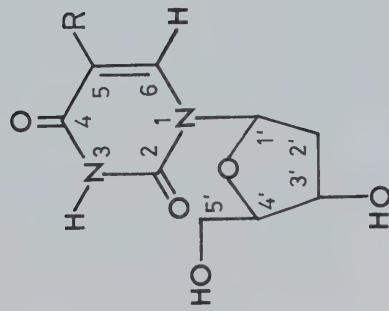
R	BIOCHEMICAL PROPERTIES
H	TdR PRECURSOR
CH_3	TdR – NORMAL DNA COMPONENT
CF_3	TdR ANALOGUE
I	TdR ANALOGUE
Br	TdR ANALOGUE
Cl	WEAK THYMIDINE SYNTHETASE INHIBITOR
F	THYMIDINE SYNTHETASE INHIBITOR

FIGURE 1   PROPERTIES and STRUCTURES of 2' DEOXYURIDINE DERIVATIVES

that primary rat hepatomas utilized more uracil than normal liver tissue[23] aroused interest in the possible effect of a fluorinated uracil analog on cell metabolism. In 1957 the first synthesis of 5-fluorouracil (FU) was accomplished[24]. It was rationalized that a fluorine substituent on the C^5 position of uracil would interfere in some way with thymine metabolism. FU was found to interfere with uracil metabolism thereby preventing the synthesis of thymidine.

2. Biochemistry

The anabolic and catabolic pathways of fluorinated pyrimidines are almost identical to those of the non-fluorinated analogs (figure 2).[25,26]. This similarity stops at the conversion of 2'-deoxyuridine-5'-monophosphate (2'-dUMP) to thymidine-5'-monophosphate (dTMP) by Thymidylate Synthetase. Phosphorylation of dTMP to the triphosphate sugar, dTTP, must occur before thymidine can be incorporated into the DNA helix. Inhibition of the conversion of 2'-dUMP to dTMP is the mechanism by which FU and FUdR exert their antitumor activity[27]. Both compounds must be converted to 5-fluoro-2'-deoxyuridine-5'-monophos-phate (FdUMP) before they can interact with Thymidylate Synthetase. FdUMP blocks the transfer of the methyl group from N^5,N^{10}-Methylene-tetrahydrofolate (CH_2-FH_4) to 2'-dUMP, thereby inhibiting the synthesis of dTMP (figure 3). This is believed to occur via nucleophilic attack of the cysteine thiol residue of the enzyme active site on the C^6 of the pyrimidine nucleus. A covalent bond is formed between the enzyme and the C^6 of FdUMP and also between the N^5,N^{10}-methylene group of CH_2-FH_4 and the C^5 of FdUMP[28]. This forms a stable complex (figure 4) which is believed to be similar to the intermediate formed during the
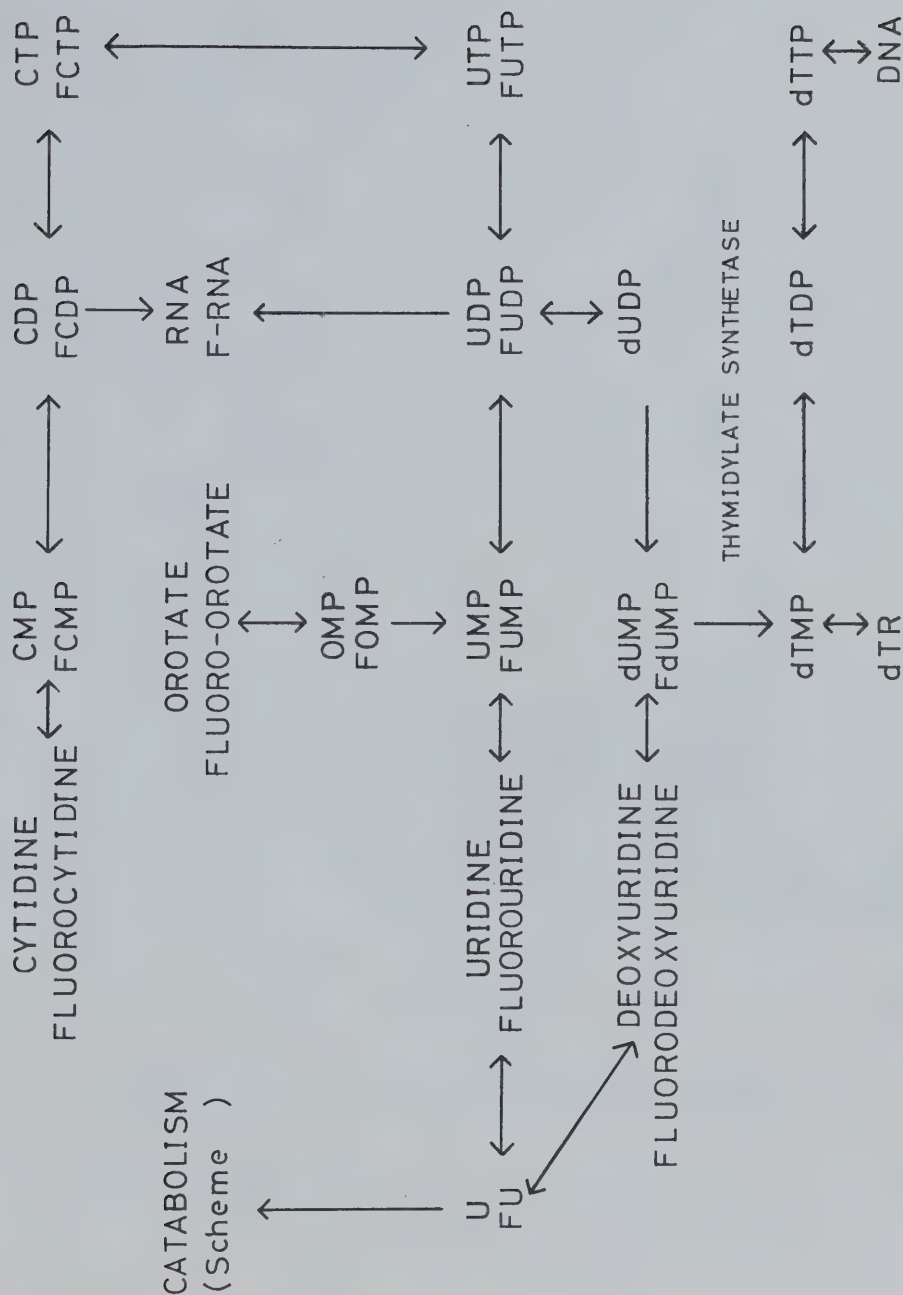
FIGURE 2 COMPARISON of the METABOLISM of FLUORINATED and NORMAL PYRIMIDINES
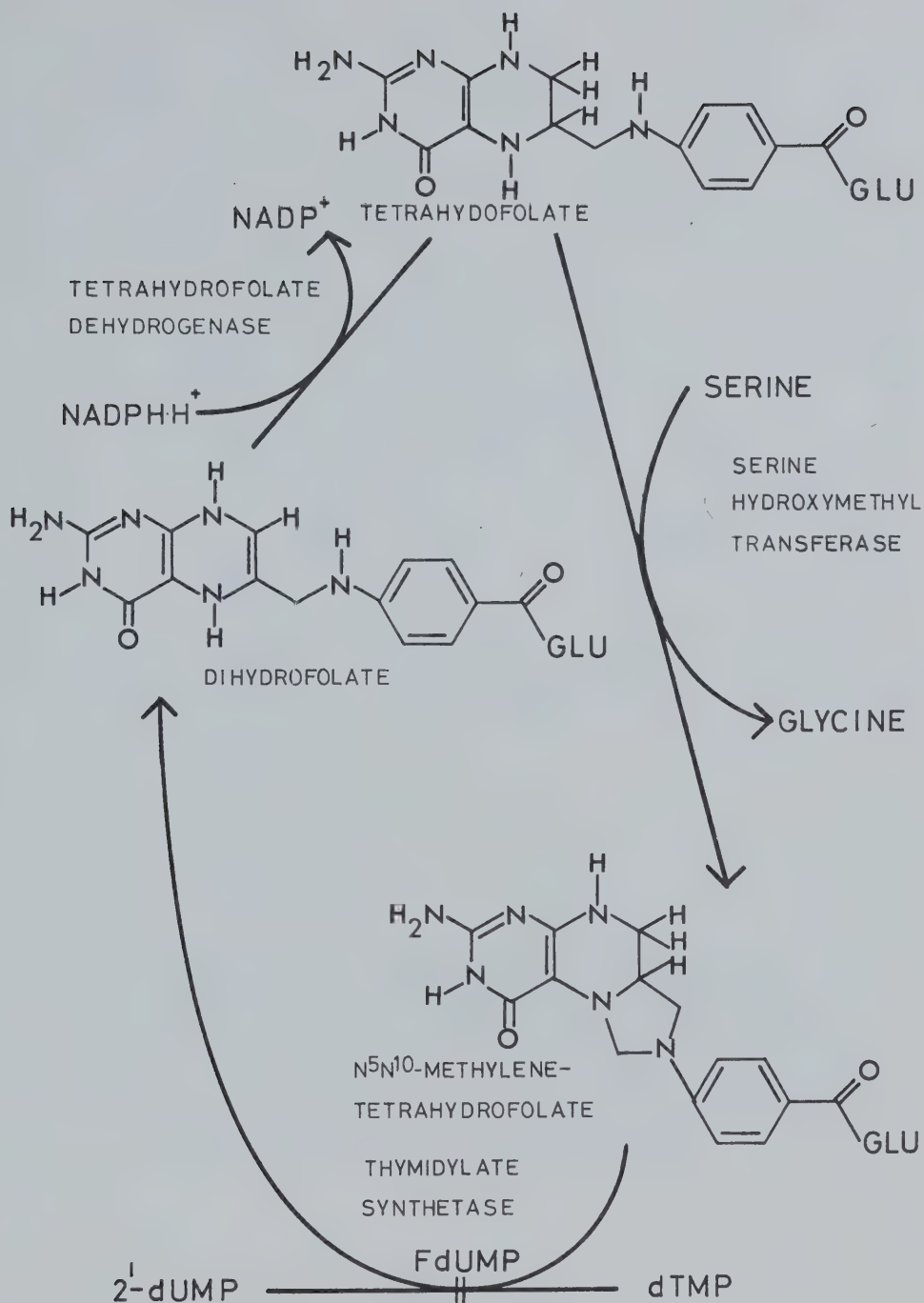
FIGURE 3 INHIBITION of the METHYLATION of

2'-DEOXYURIDINE-5'-MONOPHOSPHATE
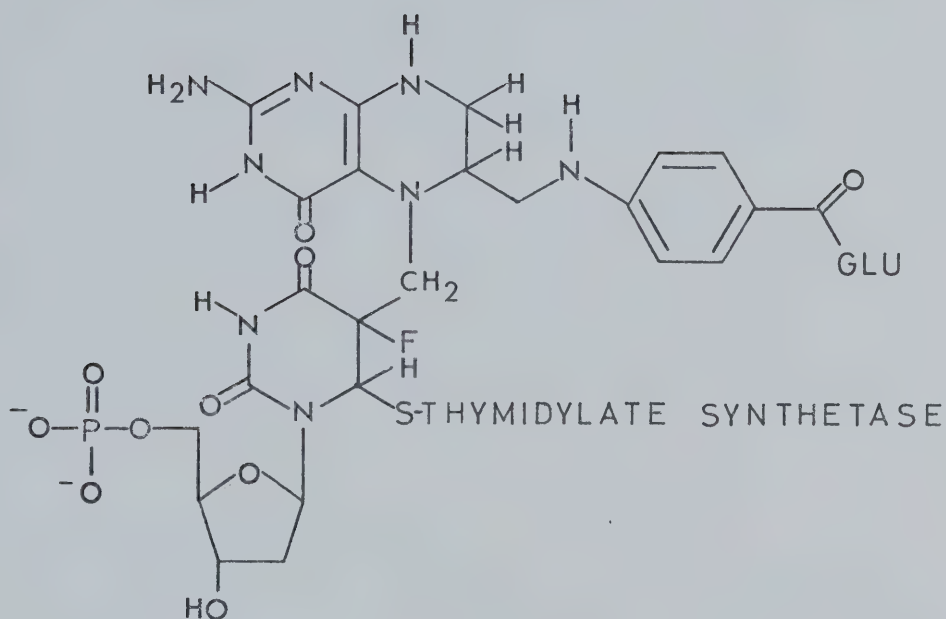
FIGURE 4· PROPOSED INTERMEDIATE FORMED by the
INTERACTION of N^5,N^{10}-METHYLENETETRAHYDRO-
FOLATE, 5-FLUORO-2'-DEOXYURIDINE-5'-MONOPHOSPHATE,
and THYMIDYLATE SYNTHETASE

normal synthesis of dTMP from 2'-dUMP. However, this complex cannot complete the methylene transfer because the C^5 fluorine bond is too strong to be cleaved under these conditions[28]. Therefore, each Thymidylate Synthetase molecule is prevented from synthesizing dTMP until the complex is reversed or new enzymes are synthesized. Thymidylate Synthetase consists of two subunits and has been found to react stoichiometrically with two mole equivalents of FUdR, presumably one with each subunit[29].

FdUMP is not phosphorylated to give the triphosphate sugar which is essential for incorporation into DNA. Therefore, it is not found in the DNA helix unlike the bromo and iodo analogs[18]. FU and, to a much smaller extent, FUdR are incorporated into RNA as the ribonucleoside[26].

3. Metabolism and Excretion

Charles Heidelberger and co-workers have done extensive work with regard to the tissue distribution, effects on various tumors, metabolism and excretion of FU and FUdR in animal models and in humans[23,30-34]. The close correlation between the anabolism of fluorinated and natural pyrimidines is depicted in the degradation pathway of uracil and FU (figure 5)[35]. The deoxyribonucleoside, FUdR, is cleaved to FU and phosphoribosyl pyrophosphate. FU then follows the same catabolic route as the free base. Enzymatic reduction of the pyrimidine nucleus to dihydrofluorouracil (DHFU) is followed by hydrolysis to α-fluoro-β-ureidopropionic acid (FUPA) which may be converted to α-fluoro-β-guanidopropionic acid (FGPA). Both acids are then converted to α-fluoro-β-alanine (FBAL) and urea or carbon dioxide and ammonia. Unlike
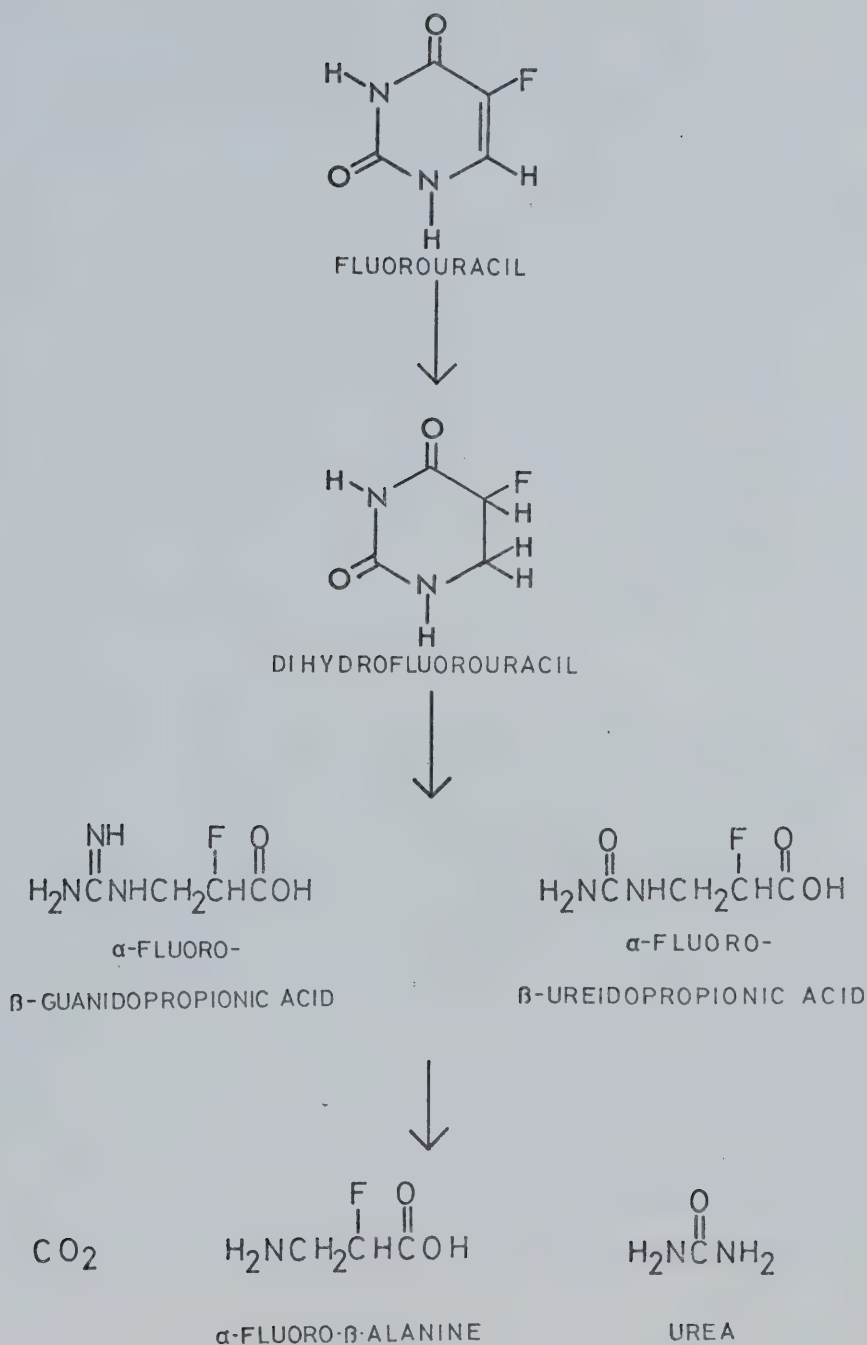
FIGURE 5   METABOLIC PATHWAY OF 5-FLUOROURACIL

β-alanine, FBAL is not further metabolized. None of the metabolites found exhibited antitumor activity[35]. The liver is the major site of metabolism of FU, although most normal tissues except the spleen can degrade the drug. Studies have shown that some tumors, such as Sarcoma 180 and Ehrlich ascites carcinoma, are unable to appreciably catabolize either FU or FUdR[36,37]. Both FU and FUdR are metabolized and excreted more quickly by human patients when ingested orally as compared to the intravenous route. Approximately 70 to 80% of the initial dose is excreted within twenty-four hours after oral ingestion compared to approximately 60% of the initial dose excreted after intravenous administration of either FU or FUdR[31,38]. Experiments using mice as animal models gave similar results[26,35,39,40].

4. Tissue Distribution

FUdR was incorporated with greater selectivity than FU by the Sarcoma 180 tumor model. However, both compounds were found to exhibit their highest concentration in the tumor when compared to other tissues, while 5-fluorouridine (FUR) was found to be much less specific for the tumor mass than for the normal tissues[35]. No radioactivity was present in the DNA after intraperitoneal (IP) injection of FUdR-2-^{14}C or FU-2-[14]C. However, the RNA was shown to incorporate radioactivity as FUR-2-[14]C. This indicated that FUdR-2-^{14}C was not incorporated into DNA. In addition, the deoxyribosyl moiety of FUdR-2-^{14}C must have been replaced by a ribosyl sugar before incorporation into RNA[26,40].

In human patients the distribution of both drugs in various tumors and surrounding tissues was studied. Parenteral administration of

FUdR-2-^{14}C or FU-2-^{14}C generally resulted in a greater localization of radioactivity in the tumor mass than in the normal tissues[34]. The magnitude of this ratio was dependent upon the route of injection, the classification of the tumor, the cellularity rating (proportion of tumor to normal cells) of the tumor and the tumor vascularity. The more metabolically active tissues demonstrated enhanced uptake of either FU or FUdR. Of these tissues, the tumors showed a greater conversion rate of either drug to the active metabolite, FdUMP, than was found in normal tissues[34]. It was concluded that the clinical response of tumors to the fluorinated pyrimidines studied was due to greater incorporation of the drug by the malignant tissue and to a higher rate of conversion of the drug into FdUMP by the tumor, than was observed for the corresponding normal tissue[41].

5. Clinical Use

The effects of FU and FUdR are primarily due to the inhibition of thymidylate synthetase by FdUMP, the active metabolite of both drugs. The incorporation of FU and FUdR into RNA as FUMP and subsequent alteration of the RNA synthesis, function and ribosomal stability is considered to be of secondary importance[41].

Intravenous administration of 15 mg/kg of FU once a week is the most commonly used dosage schedule of the many available. Though cases of severe toxicity have been associated with this routine, they are believed to be due to abnormal metabolism of the drug[34,38]. Peak levels of 10^{-3} to 10^{-4} molar concentrations were found after drug administration, followed by rapid clearance ($T_{1/2}$ = 10 to 20 minutes) from the plasma[41]. Synthesis of the active metabolite, FdUMP, was

found to occur intracellularly and reached a maximum concentration
within twenty-four hours after injection of the drug[26].

Continuous infusion of FU (10 to 40 mg/kg over 24 hours) has been
claimed to decrease the myelosuppressive side effects and enhance the
therapeutic effect[31]. This finding has not been substantiated. Oral
ingestion of FU usually exhibited a smaller response than intravenous
injection, probably due to increased metabolism and variable absorption
of the drug[34,38].

FU was distributed rapidly to all body compartments resulting in
a volume of distribution equal to that of total body water. The
cerebrospinal fluid and the brain tissue levels reached significant
concentrations after intravenous injection especially in areas of
metastatic disease[41].

Although FUdR was found to be less toxic than FU, it did not seem
to be more effective[31]. This may be a function of its rapid catabolism
to FU[42]. Neither drug is effective against either leukemias or
lymphomas, but solid tumors, in particular breast, gastrointestinal
and gynecological tumors, have regressed significantly in response to
therapy. Both drugs are carcinostatic and are considered only of
palliative importance since there have not been any cures reported
due to their use alone[43].

6. Toxicity

FU and FUdR are highly toxic like all antimetabolites. The
principle side effects are manifested as leukopenia, stomatitis,
diarrhea, anorexia, nausea and vomiting. Less frequent side effects
are thrombocytopenia, hemorrhage, gastrointestinal ulceration,

alopecia, dermatitis, nail changes and very rarely, cerebellar disturbances[42]. The latter side effect resembles the conditions caused by fluorocitrate; the formation of which has been attributed to FU and FUdR therapy[41,43].

In general, FUdR was found to be less toxic and therefore better tolerated than FU in mice. The acute LD_{50} values for FUdR and FU were determined for several different routes of administration[23]. These were greater than 1000 mg/kg intravenously and subcutaneously and 650 mg/kg intraperitoneally for FUdR in mice, compared to 250 mg/kg intravenously, 233 mg/kg subcutaneously and 188 mg/kg intra-peritoneally for FU. Repeated administration reduced the LD_{50} quite substantially. The maximum tolerated dose of FU by any route of administration was 25 mg/kg/day, significantly less than the values found for FUdR which were 100 mg/kg/day subcutaneously and 50 mg/kg/day intraperitoneally[44].

C.   FLUORINE

1. Characteristics

Elemental fluorine (F_2) is the most reactive and electronegative of all elements[45]. It is a toxic gas which was first isolated by Moisson in 1886. It is generally produced by the electrolysis of metal fluorides in a media with no other competing anions present. The weak dissociation energy of the F-F bond is 37.7 ± 0.2 kcal/mole and gives fluorine its highly reactive nature. Reactions involving elemental fluorine and organic substrates are generally exothermic resulting in the formation of a strong covalent bond between C and F

which has an energy of 93 kcal/mole[46]. Another biologically important
characteristic of fluorine is its relatively small ionic radius of
1.35 angstroms which is very close to 1.20 angstroms, the ionic radius
of hydrogen[47]. Much of the physiologically anomalous behaviour of
fluorinated analogs can be attributed to this characteristic.

The radionuclide, fluorine-18 (^{18}F), retains all of the physical
and chemical attributes of the stable isotope, fluorine-19. In
addition, its radioactive properties render it useful as a tracer in
the study of the biological distribution, behaviour and pharmaco-
kinetics of fluorinated compounds. Of the six radioactive isotopes
of fluorine, ^{18}F is the only nuclide with a physical half-life
sufficiently long enough for biomedical applications (table 1)[48].
It has a 109.7 minute half-life and is classified as a short lived
radionuclide. The unstable ^{18}F nuclei obtain stability through the
emission of 0.635 MeV positrons (β^+) which, upon approaching thermal
velocities, recombine with an electron resulting in annihilation
(figure 6).

$$^{18}_{9}F$$

β^+ 97 %
E C   3 %

$$^{18}_{8}O$$
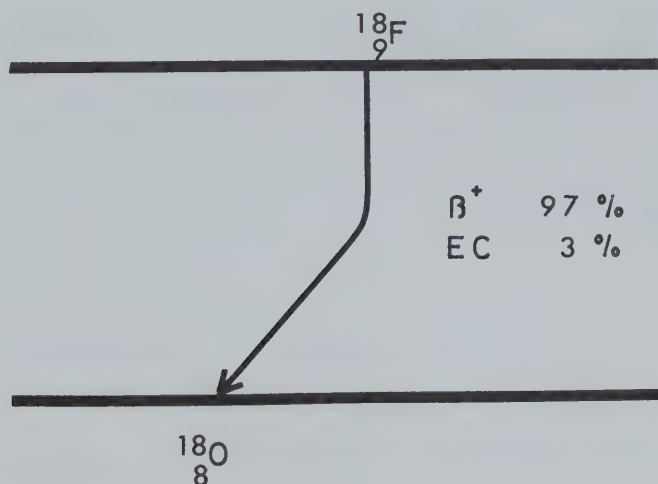
FIGURE 6   RADIOACTIVE DECAY SCHEME of FLUORINE -18

Upon recombination both the electron and positron are converted to two 0.511 MeV gamma photons, emitted from the center of annihilation, 180 degrees from each other. These coincident gamma rays offer a theoretical increase in sensitivity over images normally obtained with a single photon emitting nuclide if a positron camera is used. Fluorine-18 radiopharmaceuticals also offer the advantage of a low radiation dose to the patient due to a low initial dose and short effective half-life. In its anionic form, ^{18}F is classified as a medium toxicity isotope, lower subgroup B, with an effective half-life of 0.078 days[49].

2. Production of Fluorine-18

The chemical form of any radionuclide depends on the method of production and recovery used at the source. The anionic form of ^{18}F can be readily produced with both nuclear reactors and particle accelerators, while the most convenient source of elemental fluorine-18 (F_2-^{18}F) is an accelerator. In 1972, Lambrecht[50] reported the use of the $^{20}Ne(d,\alpha)^{18}F$ and $^{20}Ne(^3He,^4He,n)^{18}Ne(\beta^+$, 1.5 sec half-life) ^{18}F nuclear reactions as sources of F_2-^{18}F. In order to recover ^{18}F in the elemental state, Lambrecht used a neon target gas containing approximately 7% (v/v) carrier F_2-^{19}F. This method recovered 80-90% of the ^{18}F produced as F_2-^{18}F [51,52].

3. Distribution, Metabolism and Excretion

It is well known that anionic fluorine accumulates in the skeleton during the normal lifespan, as the fluoride from food and water replaces the hydroxyl moiety of hydroxyapatite in the bone matrix. This

TABLE 1

Isotopes of Fluorine

Isotope	Half-life	Radiation	Abundance	Energy (MeV)
^{16}F	10^{-19} sec	β^+	—	—
^{17}F	66.6 sec	β^+	100%	1.74 max
		γ	200%	0.511
^{18}F	109.7 min	β^+	97%	0.635 max
		e.c.	3%	
		γ	194%	0.511
^{19}F	stable	—	—	—
^{20}F	11.6 sec	β^-	100%	5.41 max
		γ	100%	1.63
^{21}F	4.4 sec	β^-	100%	5.4 max
		γ	100%	0.35
		γ	100%	1.38
^{22}F	4.0 sec	β^-	100%	11.0 max
		γ	100%	1.28
		γ	67%	2.06

formation of fluoroapatite results in a more stable and less soluble complex than the normal bone hydroxyapatite. Subsequently, it is more slowly removed from the bone matrix during the remodeling processes[53].

Oral ingestion of ^{18}F as sodium fluoride resulted in rapid systemic absorption of 75% of the dose within one hour and 90% of the dose within nine hours[54]. The fluoride concentration in the whole blood was distributed in a fashion similar to the distribution of the other halogens with the major portion occurring in the plasma. Plasma clearance was quite rapid through renal excretion and equilibration of fluoride with the extracellular fluid and tissues[55]. The soft tissue membranes are freely permeable to all halogens, but the small concentration of fluoride observed in the tissue became negligible approximately four hours after ingestion[56]. The testis, through metabolic storage, and the kidneys, through accumulation in the collecting tubule region[57], were found to be the only soft tissues demonstrating fluoride concentrations greater than blood levels. In humans, rats and mice, the skeletal tissues, neglecting excretion, incorporated the major portion of injected fluoride, which was concentrated almost exclusively in the mineralizing areas of the bone. Calcifying areas, such as the bone, teeth and to a lesser extent, the cartilage, showed uptake proportional to the vascularity of the area[54,57].

A homeostatic mechanism to control the plasma level of fluoride was evident over a range of administered doses, resulting in increased excretion and bone uptake concomitant with increased ingestion[53]. The major portion of excreted fluoride was found in the urine although a minor component was evident in the feces[53].

4. Clinical Uses of Fluorine-18 Radiopharmaceuticals

Sodium fluoride-18 was used for bone studies as early as 1940[58], eventually gaining recognition as a bone scanning agent in the early 1960's[59]. It has subsequently been replaced extensively with $^{99}Tc^m$ labeled bone seeking agents. Other uses of ^{18}F as the fluoride anion include the assessment of circulation in the femoral head[60] and imaging of myocardial infarcts[61].

Fluorine-18 has been used as a tracer for compounds with specific distribution patterns which differ from the simple fluoride ion. Tetra-fluoroborate ($BF_4-^{18}F$) ion is incorporated by the thyroid gland in a manner similar to iodide and perchlorate and has been used in thyroid studies and elucidation of the mechanism of iodide concentration by the thyroid[62]. Tetrafluoroborate has also been used as a brain scanning agent in the detection of intracranial tumors[63,64].

Fluorine-18 labeled microspheres have been used in tracheobron-chial clearance and related lung perfusion studies[65]. The particles, a polymer of fluorinated ethylene propylene, were labeled by direct irradiation of the microspheres with protons using the $^{19}F(p,pn)^{18}F$ nuclear reaction.

Some fluorinated analogs of natural biomolecules have shown preferential incorporation into certain organs and tumors. L-para-fluorophenylalanine-^{18}F has been synthesized as a potential pancreatic scanning agent as the pancreas is known to concentrate it[66]. The ortho and meta fluoro-^{18}F analogs of phenylalanine have also been synthesized as possible alternatives to L-Selenomethionine-^{75}Se, now used to image the pancreas[67-69]. The five and six fluoro isomers of

tryptophan have demonstrated some specific incorporation by both the
pancreas and solid tumors.   Both isomers have been labeled with ^{18}F
for screening as tumor and pancreatic imaging agents[66,70,71].
Concentration of L-DOPA by the brain has led to the synthesis and
testing of DL-5-fluoroDOPA-5-^{18}F as a possible brain scanning agent[72,73].
FU-5-^{18}F has been synthesized as a tumor localizing agent in view of
its successful use in breast cancer chemotherapy[50,52].   A final example
of ^{18}F-labeled compounds, aimed at specific functions, is the potential
of cholesterol-^{18}F for imaging the adrenal gland[74].

Fluorine-18 labeled compounds are useful not only in nuclear
medicine as radiopharmaceuticals, but have also found a place in drug
design, pharmacology and toxicology. Synthesis of fluoroethanol-2-^{18}F,
fluoroacetate-^{18}F, fluorotetradecanoate-2-^{18}F and related aliphatic
compounds have been studied to determine their pharmacokinetic and
tissue distribution properties[75,76]. Comparison of the behaviour of
natural and fluoro analogs may lead to a more logical method of drug
design. The tissue distribution of haloperidol-4'-^{18}F was useful in
determining the dosage and dosage form most suitable for clinical use
of the unlabeled drug[77].

5. Chemistry

Fluorine represents a unique branch of halogen chemistry and is
often discussed as a separate entity, apart from chlorine, bromine
and iodine. In addition, the short half-life of ^{18}F imposes a time
limitation on the synthetic procedures that can be used, therefore,
limiting the number of fluorination reactions of practical use. The
time for both preparation of the fluorinating agent and synthesis of

the desired product must be considered if the specific activity and overall radiochemical yield of the final product is to be of use either clinically or experimentally.

    a. Exchange Reactions

Halogen-halogen exchange or Finkelstein reactions are actually the result of an equilibrium state between two halogens, forced in one direction by various techniques to give the desired product[78]. The driving force for the fluorination of aliphatic compounds is the extremely low tendency of fluorine towards substitution once the alkyl fluoride is formed. Generally fluorine is considered a poor nucleophile and to compensate for this, most fluorine-halogen exchange reactions involve the displacement of iodine. This takes advantage of the weak C-I bond and the good leaving ability of the iodine anion. Aromatic substitution of iodine by fluorine is also possible if the ring is activated and an excess of fluorine is used.

Fluorocholesterol-^{18}F was synthesized from iodocholesterol by displacement of the iodine substituent by fluorine using the silver fluoride salt[74]. A 60% radiochemical yield was achieved when the reaction was allowed to proceed at room temperature for twenty minutes. However, many exchange reactions require more vigorous conditions, as was demonstrated by the Robinson synthesis of fluoracetate-^{18}F, fluoroethanol-2-^{18}F and fluoromethyl nitrile-^{18}F [75]. In these reactions, the ^{18}F anion was trapped on an ion exchange resin and heated at 180° in the presence of the appropriate

brominated substrate in a sealed tube for ninety minutes in order to effect exchange.

   b.   Diazonium Tetrafluoroborates

   A classic method of fluorinating aromatic compounds is the Schiemann decomposition of aryl diazonium tetrafluoroborate salts. The reaction follows an S_N1 mechanism via a phenyl cation intermediate[78]. Two methods are generally used to adapt this reaction to labeling compounds with ^{18}F. One procedure involves the diazotization of the aromatic amine in the presence of the free tetrafluoroborate-^{18}F anion. The second method prepared the diazonium tetrafluoroborate-^{19}F salt which is then labeled with ^{18}F by exchange with a metal fluoride either before or during the decomposition step.

   Hoyte et al.[66] employed the first method for the synthesis of ortho, para and meta fluorophenylalanine-^{18}F. The BF_4-^{18}F was prepared by direct proton irradiation of the lithium, sodium and potassium tetrafluoroborate salts. Approximately 75% of the radioactivity produced as ^{18}F was available as BF_4-^{18}F. This salt was reacted with the appropriate diazonium phenylalanine salt to give the diazonium tetrafluoroborate complex which decomposed upon heating to the desired isomer of fluorophenylalanine-^{18}F. This method yielded a product with specific activities ranging from 0.7 to 1.5 mCi/mmole[66].

   Haloperidol-4'-^{18}F was labeled using the second procedure[75]. The diazonium tetrafluoroborate salt of haloperidol was labeled with ^{18}F via a fluoride-18 fluoride-19 exchange reaction with

Na[18]F in an aqueous solution. The product was obtained with a specific activity of 4 to 5 μCi/mg within 140 minutes[77].

Fluorotryptophan-6-[18]F [70], fluoroDOPA-5-[18]F [73] and many other aromatic fluorides[79] have been synthesized using these techniques or other modified reaction conditions[71,72,74,80].

c. Elemental Fluorine

The reaction of elemental fluorine gas (F_2) with organic molecules was originally regarded as a nonselective process involving a free radical mechanism. This concept has changed in view of new evidence that an electrophilic mechanism may be the actual process involved[81]. Recent synthesis of fluorinated pyrimidines and their nucleoside[82-84] derivatives, steroids[85] and bridged aliphatic compounds[86], have taken advantage of this relatively new fluorination procedure using the stable isotope [19]F.

Of particular interest was the synthesis of FU-5-^{18}F reported by Lambrecht and Fowler[50,51] using F_2-[18]F. The authors prepared the F_2-^{18}F by adding F_2-^{19}F to the neon target gas to give a 7% (v/v) concentration of fluorine in neon. During the production of ^{18}F, the F_2-^{19}F acted as a scavenger and through an exchange process picked up the ^{18}F in the desired chemical form. This target gas was bubbled through a solution of uracil in trifluoro-acetic acid at -15°C. Sublimation of the residue from the above step afforded FU-5-^{18}F with a specific activity of 1.1 mCi/mg in better than 87% overall radiochemical yield. Including the sublimation step, the reaction gave a product with greater than 98% chemical purity in less than forty minutes[50,51].

d. Miscellaneous

Two methods other than the use of F_2-^{18}F have been used to produce FU-5-^{18}F. Both are nonspecific techniques which resulted in low overall radiochemical yields, but were relatively simple to perform. Lebowitz et al.[87] employed the recoil energy of the ^{18}F atoms produced by the ^{20}Ne (d,α) ^{18}F nuclear reaction to label uracil coated on the inside surface of the irradiation chamber. The labeling was random and uncontrolled and substantial degradation of the product and substrate was evident. Cation exchange chromatography was used to purify the product which was obtained in an overall labeling efficiency of 1%.

A slightly different approach was used by Anbar and Neta[88,89]. The authors used the ^{19}F $(n,2n)$ ^{18}F nuclear reaction to convert the ^{19}F of the prefluorinated FU molecule to ^{18}F. The residue was dissolved in an aqueous alkaline solution which was acidified to precipitate the desired product. The overall yield of labeled product was 8%.

III. EXPERIMENTAL

A. INSTRUMENTATION AND MATERIALS

1. Animal Models

The Lewis lung carcinoma (LLCa) and Ehrlich ascites carcinoma (EAC) tumor models were generously donated by Dr. A.R.P. Paterson of the Cancer Research Unit, University of Alberta. The LLCa cell line was maintained using BDF_1 hybrid mice as hosts and the EAC model used a Swiss albino strain (ICR), both of which were purchased locally from the University of Alberta farm. The animals were kept six to a cage and allowed food and water ad libitum.

2. Chemicals and Solvents

All chemicals were of analytical reagent grade and used without further purification. The biochemical standards such as 5-fluorouracil, 5-fluoro-2'-deoxyuridine, 5-iodo-2'-deoxyuridine, 5-bromo-2'-deoxy-uridine, 5-aminouracil, uracil and 2'-deoxyuridine were purchased from Nutritional Biochemicals, Cleveland, Ohio. Preparation of the solutions and reagents used is specifically described in the text.

The solvents were also of analytical reagent grade and used without purification with the exception of the solvents used for chromatographic analysis. These solvents were glass distilled and stored appropriately.

The Amersham Searle Company, Toronto, Canada, supplied the 5-fluorouracil-6-[3H] and 5-fluoro-2'-deoxyuridine-6-[3H] tracers which were analyzed for radiochemical purity, diluted with normal saline and stored at 4°C upon receipt. The n-hexadecane-[3H] oxidation standard was obtained from Packard Instruments, Downers Grove, Illinois.

3. Chemical Analysis

Melting points were determined with a Buchi capillary apparatus and are uncorrected. Nuclear magnetic resonance (nmr) spectra were determined for solutions of deuterium oxide (D_2O) with tetramethyl-silane (TMS) as the internal standard with a Varian A-60 spectrometer. Intrared spectra (ir) in potassium bromide, were taken on a Unicam SP-1000 spectrometer and ultraviolet (UV) determinations were taken on a Unicam 1800 spectrometer. Mass spectra (ms) were measured with an AE1-MS-9 mass spectrometer and accurate mass measurements were used in lieu of elemental analysis.

4. Gamma and Liquid Scintillation Analysis

The half-life determinations of the ^{18}F produced were measured using a Searle 1195 gamma spectrometer. The absolute activity deter-minations and the gamma spectra were obtained with a Searle-Harshaw sodium iodide well crystal (1 $\frac{3}{4}$" x 2" x $2\frac{1}{32}$" inside diameter) and a Nuclear Chicago multichannel analyzer.

Tissue sample preparation for liquid scintillation analysis was accomplished with a Packard Tricarb 306 tissue sample oxidizer. The FUdR-6-^3H tissue distribution samples were collected and analyzed in Monophase 40 liquid scintillation cocktail which was purchased from Packard Instruments, Downers Grove, Illinois. The FU-6-^3H samples were analyzed in a cocktail consisting of 700 mg 2-(4'-Biphenyl)-6-phenyl-benzoxazole (PBBO), 7.7 gm 2-(4',-tert-Butylphenyl)-5-(4"-biphenylyl)-1,3,4-oxadiazole (butyl PBD) and 170 ml Bio-Solv® (BBS3) in 1 litre scintillation grade toluene.

5.   Fluorine-18 Production

The ^{18}F used in this project was produced with the cooperation
of the staff and the Van de Graaff accelerator at the Nuclear Research
Centre, University of Alberta. The stainless steel irradiation
chamber-reaction vessel assembly was machined in the Physics workshop
and the pyrex glass target chamber reaction-vessel assembly was
obtained from the Chemistry glass blowing department; both departments
at the University of Alberta.

6.   Chromatography

All thin layer chromatography utilized Kiesel-gel silica gel with
CaSO$_4$ binder and fluorescent indicator which was supplied by Fraser
Medical Supplies, Vancouver, British Columbia. The chromatograms were
visualized in a UV cabinet at 254 nm (Applied Science Laboratories).

The high pressure liquid chromatographic analyses were performed
on prepacked Silica gel 60 columns purchased from Brinkman Instruments,
Rexdale, Ontario. The eluate was monitored for UV absorption at 254 nm
on a Pharmacia UV monitor and recorded on a model 330 Pharmacia Strip-
chart recorder. Radioactivity in the eluate was determined with a
Bicron 2" sodium iodide crystal and recorded on a Beckman 10" chart
recorder.

B.   SYNTHESES WITH STABLE FLUORINE

1.   Elemental Fluorine

a.   5-Fluorouracil

A fluorine in nitrogen gas mixture (9:1 v/v) was bubbled
slowly through a solution of uracil (34.9 mg, 0.31 mmole) in
trifluoroacetic acid (15 ml) at -10°C until micro thin layer
chromatography revealed the absence of uracil.   Removal of the
solvent in vacuo afforded a clear oil.   Sublimation of the
residue (190°C/1 mm Hg) and recrystallization of the product from
water afforded 5-fluorouracil (23.5 mg, 58%) as a white crystalline
solid with a melting point of 278-280°C (literature melting point
281-283°C)[90] which exhibited infrared (ir) and nuclear magnetic
resonance (nmr) spectra identical to those of an authentic sample;
ir (KBr):   3100-3460 (NH), 1700 (C=O) and 1260 (C-F); nmr (D_2O):
δ 7.6 (1H, d ($J_{5F,6} = 6$),C_6-H).

b.   5-Fluoro-2'-Deoxyuridine

A fluorine in neon gas mixture (1% v/v) was bubbled slowly
through a solution of 2'-deoxyuridine (5.0 mg, 0.022 mmole) in
glacial acetic acid (15 ml) at 25°C until micro thin layer
chromatography revealed the absence of 2'-deoxyuridine. Removal
of the solvent in vacuo afforded a clear oil which was redissolved
in a solution of ammonium hydroxide in methanol (5% v/v).   Prepara-
tive high pressure liquid chromatographic analysis on a 31 x 2.5
cm Merck prepacked Silica Gel G column eluted with chloroform-
95% ethanol (4:1 v/v) at 8 ml/minute gave 2.8 mg FUdR (52%) with

a retention time of 35 minutes. The FUdR exhibited infrared (ir),
nuclear magnetic resonance (nmr) and mass spectra (ms) identical
to those of an authentic sample; ir (KBr): 3410, 3080 (NH),
1700 (C=O), 1275 (C-F) and 1050 (OH); nmr (D_2O): δ 2.2 - 2.5 (2H,
m, C2'-H), 3.76 (2H, m, -O-CH_2), 4.02 (1H, m, C4'-H), 4.44 (1H, m,
C3'-H), 6.2 (1H, d($J_{1'-2'}$ = 6.5) of d($J_{1'-2'}$ = 1.5), C1'-H), 8.0
(1H, d(J_{5F-6} = 6.5), C6-H); mass calculated for $C_9H_{11}N_2O_5F$:
246.0652. Found: 246.0660.

2.   Crown Ether Synthesis

Cyclohexyl-18-crown-6 crown ether (5 mg, 0.013 mmole) was added to
a suspension of potassium fluoride (0.76 mg, 0.019 mmole) in acetonitrile
(1 ml) and allowed to reflux for 30 minutes. A solution of 5-iodo-2'-
deoxyuridine (1.09 mg, 0.003 mmole) in acetonitrile (1 ml) was then
added and refluxed with vigorous stirring for 120 minutes. Analysis
of the reaction mixture by high pressure liquid chromatography on a
24.0 x 1.3 cm Merck prepacked Silica gel G column indicated quantitative
recovery of the starting material and no trace of 5-fluoro-2'-deoxy-
uridine, the exchange product.

Various combinations of crown ethers (dibenzo-18-crown-6 and
dicyclohexyl-18-crown-6), metal fluoride salts (potassium fluoride,
sodium fluoride and lithium fluoride), solvents (dimethyl formamide,
methanol and acetonitrile) and substrates (5-bromouracil, 5-iodouracil
and their nucleosides) were reacted. None of the combinations
attempted were found to effect exchange.

C. RECOVERY OF ELEMENTAL FLUORINE-18

    1. Method A Using 10% Helium in Neon Target Gas

A target gas mixture of helium in neon (10% v/v) was irradiated with 6.5 MeV deuterons. During bombardment, the gas mixture was slowly purged, with a peristaltic pump, through 5 ml of phenol in the reaction chamber. The liquified phenol was to react with any $F_2-^{18}F$ present in the circulating target gas. A recovery of less than 1% of the theoretically produced radioactivity was obtained with this procedure.

    2. Method B Using 1% Fluorine in Neon Target Gas

A target gas mixture of fluorine in neon (1% v/v) was irradiated with 6.5 MeV deuterons. With the aid of a peristaltic pump the irradiated target gas was slowly passed through a reaction vessel containing 5 ml of liquified phenol. This method gave a recovery of $10 \pm 5\%$ of the theoretically produced radioactivity.

D. RECOVERY OF FLUORIDE-18

    1. Lithium Tetrafluoroborate-^{18}F

A target gas mixture of helium in neon (10% v/v) was irradiated with 6.5 MeV deuterons. After irradiation, an aqueous solution of $LiBF_4$ (20% w/v) was introduced into the irradiation vessel in such a manner as to coat the entire inside surface. This eluted a major portion of the ^{18}F produced which was allowed to exchange with the $LiBF_4$. A recovery of $50 \pm 10\%$ of the theoretically produced radio-activity was obtained.

2.   Potassium Fluoride-^{18}F

A target gas mixture of helium in neon (10% v/v) was irradiated with 6.5 MeV deuterons. After irradiation an aqueous solution of KF (20% w/v) was introduced into the target chamber as before. The major portion of the ^{18}F produced was eluted in this manner resulting in a yield of $70 \pm 10\%$ of the theoretical production limit.

E.   ISOTOPE CHARACTERIZATION

1.   Half-life Determination

A sample of the isotope, containing between 10^5 and 10^6 cpm, was obtained during each production cycle. A gamma spectrometer was calibrated prior to each experiment with a standard ^{137}Cs source and adjusted to count only the 0.511 MeV gamma photopeak. Each sample was counted repeatedly for one minute (dwell time of 70.33 sec/cycle) for approximately three half-lives. The half-life was calculated mathematically and a mean value of 110.68 ± 0.85 minutes was obtained over the entire series of production runs.

2.   Spectral Analysis

The spectrum of a ^{22}Na calibration standard, using a Searle-Harshaw NaI (Tl) well crystal ($1 \frac{3}{4}$ in. x 2 in. x $2\frac{1}{32}$ in. diameter), was collected and stored on a multichannel analyzer. The spectrum of the ^{18}F produced was collected in a similar manner and superimposed on the spectrum obtained for ^{22}Na. The energy correlating to each photopeak observed for the ^{18}F production sample was determined by comparison with the photopeak of known energy for ^{22}Na.

3.   Chemical Analysis

A methanolic solution of the ^{18}F produced was adjusted to pH 12 with 1 N NaOH in methanol. One ml of this solution was treated with one ml KF in methanol (5% w/v) and one ml $CaCl_2$ in methanol (10% w/v). The resultant CaF_2 precipitate was washed with ice cold $CaCl_2$ in methanol (10% w/v), dried by passing air through the precipitate cake and quantitatively transferred to a counting vial. The supernatant and wash contained 7.9% and the precipitate contained 92.1% of the total recovered radioactivity.

F.   SYNTHESES WITH FLUORINE-18

1.   Recoil Synthesis

A solution of 2'-UdR (55 mg, 0.24 mmole) in methanol (2 ml) was applied to the inside surface of the target chamber and dried with a gentle air flow to obtain a uniform coating on the upper one-third of the surface area. The chamber was evacuated to approximately 10 mm Hg and then purged with a helium in neon gas mixture (10% v/v) to remove the remaining atmospheric gases present. The inlet and outflow ports were sealed to prevent escape of the helium in neon target gas mixture (10% v/v) during irradiation. A flow of air, passing through a copper coil immersed in an ice bath, was used to cool the target chamber in order to reduce the rate of thermal degradation of 2'-UdR during irradiation. The target gas was bombarded with 6.5 MeV deuterons for two hours after which the target chamber was washed with methanol (70 ml) to dissolve the labeled product. The sample volume was reduced to

less than 1 ml and basified with a solution of ammonium hydroxide in methanol (5% v/v). Reference FUdR (0.1 mg) and FU (0.1 mg) were added to this solution, which was subsequently analyzed by high pressure liquid chromatography. A compound possessing 35% of the total radioactivity eluted was found in the elution volume correspond-ing to FUdR. This 35% amounted to 0.5% absolute radiochemical yield.

2.   Continuous Flow Synthesis

The irradiation chamber was evacuated to approximately 10 mm Hg and purged with a fluorine in neon gas mixture (1% v/v) until a positive test for fluorine gas was observed with aqueous NaI test solution at the gas exit. The gas flow rate was set at 8 ml/minute and connected to two reaction flasks in series, each containing 1.42 mg (0.006 mmole) 2'-UdR in glacial acetic acid (10 ml) at 25°C. The second reaction flask was vented through an aqueous NaI trap. The continuously flowing fluorine in neon target gas (1% v/v) was irradiated for 30 minutes with 6.5 MeV deuterons. The first reaction vessel (A) contained 5% (46 µCi) of the theoretical radioactive yield and 0.5% (6 µCi) was found in the second reaction vessel (B). High pressure liquid chromatographic analysis of the product in reaction vessel A indicated a chemical yield of 23% FUdR-5-^{19}F. In contrast, there was no reaction product observed in vessel B. There was no radioactivity due to FUdR-5-^{18}F present in either reaction vessel.

3.   Static Target Irradiation Synthesis

The irradiation chamber was evacuated and purged with a fluorine in neon gas mixture (1% v/v) as in the continuous flow method. The

assembly was sealed to prevent the escape of target gas during the two hour irradiation period. After bombardment, the outlet was vented through a solution of 2'-UDR (0.17 mg) in glacial acetic acid (2 ml) to trap any $F_2-{}^{18}F$ that may have been forced out of the target chamber upon introduction of the solvent. The irradiation chamber was then washed with a solution of 2'-UDR (5 mg, 0.022 mmole) in glacial acetic acid (70 ml) which was collected in a reaction flask. The solvent was removed in vacuo and the product redissolved in methanol. Analysis of the residue, with added reference FU (0.1 mg) and FUdR (0.1 mg), by high pressure liquid chromatography indicated a radioactive peak midway between FUdR and 2'-UDR containing 18 μCi of ^{18}F, which corresponded to approximately 1% of the absolute radiochemical yield. The elution fraction corresponding to this peak was collected, basified with a solution of ammonium hydroxide in methanol (5% v/v) and evaporated to dryness in vacuo.

G. RADIOCHEMICAL PURITY OF 5-FLUORO-2'-DEOXYURIDINE-6-^{3}H AND 5-FLUOROURACIL-6-^{3}H

1. 5-Fluoro-2'-Deoxyuridine-6-^{3}H

FUdR labeled with tritium in the C^6 position of the pyrimidine ring was purchased from Amersham/Searle in two 250 μCi lots with specific activities of 9.4 mCi/mg and 8.1 mCi/mg. Each stock solution of FUdR-6-^{3}H was diluted to give a concentration of approximately 10 μCi/ml of normal saline. The radiochemical purity of each lot of

FUdR-6-^{3}H was determined by thin layer (silica gel) chromatography using three solvent systems, each of different polarity. The solvent systems used were ethyl acetate-acetone (2:3 v/v), ethyl acetate-water (100:3 v/v) and normal butanol saturated with water. Duplicate chromatograms were developed in each solvent system and each was analyzed for radiochemical impurities by either liquid scintillation spectroscopy or autoradiography. Approximately 10 μl of the dilute solution of FUdR-6-^{3}H was applied to each chromatogram in one spot along with a small concentration of reference FUdR and FU at the origin. Each chromatogram was developed until the solvent front had moved 10 cm from the origin. The chromatograms which were to be analyzed by liquid scintillation were divided into 1 cm segments beginning 1 cm below the origin and proceeding to the solvent front. The R_f values for the reference compounds were determined by short wave ultraviolet light (UV) and noted before each segment of silica gel was transferred to a liquid scintillation vial. Fifteen ml of toluene-PPO-POPOP fluor was added to each vial and the samples were then allowed to equilibrate in the dark at 4°C until the chemilumin-escence associated with the UV indicator in the silica gel had dissi-pated. A 1 cm segment of silica gel containing no radioactivity was used as a background count rate. Each sample was counted for 20 minutes or 40,000 cpm.

2. 5-Fluorouracil-6-^{3}H

One mCi of FU labeled with tritium in the C^6 position having a specific activity of 7.7 mCi/mg was purchased from Amersham/Searle.

This stock solution was diluted to a specific activity of 10 µCi/ml of normal saline and assayed for radiochemical purity as before.

3.   Autoradiography

Radiochromatograms of both FUdR-6-^{3}H and FU-6-^{3}H were analyzed by autoradiography for radiochemical impurities. The origin and solvent front of the developed chromatograms were marked with one and two spots of FUdR-6-^{3}H respectively. The chromatograms were arranged in groups of three in each X-ray holder in order that the no screen X-ray film was in intimate contact with the silica gel. The folders were well sealed against extraneous light and weighted down to ensure good contact between the silica gel and the film. Each film was exposed for one month before it was developed. The development process included a four minute treatment with developing solution, followed by a five minute water wash. The film was then exposed to a fixing solution for eight minutes and a final water rinse.

H.   MAINTENANCE OF THE TUMOR MODELS

1.   Ehrlich Ascites Carcinoma

The Ehrlich ascites tumor model was maintained in male Swiss albino mice. A donor mouse bearing the ascitic tumor cells was sacrificed by cervical dislocation and the peritoneal cavity and fluid exposed. The fluid was collected in a 1 ml disposable syringe and the cell concentration was determined by serial dilution of a fluid sample with normal saline until the number of cells per given volume could be counted with a hemocytometer (Spencer Bright Line, American

Optical). A volume of 0.1 ml of the aspirated fluid containing approximately 1.8×10^7 cells was injected intraperitoneally into the new host. This procedure was repeated every seven days in order to maintain the tumor line.

A solid tumor was prepared for tissue distribution work by injection of 0.1 ml of the aspirated fluid into the femoral region of the right hind leg of the host five to seven days prior to use.

2. Lewis Lung Carcinoma

The Lewis lung carcinoma model was maintained in male BDF_1 hybrid mice as a solid tumor mass. A donor mouse, bearing the solid tumor, was sacrificed by cervical dislocation and the tumor mass was excised and submerged in physiological saline. Fragments, approximately 1 mm^3 in size, were removed from the tumor and transferred with forceps to a sterile 12 gauge needle barrel. The new host was anesthetized with ether to facilitate transplantation. The needle was inserted subcutaneously just below the right foreleg of the mouse and the tumor was then ejected from the needle barrel with a trochar. In order to maintain viability of the tumor line, this procedure was repeated in a ten to twelve day cycle. Tumor bearing mice required for tissue distribution work were prepared eight to ten days in advance.

I. TISSUE DISTRIBUTION STUDIES

1. Tissue Distribution of 5-Fluoro-2'-Deoxyuridine-6-^{3}H

The tissue distribution of FUdR-6-^{3}H was studied in two tumor models, the Lewis lung carcinoma and the Ehrlich ascites carcinoma,

as well as the appropriate controls. Six adult male mice, weighing 20
to 25 grams, were used in each of the four treatment groups. Each
mouse was injected intravenously with 0.83 μCi of FUdR-6-^{3}H in 0.1 ml
saline, via the dorsal tail vein. The concentration of radioactivity
in different organs was studied at 15, 30, 45, 60, 90, 120, 150, 180,
210 and 240 minute intervals after injection of FUdR-6-^{3}H. During the
designated time periods after injection, the mice were placed in
separate cages with food and water. At the end of each time interval
a blood sample was taken from the animal by cardiac puncture after
which the mouse was sacrificed by cervical dislocation. The entire
tumor, heart, liver, lungs, spleen, kidney, testis and small intestine
were excised along with the tibia, femor and aliquots of muscle from
the left hind leg. The tissues were blotted free of blood and air
dried on plastic weighing boats for one week. The samples were then
weighed and prepared for liquid scintillation analysis by combustion
on a Packard Tricarb 306 sample oxidizer. The recovery efficiency of
the radioactivity from the sample, as H_2O-^{3}H, by the oxidizer was
determined periodically by oxidation of a known quantity of tritiated
normal hexadecane standard. The mean recovery efficiency was 98%. The
H_2O-^{3}H from the samples was collected in Monophase 40^R liquid scintil-
lation cocktail. The samples were dark adapted at 4°C until chemi-
luminescence was not detected and then counted for 20 minutes or 40,000
cpm. This gave an accuracy level of 1% ± 2 δ. Both the recovery of
tritium from the oxidizer and the level of quench in each sample were
found to be constant enough to require no mathematical correction for
either variable. The per cent of the total dose incorporated into the

various tissues, the tissue to blood ratios and the tissue to muscle ratios for each animal were calculated and the results tabulated.

2. Tissue Distribution of 5-Fluorouracil-6-^{3}H

The tissue distribution patterns for FU-6-^{3}H were studied in the Lewis lung carcinoma and the Ehrlich ascites carcinoma animal models including a control group of each strain. Six adult mice weighing 20 to 25 grams were used in each of the four treatment groups. Each mouse was injected intravenously with 0.64 µCi of FU-6-^{3}H in 0.1 ml normal saline, via the dorsal vein. The distribution data was collected in an identical manner as above except that fewer time intervals were studied. These time intervals were 15, 30, 60, 120, 180 and 240 minutes after the injection of FU-6-^{3}H. A liquid scintillation cocktail of PBBO, butyl PBD and BBS3 in toluene was used to count the oxidized samples.

3. Subcellular Distribution of 5-Fluoro-2'-Deoxyuridine-6-^{3}H and 5-Fluorouracil-6-^{3}H in the Liver

Three male Swiss albino mice were injected intravenously, via the dorsal vein, with either 1.28 µCi FU-6-^{3}H or 1.66 µCi of FUdR-6-^{3}H in 0.2 ml normal saline. One hour after injection, each animal was sacrificed by cervical dislocation and the entire liver was excised, weighed and stored in ice cold isotonic sucrose. Each liver was then homogenized, using a Potter-Elvehjem homogenizer and teflon pestle, in a volume of 0.25 M sucrose, suitable to maintain a 25% w/v homogenate. The homogenate was centrifuged at 700 g for 10 minutes, the supernatant was decanted and then recentrifuged at 10,000 g for 20 minutes. A 1 ml

aliquot of the 10,000 g supernatant was diluted to 10 ml with ice cold
aqueous KCl (1.15% w/v) and centrifuged at 105,000 g for one hour. The
pellets obtained after each centrifugation were resuspended in ice
cold aqueous KCl (1.15% w/v) to a total volume of 5 ml. One ml aliquots
of the suspension were prepared for either liquid scintillation analysis
by solubilization of the solid material in Protosol [R], or protein
concentration analysis. The 105,000 g supernatant was also analyzed
for tritium and protein concentration as above. The solubilized
samples were dissolved in 12 ml of Riafluor [R], dark adapted at 4°C and
counted on a Mark III liquid scintillation spectrometer for 20 minutes
or 40,000 cpm. The results were corrected for variable quench using
the sample channels ratio technique and reported as dpm per mg of
protein.

a. Protein Determination

Each sample was analyzed for protein content using the
colorimetric method of Lowry as modified by Miller[91]. The copper
reagent was prepared by adding one volume of aqueous copper
sulphate (1% w/v), one volume of aqueous sodium potassium tartrate
(2% w/v) to twenty volumes of sodium carbonate (10% w/v) in 0.5 N
sodium hydroxide. Dilution of one volume of Folin-Phenol reagent
with ten volumes of distilled water made up the dilute Folin-Phenol
reagent. Each 1 ml sample of protein was mixed with 1 ml of copper
reagent and allowed to stand for ten minutes. Three ml of dilute
Folin-Phenol reagent were then added to the above solution, mixed
thoroughly and heated at 50°C for ten minutes. The optical density
of the cooled samples was read at 560 nm on a Unicam 1800

spectrometer and compared to control samples of bovine serum albumin (BSA) of known concentration. A standard curve of increasing concentration of BSA plotted against optical density was used to determine the sample concentration.

J.   URINARY AND FECAL EXCRETION STUDIES

1.   Excretion of 5-Fluoro-2'-Deoxyuridine-6-^{3}H

Six adult male mice, weighing 20 to 25 grams, were used in each of the four treatment groups. Each mouse was injected intravenously, via the dorsal vein, with 0.83 μCi FUdR-6-^{3}H. The mice were housed in separate cages consisting of a 600 ml glass beaker with a wire mesh floor protecting a Whatman filter paper disc covering the bottom of the beaker. The cumulative urinary and fecal output of radioactivity was determined 1, 3, 6, 12, 24, 36, 48, 60 and 72 hours after injection. The filter paper disc, containing the total urinary and fecal matter excreted, was removed at the end of each predetermined time period. The samples were air dried and prepared for liquid scintillation analysis by combustion in a tissue sample oxidizer. Preliminary results with both the external standard pulse and the sample channels ratio quench correction techniques indicated that the quench factor was relatively constant in the oxidized samples.

The results were tabulated and plotted as log per cent dose excreted versus time. The curves were visually divided into two separate components which were analyzed using a computerized curve stripping technique to determine the biological half time of each component.

2.   Excretion of 5-Fluorouracil-6-^{3}H

The excretion data for FU-6-^{3}H was obtained with the same techniques used for the FUdR-6-^{3}H data. The calculation and presentation of the results were also identical.

3.   Chromatographic Analysis of the Urine

Three adult male Swiss albino mice, weighing 20 to 25 grams, were injected intravenously via the dorsal vein with either 1.28 μCi of FU-6-^{3}H or 1.66 μCi of FUdR-6-^{3}H in 0.2 ml normal saline. One hour after injection, each mouse was sacrificed by cervical dislocation and the urine was collected and pooled for each group of three mice. The urine was applied directly onto the silica gel thin layer chromatograms along with reference FU and FUdR. Three solvent systems, ethyl acetate - acetone (2:3 v/v), ethyl acetate - water (100:3 v/v) and water saturated normal butanol were used to develop the chromatograms. Each chromatogram was developed for a distance of 15 cm from the origin for three consecutive times to increase the resolution. The chromatograms were divided into 1 cm segments beginning 1 cm below the origin and proceeding to the solvent front. The reference compounds were visualized under short wave UV light and the R$_f$ values corresponding to FU and FUdR were recorded as the section number in which they appeared. Each 1 cm fraction was counted by liquid scintillation in toluene-POPOP-PPO fluor. The radioactivity on the sections corresponding to the reference compounds was used to calculate the concentration of that component as a per cent of the total radioactivity found on the entire chromatogram.

IV. RESULTS AND DISCUSSION

A.   FLUORINATION OF URACIL AND 2'-DEOXYURIDINE

Time is the ultimate factor that must be considered during the
practical application of a short lived radionuclide to a specific
problem. The labeled compound must be synthesized and purified with
a specific and total activity high enough to be useful experimentally.
Radiopharmaceuticals labeled with ^{18}F essentially have a half-life
of 109.7 minutes and therefore represent a situation in which synthetic
and purification procedures must be accomplished as quickly as possible.
Condensation reactions, which form the fluorine containing uracil ring,
(figure 7) and similar syntheses were considered less applicable than
synthetic pathways allowing direct introduction of the ^{18}F moiety into
the preformed pyrimidine nucleus. An obvious choice would be the
simple halogen-halogen exchange reaction which has been used to
synthesize 6-fluorouracil-6-^{19}F [92] and label ethanol[76], cholesterol[74]
and some acetates[75] with ^{18}F. Substitution of fluorine for iodine or
bromine would seem to be favored if one considers bond strengths
(C-F = 93 kcal/mole; C-Br = 58 kcal/mole; C-I = 43 kcal/mole) and ease
of displacement. However, the pyrimidine-2,4-dione nucleus is inher-
ently electronegative at the C^5 position, even with an electronegative
iodine or bromine substituent, and hence favors electrophilic substitu-
tion over nucleophilic displacement as demonstrated in figure 8. The
use of a crown ether, phase transfer catalyst, to increase the nucleo-
philicity of the fluoride anion ("naked fluoride") failed to effect
substitution with either 5-bromouracil, 5-iodouracil or their nucleosides.
The classic fluorination of aromatic compounds via the decomposi-
tion of isolated aryl diazonium tetrafluoroborate salts has been used
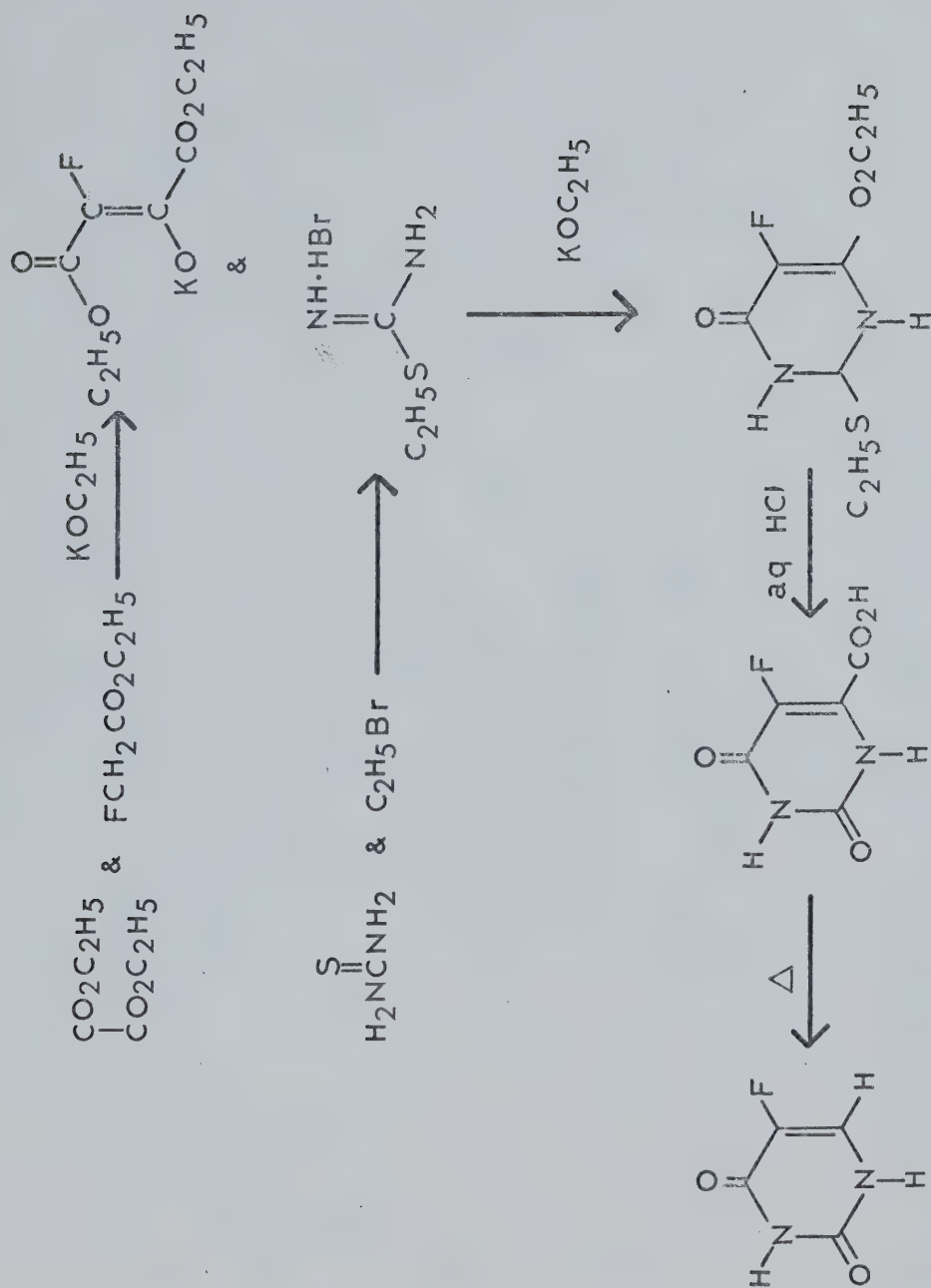
FIGURE 7   RING CONDENSATION REACTION for the SYNTHESIS of 5-FLUOROURACIL

51
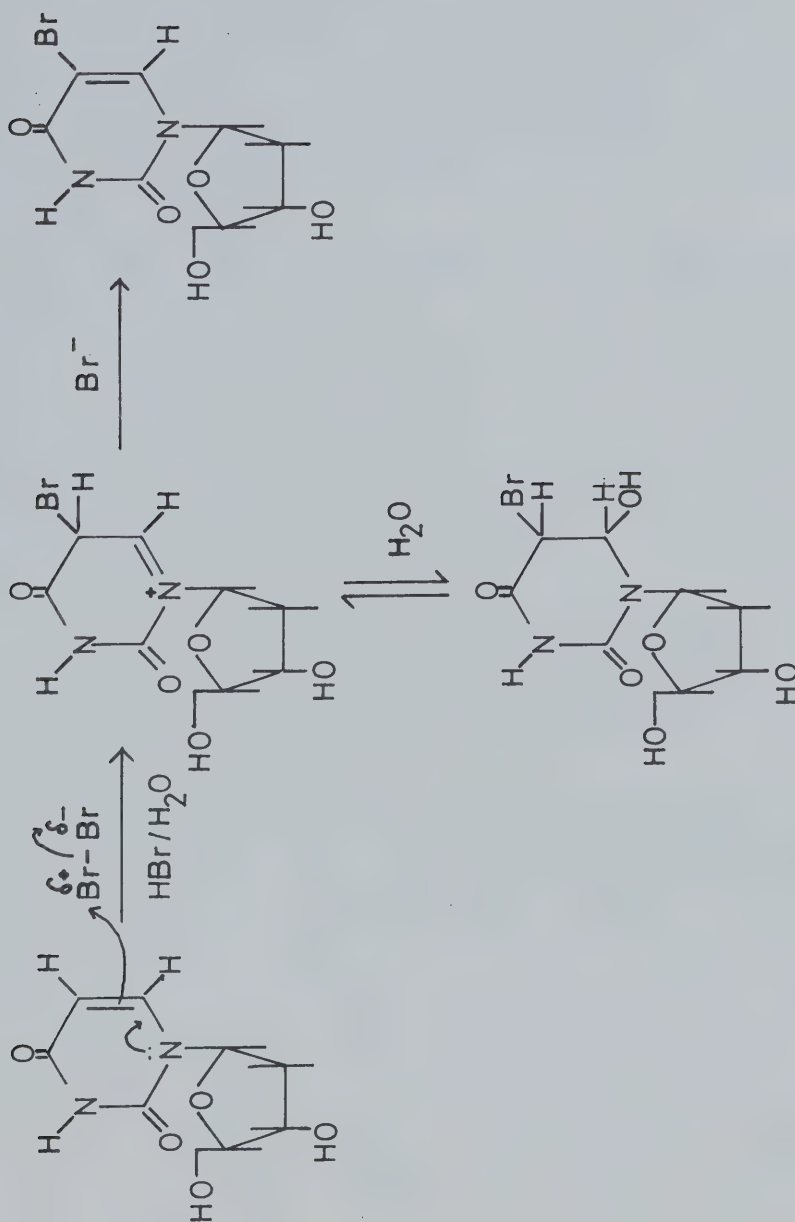
FIGURE 8   BROMINATION MECHANISM DEMONSTRATING

the ELECTROPHILIC NATURE of the C⁵ of 2'-DEOXYURIDINE

successfully to label tryptophan[70], para-fluorophenylalanine[66-69] and DOPA[72,73] with ^{18}F. Unfortunately pyrimidines form unstable diazonium tetrafluoroborate salts which cannot be isolated[93]. Other methods in which the pyrimidine diazonium salt is decomposed in the presence of fluoroboric or hydrofluoric acid have had limited success. The attempted isolation of the products of the 5-amino-pyrimidine series have resulted in hydrolytic ring cleavage[93].

More recent techniques have employed trifluoromethyl hypofluorite (CF_3OF) and elemental fluorine (F_2) as electrophilic fluorinating reagents. Trifluoromethyl hypofluorite, a well docomented and efficient procedure, has been used to fluorinate uracil[94,95], cytosine[96,97] and 1-(tetrahydro-2-furanyl)-5-fluorouracil[98]. Fluorine gas was selected in lieu of CF_3OF since it was believed that $F_2-^{18}F$ would be much more accessible than $CF_3OF-^{18}F$. 5-Fluorouracil and its nucleoside derivatives have been synthesized using $F_2-^{19}F$ [82-84] and Lambrecht[50,51] recently reported the synthesis of FU-5-^{18}F in high chemical and radiochemical yield using $F_2-^{18}F$.

Initial experiments on the fluorination of uracil using conditions similar to those outlined by Lambrecht afforded FU-^{19}F in 58% chemical yield. No attempt was made to optimize the reaction conditions. The reaction of 2'-UdR in trifluoroacetic acid with F_2/N_2 (1:9 v/v) gave a complex reaction mixture. Thin layer chromatographic analysis of the reaction mixture revealed six distinct bands, four of which exhibited Rf values corresponding to 2'-UdR, uracil, FUdR and FU. The remaining bands were not identified. In view of the observation that 2'-UdR and FUdR are susceptible to cleavage of the β-glycosidic bond in the

presence of acid, it was thought that trifluoroacetic acid may not be the most suitable solvent for this reaction. Fluorination of 3',5'-diacetyl-2'-deoxyuridine with F_2/N_2 (1:9 v/v) using glacial acetic acid as the solvent afforded 5-fluoro-3',5'-diacetyl-2'-deoxyuridine in satisfactory yield. However, hydrolysis of the protected sugar proved to be too time consuming and also reduced the overall chemical yield of FUdR. Further studies indicated that direct fluorination of 2'-UdR in glacial acetic acid at 16°C using a F_2/Ne (1% v/v) gas mixture afforded FUdR in 56% chemical yield. A slight decrease in yield was noted when the reaction was carried out at room temperature. Analysis of the reaction mixture using high pressure liquid chromatography (HPLC) indicated the presence of FU and 2'-UdR in addition to the desired FUdR.

Both micro thin layer chromatography and HPLC, used to monitor the progress of the reaction, exhibited a new product whose Rf value appeared midway between that of 2'-UdR and FUdR. This product disappeared when the crude reaction mixture was taken up in ammonium hydroxide in methanol (5% v/v) and a compound with an Rf value corresponding to FUdR appeared. No change was observed when the reaction mixture was dissolved in anhydrous methanol.

These observations may be explained by referring to figures 9 and 10. If the intermediate adduct, 5,6-dihydro-5-fluoro-6-hydroxyuracil, postulated by Barton[94] arose via a reaction analogous to the mechanism proposed by Robins[97], a similar adduct can be envisioned for our reaction. On the addition of CF_3OF to uracil, Robins proposed that the solvent may act as a nucleophile and attack at the C^6 position. In our reaction, hydroxyl, acetate or fluoride may act as the nucleophile,

54
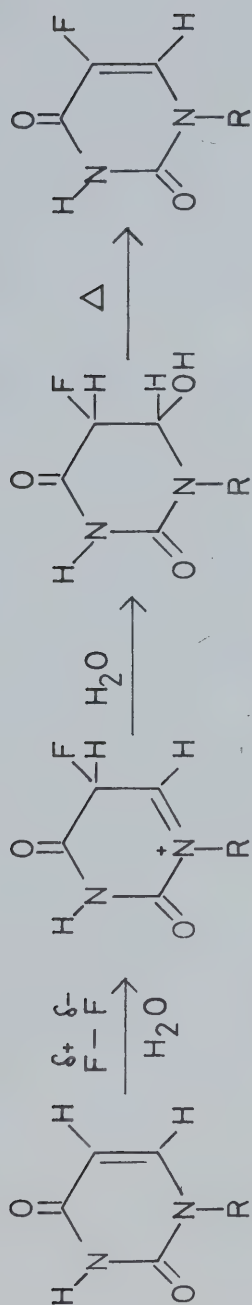
FIGURE 9   DIRECT FLUORINATION of URACIL with ELEMENTAL FLUORINE
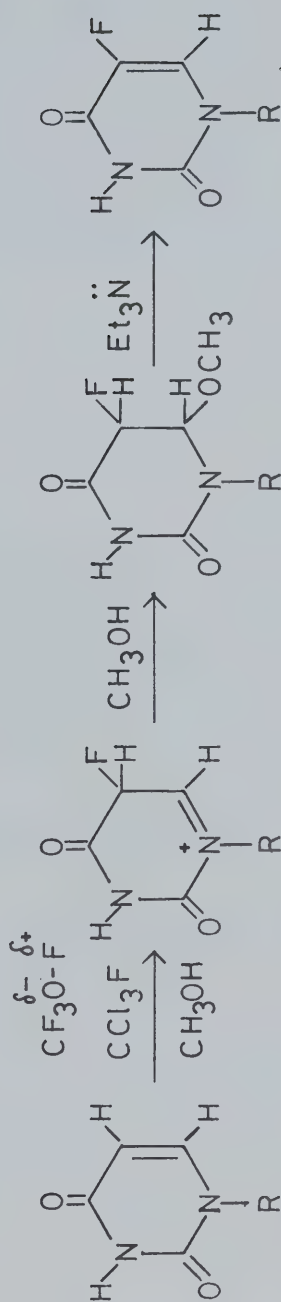
FIGURE 10   DIRECT FLUORINATION of URACIL with TRIFLUOROMETHYL HYPOFLUORITE

giving a C[6] substituted 5,6-dihydro-5-fluorouracil intermediate. Cech
and Holy[84] have also noted a primary reaction product that required
either sharp drying, heating or treatment with a tertiary base to be
transformed into the desired 5-fluorouracil derivative. These
primary addition products were unstable and less polar than the
starting materials and were postulated to be the 5,6-dihydro-5,6-
difluorouracil derivatives.

B.   PRODUCTION OF FLUORINE-18

      1.   Production Systems

The ^{18}F used in this study was produced with a 7 MV Van de Graaff
accelerator located at the Nuclear Research Center, University of
Alberta, Edmonton, Alberta. Although many reactions are possible for
the production of ^{18}F, the ^{20}Ne(d,α)^{18}F nuclear reaction was chosen
for the following reasons:

1.   It has a favourable cross section in the available energy range
      (figure 11)[108].

2.   The neon target gas is inert and would not interfere with
      subsequent chemical reactions with the ^{18}F.

3.   It allowed for a variety of recovery methods to be explored.

      The production facilities consisted of three major components
including the accelerator, the beam line and the target assembly
(figure 12). Minor modifications were applied to the target assemblies
to allow different methods for the recovery of ^{18}F to be evaluated. The
accelerator and beam line remained unaltered.
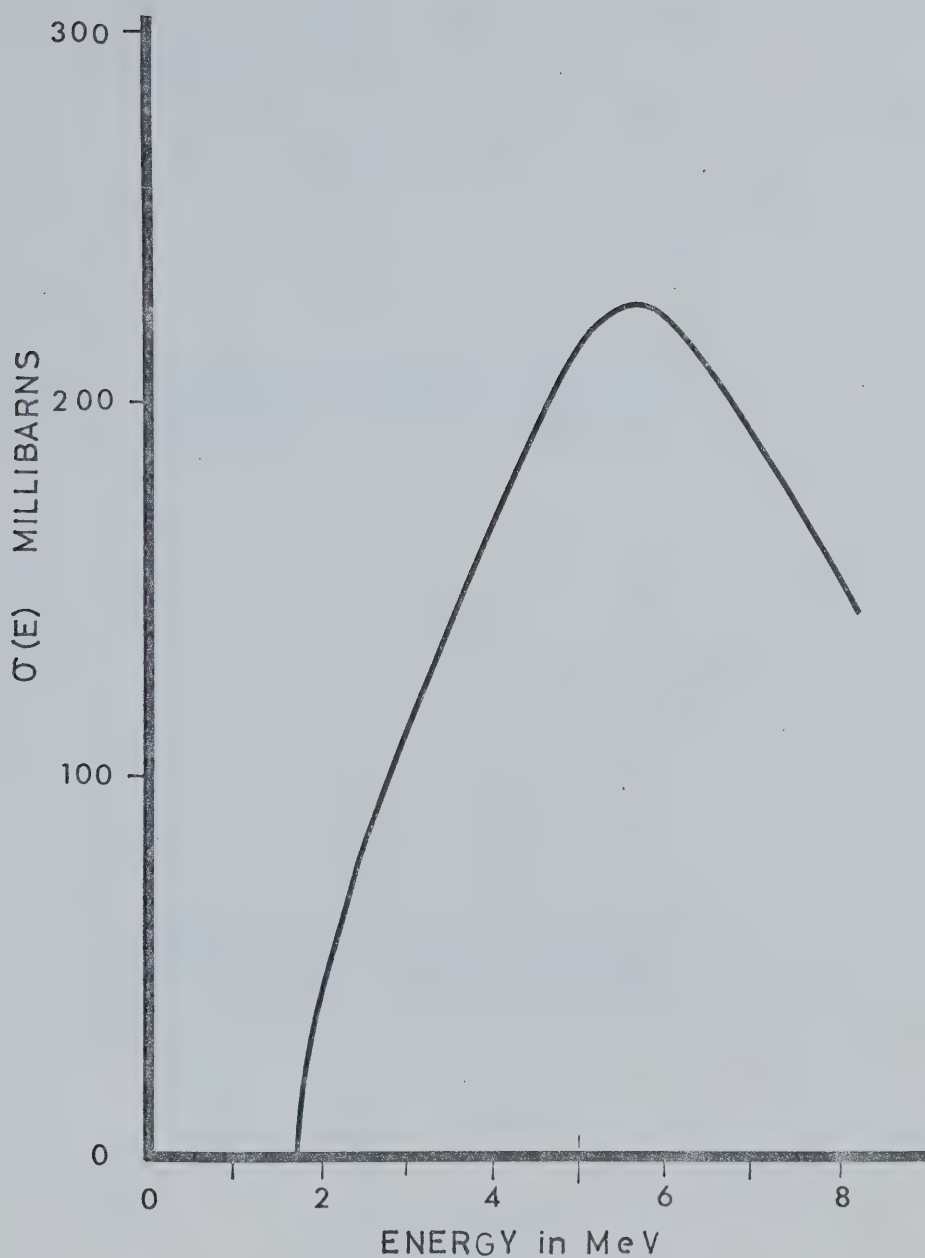
FIGURE 11 CROSS SECTION of $^{20}Ne(d,\alpha)^{18}F$ REACTION

57
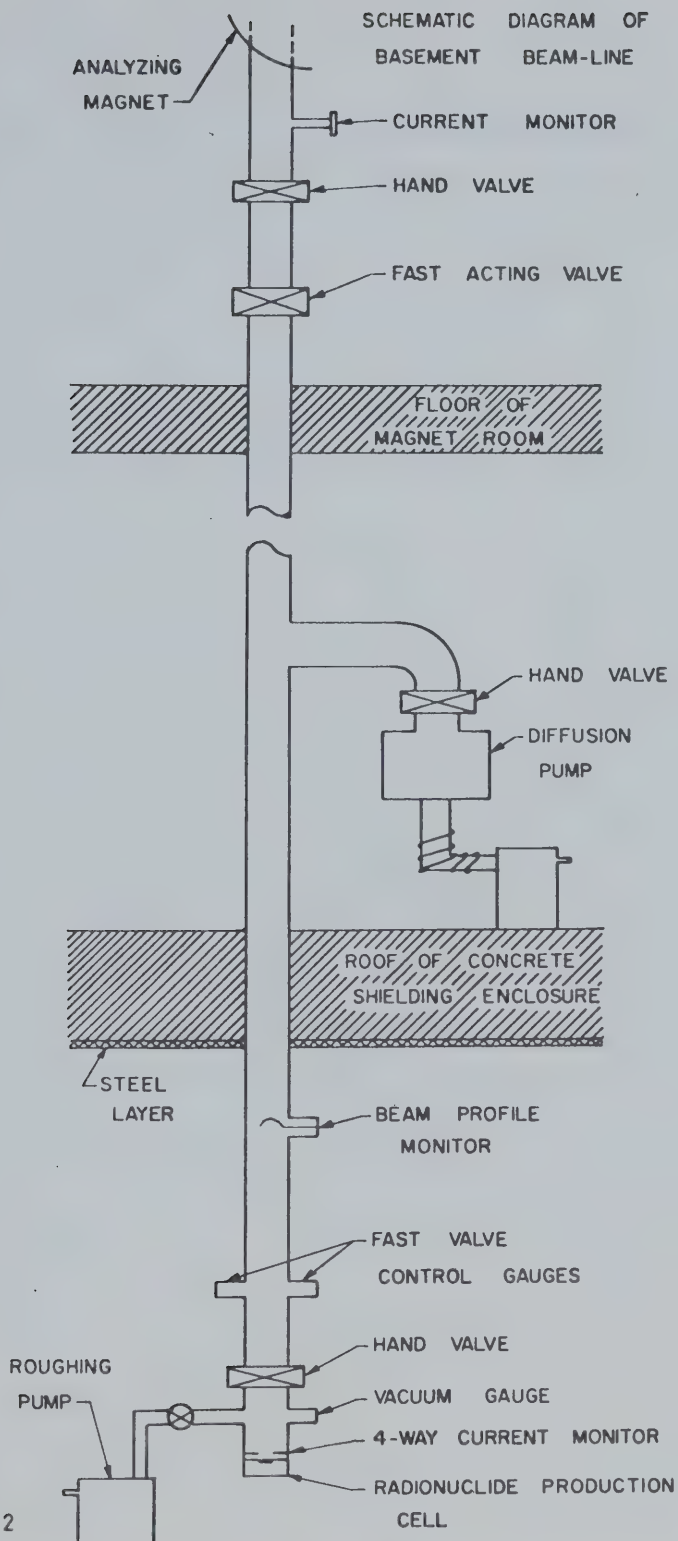
FIGURE 12

2.   Target Assemblies

A detailed description of the accelerator and beam line is beyond the scope of this project and is covered in a recent review[99]. The production cell was designed so that a sufficient cross section of neon gas would be present and the irradiated gas would be directly accessible for chemical reaction. Figure 13 is a schematic diagram comparing two different target assemblies used. Each isolated the neon target gas from the beam line vacuum by a thin molybdenum foil (5×10^{-3} mm). The two inlet ports were located so that either the target gas or a recovery solvent could be introduced into the target chamber after the complete assembly had been attached to the beam line. The inner surface of the target cell walls were either siliconized stainless steel or siliconized pyrex glass. The initial assembly was totally fabricated from stainless steel, but the target cell and reaction vessels themselves were eventually replaced by glass equipment. This allowed more efficient cooling of the target chamber during irradiation and a more practical reaction vessel. Both assemblies had a tantalum disc located at the bottom of the irradiation chamber to act as a beam stop and current monitor. An outlet port at the bottom of the target vessel allowed recovery of either the irradiated target gas or the eluting solvent containing the ^{18}F produced during irradiation of a fixed volume of neon. In addition, this port was necessary for maintaining the continuous flow reaction.

3.   Recovery Systems

The closed loop recirculating gas target cell system (figure 14) utilized a peristaltic pump to slowly recirculate the neon target gas

DEUTERON BEAM

MOLYBDENUM FOIL

INLET PORTS

NEON TARGET GAS

STAINLESS STEEL CELL

PYREX CELL

Ta BEAM STOP

TO RECOVERY VESSEL

AIR FLOW
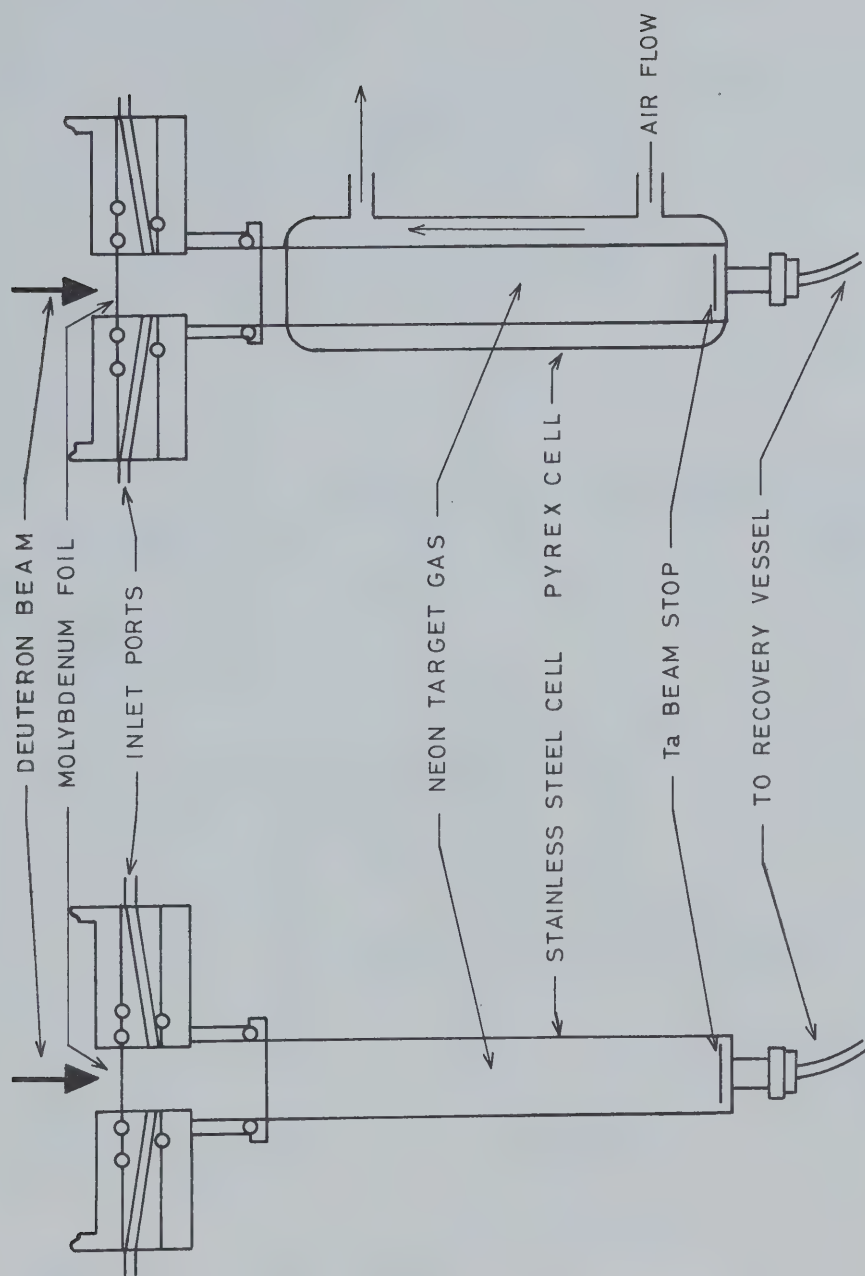
FIGURE 13   FLUORINE-18 PRODUCTION CELLS

DEUTERON BEAM

1% F$_2$ in Ne →

GLASS TARGET CELL

aq .NaI TRAP

GLASS REACTION
VESSELS

CONTINUOUS
FLOW

DEUTERON BEAM

STAINLESS STEEL
TARGET CELL

1% F$_2$-Ne →

STAINLESS STEEL
REACTION VESSEL

PERISTALTIC
PUMP

RECIRCULATING FLOW
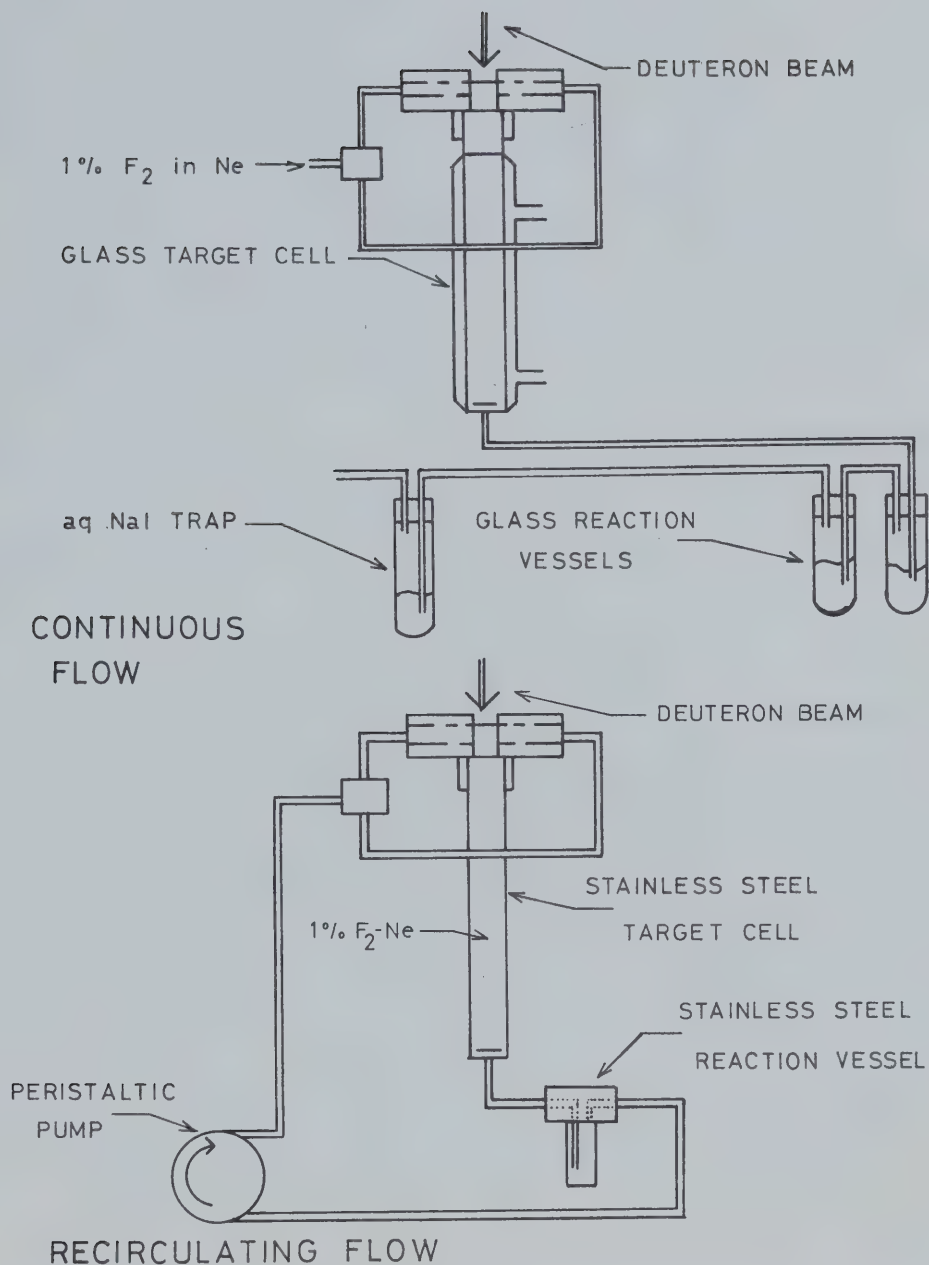
FIGURE 14   FLUORINE-18 RECOVERY SYSTEMS

through the reaction vessel. The F_2-^{18}F produced was removed from the gas stream by chemical reaction with the substrate in the reaction chamber. The unreacted neon was recirculated through the irradiation chamber to be converted into more ^{18}F. When the target gas used was helium in neon (10% v/v), less than 1% of the theoretical radioactive yield was found to be incorporated into the liquified phenol, which acted as the reaction substrate for F_2-^{18}F. In an effort to increase the amount of ^{18}F available as F_2-^{18}F, a mixture of fluorine in neon (1% v/v) was substituted as the target gas. The carrier fluorine reduced the absorption of F_2-^{18}F in the target assembly by passivating or saturating the inside surface area with F_2-^{19}F. The F_2-^{19}F also promoted the combination of ^{18}F atoms with ^{19}F atoms to produce F_2-^{18}F rather than ^{18}F anion. Using this technique, recovery was found to be 10 ± 5% of the total theoretical radioactive yield.

In anticipation of possible synthetic routes using the anionic form of ^{18}F, sodium fluoride and lithium tetrafluoroborate labeled with ^{18}F were prepared. An aqueous solution of either sodium fluoride or lithium tetrafluoroborate was introduced into the target cell after irradiation of the neon gas. This eluted the ^{18}F adsorbed to the inner surface of the target chamber and allowed a passive exchange of ^{18}F for ^{19}F to occur. The resultant recoveries of potassium fluoride-^{18}F and lithium tetrafluoroborate-^{18}F were 70 ± 10% and 50 ± 10% respectively, based on the total radioactivity theoretically produced.

4.   Isotope Characterization and Radionuclidic Purity

    a. Half-life

    The half-life of the isotope, ^{18}F, produced was calculated

for each production run. The sample was counted repeatedly using

a gamma spectrometer calibrated to discriminate for the 0.511 MeV

photopeak only. The dwell time of the gamma spectrometer was

determined as 70.33 sec/cycle. The actual elapsed time between

sample counts was calculated and the data substituted into the

formula:[100]

$$In \ n_2 = In \ n_1 - \frac{0.693t_2}{t\frac{1}{2}}$$ (1)

which was used to calculate the half-life of the isotope. A mean

value of 110.68 ± 0.85 minutes was obtained over the entire study,

which agreed to within 0.9% of the accepted value for the half-life

of ^{18}F [48]. The semilog plot of the count rate versus time was

found to be linear, which suggested that only a single isotope

contributed towards the decay rate measured.

    b. Spectral Analysis

    Fluorine-18 is a pure positron emitting isotope and its

gamma scintillation (NaI (Tl)) spectrum consists of two peaks.

The first of these peaks corresponds to 0.511 MeV, due to gamma

photons emitted during positron annihilation, while the other

occurs at 1.022 MeV due to coincidence summation of two 0.511 MeV

gammas. These two peaks should be superimposable on a spectrum

from any positron emitting isotope, such as ^{22}Na. The spectra

of a ^{22}Na standard and the ^{18}F production sample were recorded

on a multichannel analyzer using a NaI (Tl) well crystal (figure 15). The ^{18}F spectrum was identical to the portion of the ^{22}Na spectrum which was due to positron emission alone. The spectrum of the ^{18}F production sample, after the 1.022 MeV photopeak, was flat, indicating that no radionuclides with gamma energies greater than 1.022 MeV were present in the sample. The shape of the 0.511 and 1.022 MeV photopeaks were essentially symmetrical suggesting that no contaminating radionuclides with similar energy gammas were hidden beneath either photopeak. The two additional photopeaks observed for ^{22}Na were due to a 1.275 MeV gamma, also emitted by that nuclide, and a coincidence photopeak of 1.78 MeV resulting from the summation of a 0.511 MeV and a 1.275 MeV gamma ray. This evidence suggested that the ^{18}F production sample contained only positron emitting radionuclides.

c. Chemical Analysis

The poor recovery of radioactivity by the liquified phenol and the relatively high yields of potassium fluoride-^{18}F and lithium tetrafluoroborate-^{18}F indicated that the chemical form of the ^{18}F produced was the anionic fluoride. Carrier sodium fluoride was added to an alkaline sample of the crude reaction mixture. Addition of excess calcium chloride quantitatively precipitated the fluoride ions in solution as calcium fluoride. The precipitate accounted for 92.1% and the supernatant con- tained 7.9% of the recovered radioactivity. Preliminary studies in which FU-6-^{3}H and FUdR-6-^{3}H were present in solution during the precipitation of the fluoride indicated that neither of
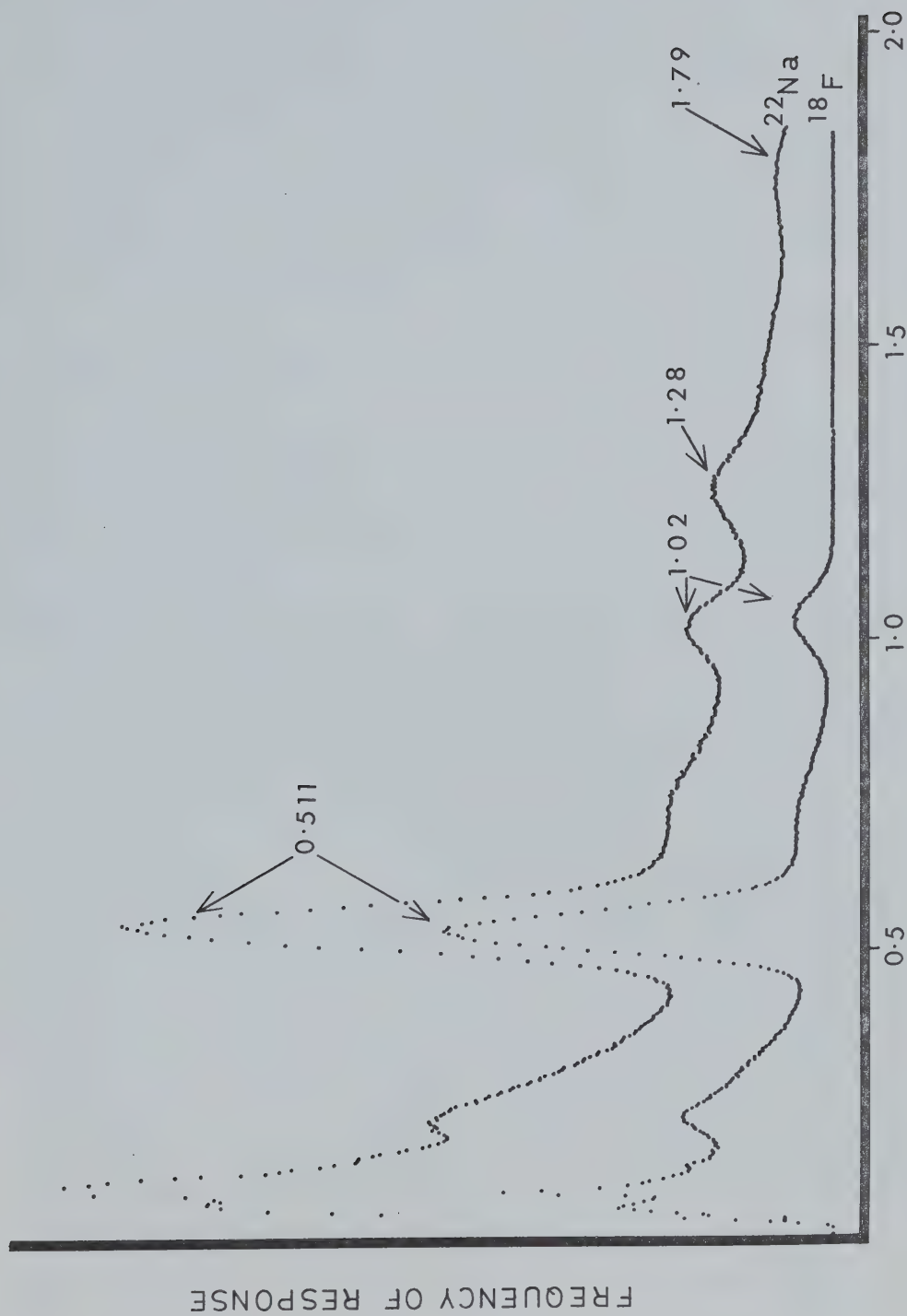
FIGURE 15   GAMMA SPECTRA OF FLUORINE-18 AND SODIUM-22

these compounds is co-precipitated with the calcium fluoride. These results suggested that 92.1% of the radioactivity recovered for the radiofluorination of 2'-deoxyuridine was present in a form which would precipitate as calcium fluoride. The radioactivity present in the supernatant can be attributed to organically bound ^{18}F and the remainder to a minute portion of unprecipitated fluoride.

C.   RADIOFLUORINATION OF 2'-DEOXYURIDINE

The majority of medical applications of ^{18}F initially employed the fluoride anion for bone scanning[59,101] and fluoride metabolism[53,102] or the tetrafluoroborate salt for thyroid studies[63] and imaging of intracranial lesions and tumors. Fluorine-18 can be produced directly as either the fluoride or the tetrafluoroborate salt and therefore require only purification and sterilization before use. More recent approaches to improve organ scanning agents necessitates binding radionuclides covalently to biomolecules with known or suspected organ specificity. This in turn requires more suitable forms of the isotopes as specialized reactants. Until recently, chemical labeling with ^{18}F has involved mainly nucleophilic reactions because the electrophilic reactants available were not applicable to short lived radionuclides. Therefore, halogen exchange and displacement reactions with fluoride anion[74-76], addition reactions to alkenes and epoxides with hydrogen fluoride[103,104] and aromatic fluorination via decomposition of the tetrafluoroborate salts[66-73, 79] were the first reactions used to label organic molecules. However, these reactions

are not applicable to fluorination of pyrimidines at the C^5 position
which is inherently electronegative.

Direct irradiation of compounds containing fluorine substituents
utilizing the $^{19}F(n,2n)^{18}F$ or $^{19}F(p,pn)^{18}F$ nuclear reaction have been
used to circumvent the problem of the availability of useful fluorin-
ating reagents. This method is applicable to both aromatic and
aliphatic compounds, however, the radiochemical yields are considerably
higher for the aromatic compounds due to the stabilizing effect of the
delocalized electrons on the transition from ^{19}F to ^{18}F. Anbar and
Neta[88] reported radiochemical yields ranging from 8% for FU-5-^{18}F to
20% for more stable fluorinated aromatic nuclei. The facilities for
this reaction were not available; therefore another method which did
not require chemical synthetic procedures was examined. This method
used the recoil energy afforded ^{18}F atoms upon production to label
the desired compound. The synthesis of FU-5-^{18}F in 1% radiochemical
yield by recoil labeling has been reported using the nuclear reaction
$^{20}Ne(d,\alpha)^{18}F$ [87,105].

These high energy recoil atoms of ^{18}F must reach thermal energy
for the labeling process. However if too many collisions occur before
the interaction of the ^{18}F nuclei with the substrate, it may become
nonreactive even though it is within the desired energy range.

The recoil labeling species is probably a mixture of neutral
and electronically excited atoms[87]. An increase in yield is therefore
expected with a decrease in pressure of the target gas. Although low
radiochemical yields, significant substrate decomposition and poor
control over label position are disadvantageous, the ease of synthesis

and high specific activity of the product suggested that the recoil method may be practical.

The recoil labeling of 2'-UdR was effected using an argon in neon (10% v/v) target gas mixture at atmospheric pressure. The substrate was coated uniformly over the upper one-third of the inner surface of the target vessel to take advantage of the maximum flux of ^{18}F atoms produced in that region. The average radiochemical yield of FUdR-5-^{18}F obtained overall was 0.5% of the absolute radioactivity produced. Absolute radioactivity produced refers to the total radio-activity recovered after bombardment as determined in a calibrated well crystal (NaI (Tl)) and calculated back to time zero (end of bombardment). A significant amount of degradation resulting in a complex mixture of radiolabeled and non-labeled radiolysis products was observed (figure 16).

Cleavage of the nucleoside β-glycosidic bond to afford uracil and FU-5-^{18}F was demonstrated by high pressure liquid chromatography. Only 1 to 2% of the absolute radioactivity produced was recovered in the column effluent, of which an average of 35% was found in an elution volume synonymous with that of carrier FUdR. The yield of FUdR-5-^{18}F available for biological experimentation was too low to be of practical use.

Lambrecht's successful preparation of FU-5-^{18}F prompted attempts to prepare ^{18}F as elemental fluorine with the Van de Graaff accelerator using the ^{20}Ne (d,α) ^{18}F nuclear reaction. Fluorine gas was added to the neon target gas (1% v/v) to enhance the recovery of ^{18}F in its elemental state. Two different techniques were employed to recover
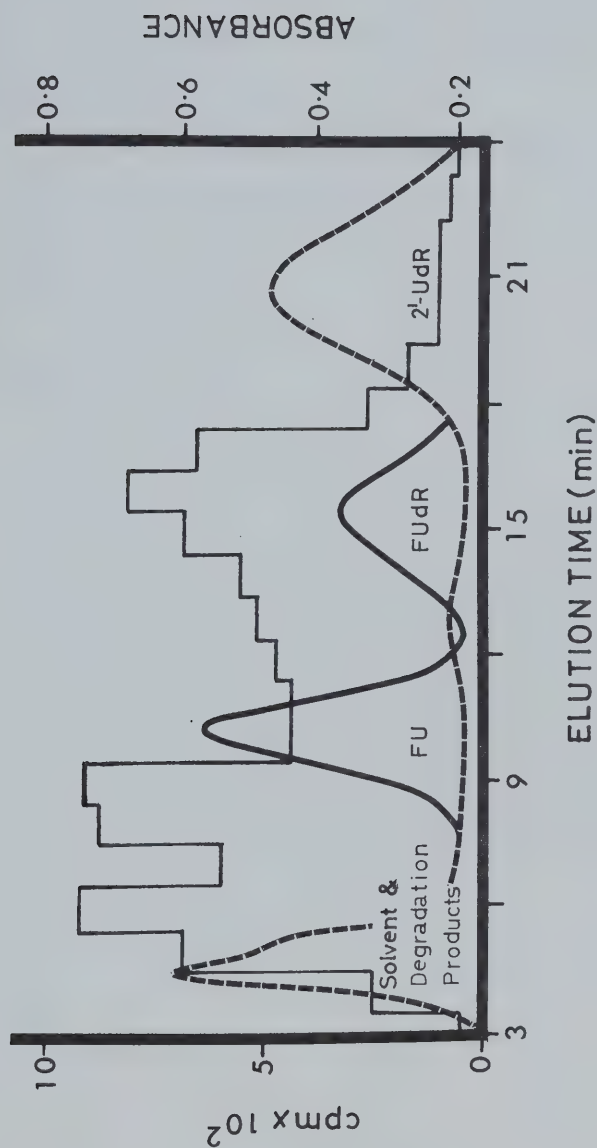
FIGURE 16

Composite chromatogram from column chromatography of the FUdR-5-^{18}F recoil synthesis product. The histogram represents radioactivity in consecutive 1 ml aliquots of column effluent. The ultraviolet absorption profile (254 nm) is shown by the broken line (— —); the solid line (——) depicts typical elution curves for FU and FUdR.

the F_2-^{18}F for reaction; viz, a continuous flow of F_2/Ne (1% v/v) through the target chamber-reaction vessel assembly during bombardment and bombardment of a volume of static F_2/Ne gas (1% v/v) and subsequent elution of the F_2-^{18}F with a solution of 2'-UdR in glacial acetic acid (5 mg/70 ml).

Three variations of the continuous flow method were investigated:

1. Continuous flow of F_2/Ne (1% v/v) gas through the target chamber-reaction vessel assembly in a closed loop, throughout the total irradiation period;

2. Continuous flow of F_2/Ne (1% v/v) gas through the target chamber-reaction vessel assembly in a closed loop, initiated midway through the irradiation period; and

3. Continuous flow of F_2/Ne (1% v/v) gas from an external source through the target chamber-reaction flask assembly in an open, vented system throughout the total irradiation period.

All three systems gave similar results and only the third system will be described in detail. A recovery of 5 to 10% of the absolute amount of radioactivity produced was present in the reaction vessel containing 2'-UdR in glacial acetic acid. The low recovery of ^{18}F was attributed to the low concentration of scavenger F_2 gas present in the neon and the large surface area inherent in the continuous flow design. The irradiated F_2/Ne (1% v/v) target gas was passed through two reaction flasks, each containing 2'-UdR in glacial acetic acid and a third flask containing aqueous sodium iodide (5% w/v) to trap any F_2-^{18}F not dissolved in the glacial acetic acid. Less than 20% of the radioactivity found in the first vessel was observed in the

second vessel and a negligible amount was found in the aqueous sodium
iodide trap. These observations parallel those experiments in which
unirradiated F_2/Ne (1% v/v) was bubbled through a series of two reaction
flasks containing 2'-UdR in glacial acetic acid. The first reaction
vessel in line exhibited a substantially higher concentration of
reaction product with respect to the second.

It was anticipated that the F_2-^{18}F produced was adsorbed on the
inner walls of the target assembly. Therefore, a second method to
increase the recovery of F_2-^{18}F was attempted. A constant volume
of F_2/Ne (1%) target gas was irradiated. After bombardment, a solution
of 2'-UdR in glacial acetic acid (5 mg/70 ml) was introduced directly
into the irradiation vessel to elute the F_2-^{18}F adsorbed on the inner
surfaces. During injection of the elution solvent, the target assembly
was vented through a small volume (5 ml) of the elution solvent to trap
any free F_2-^{18}F that might be forced out. The eluate was collected in
a reaction flask and allowed to stand with gentle agitation for thirty
minutes. Approximately 80 to 85% of the absolute radioactivity
produced was lost upon evaporation of the solvent, possibly in the
form of hydrogen fluoride. Analysis of the remaining sample by high
pressure liquid chromatography indicated that only 1 to 2% of this
radioactivity was present in the eluate. The eluate was monitored by
UV absorption (254 nm) and a gamma scintillation detector (NaI (Tl))
which revealed a peak of radioactivity corresponding to an elution
volume midway between FUdR and 2'-UdR (figure 17). This peak was
determined to represent 35% of the total eluted radioactivity. A
similar peak was observed during the fluorination of 2'-UdR with

F_2-^{19}F/Ne (1% v/v). This product may be explained as an unstable reaction intermediate or adduct which was found to give the desired FUdR-^{19}F upon treatment with ammonium hydroxide in methanol (5% v/v). This peak, representing 15 to 30 μCi of radioactivity, was collected, treated with ammonium hydroxide in methanol and reduced in volume to dryness in vacuo. The product was redissolved in normal saline, sterilized by millipore filtration and administered to a mouse bearing a Lewis lung carcinoma, for imaging.

D. RADIOCHEMICAL PURITY

The radiochemical purity of FUdR-6-^{3}H and FU-6-^{3}H was determined by thin layer chromatography on silica gel plates using three solvent systems of different polarity (Table 2). Both of the samples of FUdR-6-^{3}H conformed to the distributor's claim of 98% radiochemical purity. A range of 93.8 to 99.6% was determined experimentally with an overall mean value equal to 96.5%,;therefore, the FUdR-6-^{3}H was considered suitable for use without further purification.

The FU-6-^{3}H was not 96-97% radiochemically pure as claimed by the distributor, but was found to be 84.0 to 90.0% pure. This was not considered to be of adequate purity for experimental use and was subsequently purified by preparative thin layer chromatography. This procedure increased the mean value of the product's radiochemical purity from 87% to 96%. The 9% increase brought the FU-6-^{3}H within acceptable limits. Approximately 83% of the original FU-6-^{3}H was recovered in the final step of the chromatographic procedure. The radiochemical purity of each sample was calculated as the ratio of
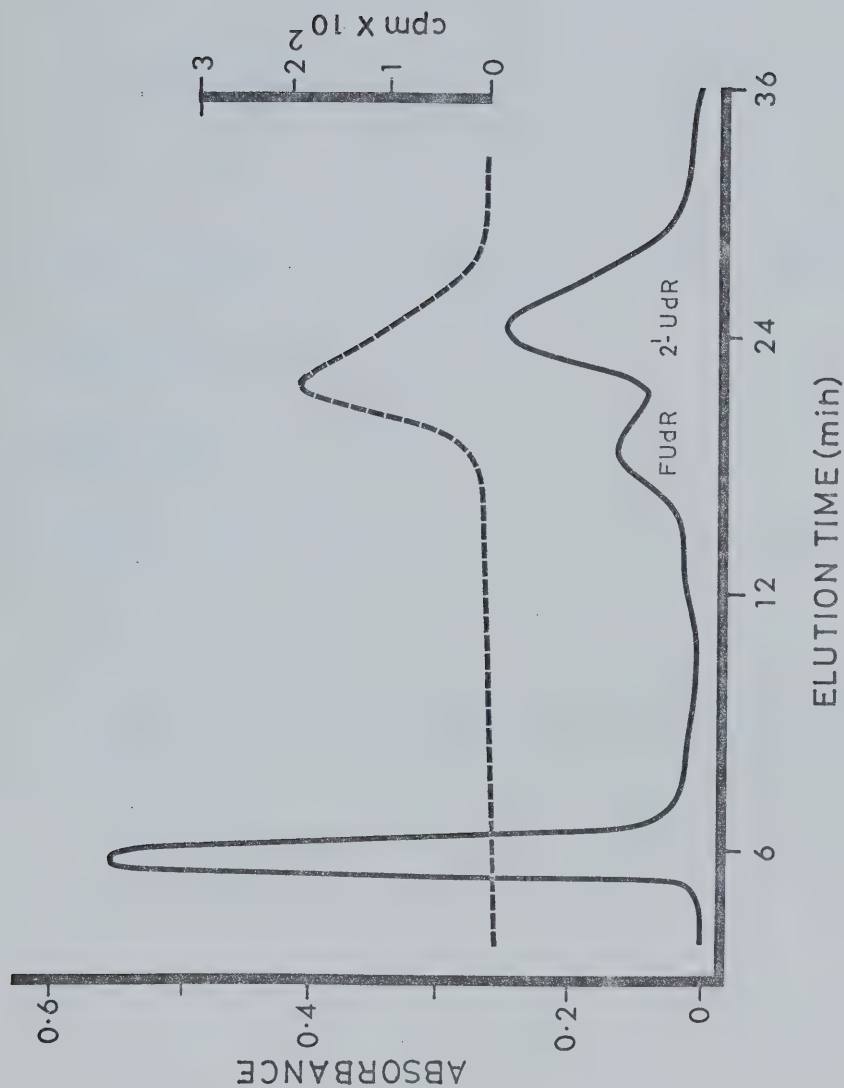
FIGURE 17

Ultraviolet absorption (———) and radiochromatograms (— —) of FUdR-5-^{18}F and reaction products after reaction of ^{18}F gas with 2'-UdR in glacial acetic acid. Separations were achieved by eluting a silica gel column with chloroform:ethanol (4:1 v/v) at a flow rate of 8.2 ml min^{-1}.

TABLE 2

Radiochemical Purity of 5-Fluoro-2'-Deoxyuridine-6-^{3}H
and 5-Fluorouracil-6-^{3}H [a]

| Solvent system | FUdR-6-^{3}H | | | FU-6-^{3}H | |
	Lot 1	Lot 1[b]	Lot 2	Impure[c] sample	Purified[d] sample
ethyl acetate - acetone (2:3 v/v)	99.6	94.1	93.8	90.0	93.4
ethyl acetate - water (100:3 v/v)	97.5	91.9	94.9	85.7	95.9
nButanol - water (saturated)	96.2	——	97.0	84.0	98.1

a. % calculated as radioactivity associated with the reference compound, divided by the radioactivity on the entire chromatogram.

b. Radiochemical purity after 1 year storage at 4°C.

c. Radiochemical purity prior to chromatographic purification.

d. Radiochemical purity after chromatographic purification.

the amount of radioactivity found on the silica gel segments corre-
sponding to the reference material to the total amount of radioactivity
found on the chromatogram. Background was subtracted from each sample
before calculations were made.

The tritiated compounds were diluted in normal saline to a
specific activity of approximately 10 μCi/ml and stored at 4°C. The
effect of these storage conditions on the first sample of FUdR-6-[3]H
was determined after one year. The radiochemical purity decreased
from a mean value of 97.7% to 93.0%.

Each set of three radiochromatograms of each tritiated compound was
autoradiographed. The autoradiogram of FU-6-^{3}H, after preparative thin
layer chromatographic purification, depicted in plate 1 is typical for
each compound. Radiochemical purity is indicated by the absence of expo-
sure at the origin and solvent front as well as the presence of only one
spot having a chromatographic mobility corresponding to the reference FU.

E.   TISSUE DISTRIBUTION

The tissue distribution of FUdR-6-^{3}H and FU-6-^{3}H was studied in
two tumor models: the Ehrlich ascites carcinoma and the Lewis lung car-
cinoma, as well as the appropriate controls. The results were expressed
as a per cent of the injected dose incorporated by each organ and the
relative tissue to blood and tissue to muscle ratios. The calculations
involving the bone marrow data were based on the assumption that the
bone marrow contributes approximately 20% of the total weight of the
femur[8]. The gastrointestinal tract (GIT) and muscle were calculated on
a per cent per gram dry weight of tissue basis while the other tissues
were on a per cent per total organ basis. Therefore, for comparative
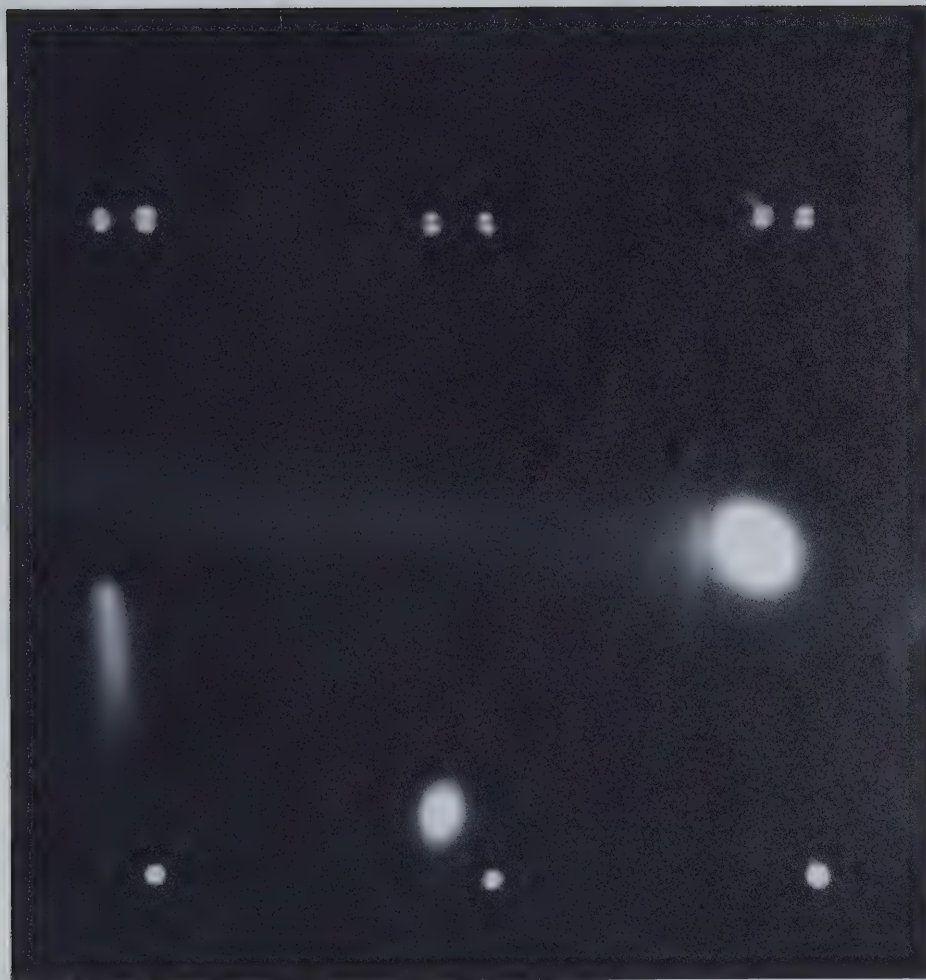
purposes the tumor uptake was calculated on both a gram of tissue and the entire tissue mass basis. The tissue distribution of the control animals was found to be identical to the tumor models and for this reason the control data has been included for comparison, but has not been discussed in detail to avoid unnecessary repetition.

1. Tissue Distribution of 5-Fluoro-2'-Deoxyuridine-6-^{3}H in the Ehrlich Ascites Carcinoma

After intravenous injection of FUdR-6-^{3}H, the radioactivity reached a maximum concentration in each tissue within fifteen minutes with the exception of the tumor and the gastrointestinal tract (Tables 3 and 4; figure 18). The liver concentrated up to 30% of the injected dose at 15 minutes and then the concentration steadily decreased to a value of 3% at 4 hours. The other tissues of interest exhibited peak levels at 15 minutes, concentrating less than 5% of the radio-activity. These levels declined to insignificant concentrations after approximately 2 hours. The gastrointestinal tract levels fluctuated considerably, due to very large standard deviations from the mean value for some of the time intervals; notably 1.0 and 4.0 hours. The gastrointestinal tract appears to have concentrated a large fraction of the radioactive dose quite rapidly and remained relatively constant, thereby not exhibiting the marked trend towards lower levels of radio-activity portrayed by the other tissues. The levels of radioactivity in the tumor mass peaked at 30 minutes and then decreased slowly throughout the time interval studied, following a pattern more closely related to the gastrointestinal tract than the other tissues.

TABLE 3

Tissue Incorporation After Injection of 5-Fluoro-2'-Deoxyuridine-6-^{3}H in Ehrlich Ascites Carcinoma[a,c]

Time (minutes) after administration

	15	30	60	120	180	240
Spleen	1.60 ± 0.70	1.60 ± 0.94	2.08 ± 1.05	2.88 ± 0.34	1.83 ± 0.82	2.37 ± 1.14
Liver	30.22 ± 6.82	22.09 ± 2.76	13.38 ± 6.12	6.48 ± 1.27	5.26 ± 2.45	3.05 ± 1.18
GIT [b] *	28.08 ± 6.26	26.93 ± 10.02	22.39 ± 13.70	29.22 ± 5.30	36.22 ± 3.45	20.99 ± 8.45
Muscle[b]	3.41 ± 0.82	1.78 ± 0.44	1.29 ± 0.44	1.13 ± 0.31	1.17 ± 0.29	0.72 ± 0.34
Kidney	4.25 ± 1.10	2.78 ± 0.29	3.12 ± 1.52	1.17 ± 0.21	0.84 ± 0.45	0.41 ± 0.13
BM *	0.24 ± 0.14	0.28 ± 0.12	0.31 ± 0.16	0.27 ± 0.06	0.30 ± 0.05	0.23 ± 0.11
Lung	0.29 ± 0.04	0.16 ± 0.03	0.13 ± 0.06	0.11 ± 0.03	0.06 ± 0.04	0.06 ± 0.02
Heart	0.14 ± 0.03	0.42 ± 0.32	0.05 ± 0.02	0.04 ± 0.01	0.03 ± 0.005	0.02 ± 0.008
Blood	2.73 ± 0.60	0.35 ± 0.12	0.80 ± 0.36	0.34 ± 0.05	0.29 ± 0.08	0.17 ± 0.08
Testes	0.11 ± 0.04	0.09 ± 0.06	0.06 ± 0.02	0.06 ± 0.02	0.05 ± 0.02	0.05 ± 0.02
Tumor	3.14 ± 1.67	2.64 ± 1.64	1.40 ± 0.49	3.16 ± 0.92	4.29 ± 1.01	2.12 ± 0.48
Tumor[b]	13.71 ± 4.06	16.20 ± 13.33	9.55 ± 2.47	9.80 ± 3.75	11.72 ± 6.57	6.75 ± 3.37
Stomach	0.60 ± 0.20	0.47 ± 0.17	0.50 ± 0.08	0.39 ± 0.11	0.57 ± 0.03	0.40 ± 0.24

a. Expressed as % dose per whole organ dry weight.

b. Expressed as % dose per gram tissue dry weight.

c. Each value is the mean ± standard deviation of 6 aminals.

* GIT - gastrointestinal tract; BM - bone marrow.

TABLE 4

Tissue Incorporation After Injection of 5-Fluoro-2'-Deoxyuridine-6-^{3}H in Swiss Albino Controls[a,c]

Time (minutes) after administration

	15	30	60	120	180	240
Spleen	0.74 ± 0.33	0.53 ± 0.13	0.80 ± 0.31	0.55 ± 0.28	0.49 ± 0.20	0.43 ± 0.15
Liver	31.02 ± 19.48	27.61 ± 6.15	11.21 ± 3.33	3.73 ± 2.73	1.45 ± 0.92	0.78 ± 0.52
GIT[b] *	29.96 ± 14.39	35.36 ± 9.91	29.32 ± 13.30	29.49 ± 5.49	20.52 ± 7.66	27.19 ± 9.68
Muscle[b]	5.05 ± 1.48	2.57 ± 1.28	1.56 ± 0.29	0.97 ± 0.55	0.85 ± 0.60	0.46 ± 0.34
Kidney	7.12 ± 1.70	5.01 ± 1.75	2.81 ± 0.43	0.92 ± 0.63	0.37 ± 0.17	0.28 ± 0.16
BM*	0.25 ± 0.06	0.22 ± 0.08	0.26 ± 0.09	0.15 ± 0.07	0.15 ± 0.05	0.12 ± 0.04
Lung	0.32 ± 0.07	0.28 ± 0.20	0.19 ± 0.08	0.07 ± 0.03	0.04 ± 0.02	0.05 ± 0.02
Heart	0.25 ± 0.08	0.11 ± 0.03	0.08 ± 0.02	0.03 ± 0.02	0.015± 0.005	0.015± 0.005
Blood	4.73 ± 0.68	2.06 ± 0.60	1.06 ± 0.35	0.38 ± 0.31	0.14 ± 0.09	0.11 ± 0.08
Testes	0.18 ± 0.04	0.13 ± 0.04	0.12 ± 0.06	0.10 ± 0.05	0.06 ± 0.02	0.05 ± 0.02
Stomach	0.89 ± 0.15	0.70 ± 0.21	0.82 ± 0.16	0.48 ± 0.28	0.40 ± 0.18	0.44 ± 0.21

a. Expressed as % dose per whole organ dry weight.

b. Expressed as % dose per gram tissue dry weight.

c. Each value is the mean ± standard deviation of 6 animals.

* GIT - gastrointestinal tract; BM - bone marrow.
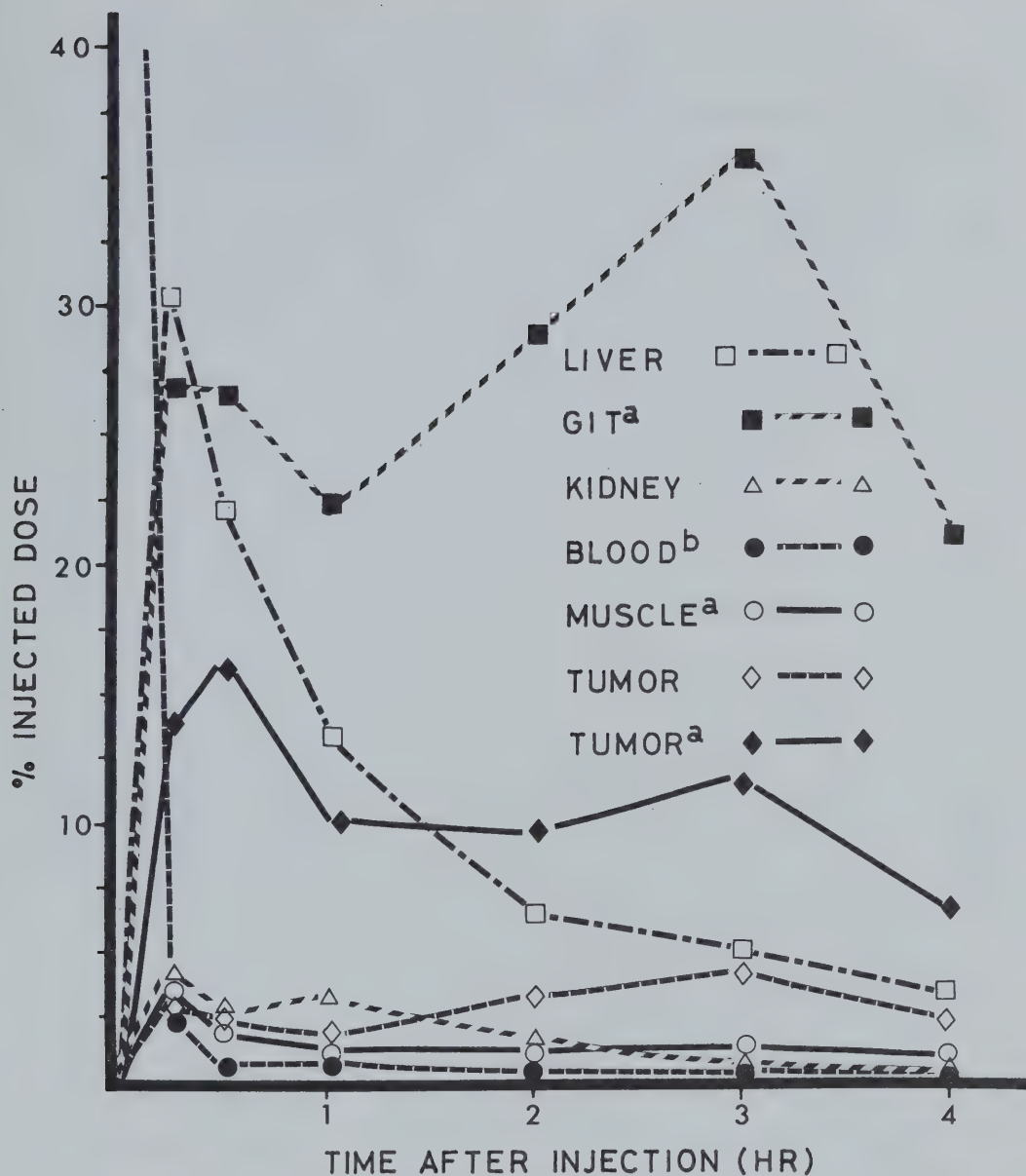
FIGURE 18

Tissue incorporation after injection of 5-fluoro-2'-deoxyuridine-6-^{3}H in Ehrlich ascites carcinoma. Expressed as % of injected dose per whole organ dry weight. Each determination is the mean of 6 animals.

a. Expressed as % of injected dose per gram tissue dry weight.

b. Expressed as % of injected dose per estimated total blood volume (1.5 ml) per mouse.

The testis, lung and tumor have a greater wet to dry weight ratio than the other tissues and the effect of these differences should be considered during interpretation of the tissue to blood and tissue to muscle ratios. The tissue to blood ratios in Table 5 demonstrated that the concentration of radioactivity was greatest in the tissues with high proliferation rates. The ratios of gastrointestinal tract and bone marrow to blood levels steadily increased suggesting active uptake of FUdR-6-^{3}H, whereas the liver and kidney seemed to remain at relatively constant levels with respect to the blood radioactivity. The tumor to blood ratio steadily increased reaching a plateau at approximately 2.5 hours and a maximum value of 17 at 3.0 hours. There was no significant difference between the tumor, liver and kidney to blood ratios at 4.0 hours.

The tissue to muscle ratios (Table 6) followed a pattern similar to the tissue to blood data, although of lesser magnitude. The gastro-intestinal tract, bone marrow and tumor showed steadily increasing ratios whereas the liver and kidney to muscle ratios reached a maximum at one hour and then declined. The tumor to muscle ratio peaked at 3 hours, reaching a level of 17 which is not significantly different from the kidney to muscle ratio. The initial high values in the liver and kidney were expected as they reflect the very fast metabolism and excretion of FUdR-6-^{3}H. The liver is the major metabolic site and the kidney is the major excretory route of the drug[35].

2.   Tissue Distribution of 5-Fluorouracil-6-^{3}H in the Ehrlich
     Ascites Carcinoma

The liver concentrated the greatest fraction of the radioactivity injected as FU-6-^{3}H with respect to the other tissues, reaching a

TABLE 5

Tissue to Blood Ratios After Injection of 5-Fluoro-2'-Deoxyuridine-6-^{3}H in Ehrlich Ascites Carcinoma[a,b]

Time (minutes) after administration

	15	30	60	120	180	240
Spleen	3.5 ± 1.1	33.1 ± 25.0	16.8 ± 11.6	33.2 ± 6.0	40.4 ± 9.5	86.7 ± 49.8
Liver	5.7 ± 1.9	37.2 ± 16.2	11.6 ± 7.8	9.5 ± 1.8	16.9 ± 10.1	10.5 ± 3.5
GIT*	3.6 ± 1.0	34.7 ± 22.4	15.3 ± 8.6	32.0 ± 8.6	49.6 ± 17.2	51.1 ± 20.2
Muscle	0.4 ± 0.1	2.1 ± 1.0	0.6 ± 0.2	1.1 ± 0.2	1.5 ± 0.2	1.6 ± 0.4
Kidney	8.3 ± 2.6	46.2 ± 24.1	19.8 ± 8.5	19.8 ± 5.1	16.5 ± 4.0	20.6 ± 14.1
BM*	3.2 ± 1.5	29.2 ± 19.8	11.0 ± 5.5	29.3 ± 4.4	31.3 ± 13.3	57.7 ± 23.7
Lung	0.9 ± 0.2	4.5 ± 2.5	1.4 ± 0.6	2.9 ± 0.4	2.2 ± 0.7	3.2 ± 0.8
Heart	0.6 ± 0.2	21.6 ± 21.0	0.8 ± 0.2	1.3 ± 0.2	1.0 ± 0.1	1.4 ± 0.3
Blood	1.0 ± 0.0	1.0 ± 0.0	1.0 ± 0.0	1.0 ± 0.0	1.0 ± 0.0	1.0 ± 0.0
Testes	0.8 ± 0.3	4.9 ± 3.6	1.6 ± 0.8	3.1 ± 1.0	2.9 ± 1.1	5.8 ± 2.7
Tumor	1.8 ± 0.3	15.4 ± 11.1	4.7 ± 1.3	10.5 ± 4.0	16.8 ± 11.1	16.4 ± 6.1
Stomach	1.4 ± 0.5	9.8 ± 4.8	4.4 ± 2.2	9.5 ± 2.9	14.6 ± 6.3	17.4 ± 8.2

a. Ratios calculated on dry tissue weight basis.

b. Each value is the mean ± standard deviation of 6 animals.

* GIT - gastrointestinal tract; BM - bone marrow.

TABLE 6

Tissue to Muscle Ratios After Injection of 5-Fluoro-2'-Deoxyuridine-6-^{3}H in Ehrlich Ascites Carcinoma[a],[b]

Time (minutes) after administration

	15	30	60	120	180	240
Spleen	8.6 ± 4.8	14.4 ± 6.5	27.0 ± 14.2	30.6 ± 9.4	28.0 ± 9.1	60.5 ± 43.6
Liver	12.9 ± 2.2	18.9 ± 5.8	20.7 ± 17.1	8.5 ± 1.8	11.5 ± 6.4	6.7 ± 1.5
GIT *	8.2 ± 1.2	15.2 ± 3.6	24.6 ± 9.7	28.8 ± 8.7	33.4 ± 8.7	32.7 ± 10.4
Muscle	1.0 ± 0.0	1.0 ± 0.0	1.0 ± 0.0	1.0 ± 0.0	1.0 ± 0.0	1.0 ± 0.0
Kidney	19.3 ± 6.5	22.0 ± 6.1	33.2 ± 12.4	18.0 ± 6.9	11.4 ± 3.6	13.4 ± 8.4
BM *	7.3 ± 2.4	12.8 ± 4.0	18.3 ± 7.6	26.6 ± 7.3	22.1 ± 10.3	36.6 ± 9.1
Lung	2.0 ± 0.3	2.1 ± 0.4	2.5 ± 1.0	2.6 ± 0.5	1.5 ± 0.6	2.1 ± 0.7
Heart	1.3 ± 0.3	8.0 ± 5.9	1.4 ± 0.5	1.1 ± 0.1	0.7 ± 0.1	0.9 ± 0.3
Blood	2.4 ± 0.8	0.6 ± 0.3	1.8 ± 0.6	0.9 ± 0.2	0.7 ± 0.1	0.7 ± 0.2
Testes	1.7 ± 0.4	2.0 ± 1.0	2.7 ± 1.0	2.8 ± 1.5	2.1 ± 0.8	3.7 ± 1.2
Tumor	4.2 ± 1.4	8.0 ± 6.0	7.9 ± 1.7	10.3 ± 4.1	16.7 ± 8.3	11.0 ± 5.6
Stomach	3.1 ± 0.7	4.7 ± 1.01	7.3 ± 3.0	8.6 ± 3.3	10.1 ± 4.3	12.6 ± 10.7

a. Ratios calculated on a dry tissue weight basis.

b. Each value is the mean ± standard deviation of 6 animals.

* GIT - gastrointestinal tract; BM - bone marrow.

maximum at 15 minutes after injection (Tables 7 and 8; figure 19). This was followed by a rapid loss of radioactivity, reaching a level comparable to the other tissues at 2 hours. The gastrointestinal tract did not incorporate as much radioactivity after injection of FU-6-^{3}H as it did after FUdR-6-^{3}H administration. The level of radioactivity in the kidney peaked at 30 minutes then subsequently decreased to reach a negligible level at 2 hours. The tumor reached a maximum rapidly after injection, which was maintained for approximately 1 hour before the level gradually subsided. The tumor incorporated a higher proportion of radioactivity than the muscle or gastrointestinal tract when compared on a per gram basis. When the tissues were compared on an uptake per organ basis, the liver was the only tissue to incorporate more radioactivity than the tumor mass. However, this may have changed with an increase in time as the slope of the line representing loss of radioactivity from the liver was greater than the slope for the tumor.

The tissue to blood ratios (Table 9) demonstrated the rapid clearance of radioactivity from the blood. The kidney maintained the highest tissue to blood ratio which correlates with the rapid excretion rate found for FU-6-^{3}H. The ratio of liver to blood reached a maximum at 15 minutes then slowly decreased in magnitude with time; possibly a reflection of the rapid metabolism of the drug. The tumor and bone marrow to blood ratios followed similar patterns exhibiting a slow increase with time. Four hours after the injection of FU-6-^{3}H, the liver, tumor and bone marrow had the same tissue to blood ratios, which were approximately 7 to 1.
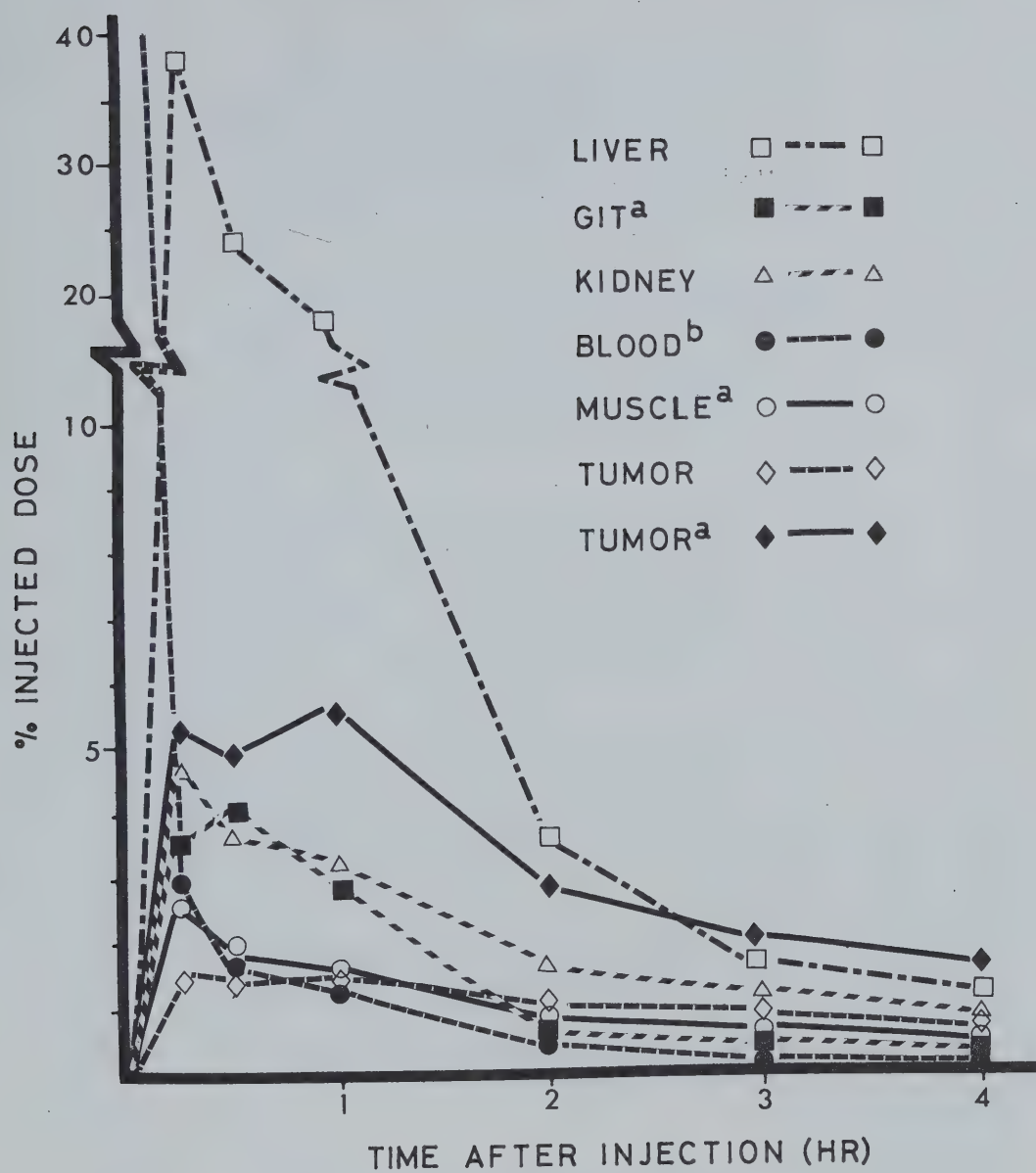
FIGURE 19

Tissue incorporation after injection of 5-fluorouracil-6-^{3}H in Ehrlich
Ascites carcinoma. Expressed as % of injected dose per whole organ
dry weight. Each determination is the mean of 6 animals.

a. Expressed as % of injected dose per gram tissue dry weight.

b. Expressed as % of injected dose per estimated total blood volume
   (1.5 ml) per mouse.

TABLE 7

Tissue Incorporation After Injection of 5-Fluorouracil-6-^{3}H in Ehrlich Ascites Carcinoma[a,c]

Time (minutes) after administration

	15	30	60	120	180	240
Spleen	0.22 ± 0.06	0.24 ± 0.07	0.20 ± 0.08	0.12 ± 0.02	0.10 ± 0.02	0.10 ± 0.03
Liver	37.72 ± 4.20	24.53 ± 6.24	15.99 ± 1.21	3.66 ± 1.14	1.86 ± 0.48	1.19 ± 0.57
GIT[b] *	4.47 ± 0.85	3.63 ± 0.89	3.13 ± 0.97	1.46 ± 0.63	1.19 ± 0.74	0.83 ± 0.38
Muscle[b]	2.55 ± 0.19	1.80 ± 0.55	1.75 ± 1.43	0.87 ± 0.45	0.89 ± 0.73	0.51 ± 0.21
Kidney	3.34 ± 0.61	3.99 ± 0.59	2.79 ± 0.50	0.77 ± 0.18	0.37 ± 0.11	0.21 ± 0.09
BM *	0.08 ± 0.02	0.06 ± 0.02	0.05 ± 0.01	0.03 ± 0.01	0.03 ± 0.02	0.025 ± 0.005
Lung	0.18 ± 0.02	0.17 ± 0.04	0.14 ± 0.04	0.05 ± 0.01	0.05 ± 0.02	0.04 ± 0.01
Heart	0.10 ± 0.02	0.07 ± 0.01	0.06 ± 0.01	0.02 ± 0.004	0.02 ± 0.004	0.02 ± 0.01
Blood	2.41 ± 0.83	1.51 ± 0.33	1.06 ± 0.56	0.28 ± 0.10	0.14 ± 0.04	0.14 ± 0.13
Testes	0.05 ± 0.01	0.06 ± 0.01	0.06 ± 0.04	0.02 ± 0.008	0.02 ± 0.01	0.02 ± 0.02
Tumor	1.45 ± 0.78	1.62 ± 0.45	1.28 ± 0.56	0.75 ± 0.33	0.58 ± 0.28	0.39 ± 0.16
Tumor[b]	5.31 ± 1.10	5.06 ± 1.08	5.71 ± 1.67	2.91 ± 0.74	2.08 ± 0.75	1.60 ± 0.41
Stomach	0.26 ± 0.05	0.19 ± 0.02	0.19 ± 0.04	0.08 ± 0.02	0.05 ± 0.02	0.05 ± 0.02

a. Expressed as % dose per whole organ dry weight.

b. Expressed as % dose per gram dry weight.

c. Each value is the mean ± standard deviation of 6 animals.

* GIT - gastrointestinal tract; BM - bone marrow.

TABLE 8

Tissue Incorporation After Injection of 5-Fluorouracil-6-^{3}H in Swiss Albino Controls[a,b,c]

Time (minutes) after administration

	15	30	60	120	180	240
Spleen	0.14 ± 0.02	0.07 ± 0.02	0.06 ± 0.02	0.04 ± 0.02	0.03 ± 0.004	0.03 ± 0.008
Liver	35.61 ± 5.18	23.45 ± 6.21	11.81 ± 4.04	4.16 ± 1.20	1.33 ± 0.39	0.55 ± 0.09
GIT[b]	5.40 ± 0.79	5.18 ± 1.15	3.48 ± 0.82	1.54 ± 0.44	1.00 ± 0.28	0.74 ± 0.42
Muscle[b]	2.84 ± 0.67	2.25 ± 1.24	1.77 ± 1.09	0.97 ± 0.16	0.53 ± 0.13	0.31 ± 0.08
Kidney	4.06 ± 0.40	3.59 ± 0.90	1.70 ± 0.70	0.60 ± 0.10	0.21 ± 0.03	0.11 ± 0.05
BM	0.08 ± 0.01	0.06 ± 0.02	0.05 ± 0.02	0.02 ± 0.004	0.02 ± 0.005	0.01 ± 0.004
Lung	0.22 ± 0.03	0.18 ± 0.05	0.11 ± 0.03	0.06 ± 0.02	0.04 ± 0.01	0.015± 0.005
Heart	0.13 ± 0.01	0.09 ± 0.02	0.05 ± 0.02	0.02 ± 0.004	0.01 ± 0.005	0.01 ± 0.001
Blood	2.72 ± 0.50	1.80 ± 0.46	0.70 ± 0.31	0.24 ± 0.10	0.33 ± 0.37	0.06 ± 0.02
Testes	0.07 ± 0.04	0.08 ± 0.07	0.03 ± 0.01	0.02 ± 0.005	0.02 ± 0.02	0.01 ± 0.004
Stomach	0.25 ± 0.03	0.19 ± 0.03	0.14 ± 0.05	0.08 ± 0.008	0.05 ± 0.005	0.03 ± 0.01

a. Expressed as % dose per whole organ dry weight.

b. Expressed as % dose per gram dry weight.

c. Each value is the mean ± standard deviation of 6 animals.

* GIT - gastrointestinal tract; BM - bone marrow.

TABLE 9

Tissue to Blood Ratios After Injection of 5-Fluorouracil-6-^{3}H in Ehrlich Ascites Carcinoma[a,b]

Time (minutes) after administration

	15	30	60	120	180	240
Spleen	0.6 ± 0.2	1.0 ± 0.3	1.3 ± 0.2	2.9 ± 0.9	4.8 ± 1.6	6.4 ± 3.1
Liver	9.7 ± 3.9	9.0 ± 1.9	9.2 ± 3.2	8.8 ± 3.6	8.4 ± 2.1	7.4 ± 2.4
GIT*	0.8 ± 0.5	0.9 ± 0.3	1.1 ± 0.2	2.0 ± 0.6	3.9 ± 3.4	3.8 ± 2.6
Muscle	0.4 ± 0.2	0.4 ± 0.1	0.5 ± 0.2	1.2 ± 0.7	2.5 ± 2.0	1.8 ± 1.0
Kidney	8.9 ± 3.4	14.7 ± 4.0	17.7 ± 8.6	18.1 ± 8.7	15.5 ± 0.9	25.9 ± 9.2
BM*	1.0 ± 0.4	1.6 ± 0.3	1.8 ± 0.4	4.0 ± 1.2	7.2 ± 4.4	7.4 ± 3.5
Lung	0.8 ± 0.3	1.0 ± 0.1	1.1 ± 0.4	1.9 ± 0.7	2.8 ± 0.8	2.8 ± 1.1
Heart	0.6 ± 0.2	0.6 ± 0.1	0.7 ± 0.2	1.1 ± 0.4	1.6 ± 0.4	1.8 ± 0.7
Blood	1.0 ± 0.0	1.0 ± 0.0	1.0 ± 0.0	1.0 ± 0.0	1.0 ± 0.0	1.0 ± 0.0
Testes	0.5 ± 0.2	0.6 ± 0.1	1.2 ± 0.7	1.3 ± 0.6	2.3 ± 1.1	4.8 ± 5.8
Tumor	0.9 ± 0.3	1.2 ± 0.2	2.1 ± 0.6	4.3 ± 1.8	6.5 ± 2.3	6.6 ± 2.9
Stomach	1.0 ± 1.2	0.8 ± 0.1	1.2 ± 0.4	2.1 ± 1.0	1.7 ± 1.0	3.4 ± 1.4

a. Ratios calculated on a dry tissue weight basis.

b. Each value is the mean ± standard deviation of 6 animals.

* GIT - gastrointestinal tract; BM - bone marrow.

The data on Table 10 represents the tissue to muscle ratios found after injection of FU-6-^{3}H. In general, the tissue to muscle ratios followed a similar pattern to the tissue to blood ratios; however a difference was noted for the kidney. The gradually increasing ratio found for the kidney to blood data was replaced by a rapid increase which reached a maximum at 30 minutes followed by a rapid decline. The gradual increase can be attributed to active absorption of the radioactivity into the kidney from the blood. The kidney to muscle ratios may have decreased because the kidney actively excreted the radioactivity more rapidly than the muscle could excrete it passively. The tumor to muscle ratios were somewhat higher than the gastrointestinal tract to muscle ratios, both reaching a maximum at 1 hour and staying relatively constant up to 4 hours after injection.

3. Tissue Distribution of 5-Fluoro-2'-Deoxyuridine-6-^{3}H in the Lewis Lung Carcinoma

The liver incorporated the largest fraction of the radioactivity injected as FUdR-6-^{3}H reaching a maximum of 22% in 15 minutes. However, this level rapidly decreased to below the values found for the gastrointestinal tract and tumor after 2 hours (Tables 11 and 12; figure 20). After 2 hours the tumor and gastrointestinal tract represented the greatest fraction of radioactivity on a per cent per gram basis with neither tissue bearing a significantly greater portion. Comparison of the tissues on a per cent per whole organ basis proved the tumor to have incorporated the largest fraction of the injected dose, reaching a plateau at approximately 4%. After 2 hours the kidney and blood contained relatively insignificant amounts of radioactivity.

TABLE 10

Tissue to Muscle Ratios After Injection of 5-Fluorouracil-6-^{3}H in Ehrlich Ascites Carcinoma[a,b]

Time (minutes) after administration

	15	30	60	120	180	240
Spleen	1.6 ± 0.2	2.4 ± 0.6	2.5 ± 0.8	2.7 ± 1.0	2.8 ± 1.6	3.7 ± 1.6
Liver	23.3 ± 2.4	21.9 ± 5.9	18.7 ± 3.2	7.9 ± 2.7	5.1 ± 3.0	4.6 ± 1.5
GIT*	1.8 ± 0.2	2.1 ± 0.5	2.3 ± 0.8	1.9 ± 1.2	2.1 ± 2.1	2.3 ± 1.9
Muscle	1.0 ± 0.0	1.0 ± 0.0	1.0 ± 0.0	1.0 ± 0.0	1.0 ± 0.0	1.0 ± 0.0
Kidney	21.6 ± 5.2	35.8 ± 11.7	34.9 ± 17.1	15.2 ± 5.2	9.4 ± 5.5	12.2 ± 6.6
BM*	2.5 ± 0.4	3.7 ± 0.7	3.5 ± 1.2	3.7 ± 1.3	4.9 ± 2.6	4.3 ± 1.5
Lung	1.9 ± 0.3	2.4 ± 0.6	2.3 ± 0.8	1.7 ± 0.4	1.6 ± 0.7	1.7 ± 0.6
Heart	1.4 ± 0.3	1.6 ± 0.3	1.5 ± 0.7	1.0 ± 0.1	0.9 ± 0.4	1.2 ± 0.6
Blood	2.7 ± 1.0	2.5 ± 0.6	2.0 ± 0.7	1.0 ± 0.5	0.6 ± 0.4	0.8 ± 0.6
Testes	1.1 ± 0.1	1.5 ± 0.3	2.5 ± 2.1	1.1 ± 0.2	1.2 ± 0.5	2.5 ± 2.6
Tumor	2.1 ± 0.5	3.0 ± 0.8	4.1 ± 1.3	3.7 ± 0.8	3.7 ± 2.3	3.9 ± 1.6
Stomach	1.9 ± 1.0	2.1 ± 0.4	2.4 ± 1.2	2.0 ± 0.4	1.7 ± 1.0	2.0 ± 0.5

a. Ratios calculated on a dry tissue weight basis.

b. Each value is the mean ± standard deviation of 6 animals.

* GIT - gastrointestinal tract; BM - bone marrow.

TABLE 11

Tissue Incorporation After Injection of 5-Fluoro-2'-Deoxyuridine-6-^{3}H in Lewis Lung Carcinoma[a,c]

Time (minutes) after administration

	15	30	60	120	180	240
Spleen	0.70 ± 0.36	0.85 ± 0.13	0.60 ± 0.43	0.65 ± 0.32	0.71 ± 0.40	1.20 ± 0.68
Liver	22.05 ± 15.31	14.22 ± 7.84	5.22 ± 1.04	1.79 ± 0.94	0.82 ± 0.50	0.65 ± 0.23
GIT*	31.00 ± 6.04	27.88 ± 17.36	27.46 ± 7.67	33.62 ± 3.64	28.31 ± 8.61	22.44 ± 7.84
Muscle[b]	5.64 ± 2.00	2.13 ± 0.52	0.93 ± 0.14	2.37 ± 3.05	0.67 ± 0.15	0.73 ± 0.21
Kidney	4.88 ± 0.64	4.21 ± 1.02	2.11 ± 0.95	0.52 ± 0.16	0.30 ± 0.07	0.26 ± 0.12
BM*	0.36 ± 0.16	0.34 ± 0.07	0.34 ± 0.12	0.23 ± 0.04	0.22 ± 0.07	0.32 ± 0.09
Lung	0.30 ± 0.10	0.24 ± 0.04	0.12 ± 0.05	0.07 ± 0.01	0.05 ± 0.01	0.06 ± 0.02
Heart	0.21 ± 0.03	0.12 ± 0.02	0.05 ± 0.02	0.04 ± 0.04	0.03 ± 0.01	0.02 ± 0.005
Blood	4.06 ± 1.50	2.34 ± 0.54	1.12 ± 0.63	0.36 ± 0.20	0.21 ± 0.08	0.21 ± 0.13
Testes	0.15 ± 0.02	0.14 ± 0.04	0.09 ± 0.02	0.08 ± 0.02	0.05 ± 0.01	0.07 ± 0.02
Tumor	3.70 ± 2.25	3.07 ± 1.74	5.38 ± 1.37	2.47 ± 1.16	4.38 ± 2.19	4.41 ± 1.79
Tumor[b]	31.67 ± 10.68	22.46 ± 4.44	25.31 ± 4.11	19.88 ± 10.53	23.25 ± 6.68	20.17 ± 3.65
Stomach	0.50 ± 0.17	0.31 ± 0.06	0.49 ± 0.55	0.21 ± 0.07	0.46 ± 0.33	0.17 ± 0.02

a. Expressed as % dose per whole organ dry weight.

b. Expressed as % dose per gram dry weight.

c. Each value is the mean ± standard deviation of 6 animals.

* GIT – gastrointestinal tract; BM – bone marrow.

TABLE 12

Tissue Incorporation After Injection of 5-Fluoro-2'-Deoxyuridine-6-^{3}H in BDF$_1$ Controls[a,c]

Time (minutes) after administration

	15	30	60	120	180	240
Spleen	0.32 ± 0.10	0.27 ± 0.19	0.26 ± 0.11	0.24 ± 0.08	0.20 ± 0.10	0.14 ± 0.05
Liver	30.98 ± 17.42	17.90 ± 11.45	9.63 ± 2.15	2.41 ± 1.89	1.18 ± 0.72	0.51 ± 0.26
GIT[b] *	35.70 ± 7.10	39.05 ± 23.31	42.67 ± 3.35	35.84 ± 9.40	36.96 ± 9.47	35.03 ± 4.55
Muscle[b]	5.18 ± 1.18	4.25 ± 3.76	1.61 ± 0.17	1.15 ± 0.29	2.77 ± 2.77	0.76 ± 0.44
Kidney	4.98 ± 0.43	3.13 ± 0.79	2.00 ± 0.74	0.64 ± 0.88	0.35 ± 0.22	0.19 ± 0.06
BM *	0.27 ± 0.08	0.24 ± 0.10	0.27 ± 0.06	0.23 ± 0.04	0.25 ± 0.07	0.15 ± 0.06
Lung	0.24 ± 0.08	0.18 ± 0.10	0.16 ± 0.04	0.04 ± 0.03	0.07 ± 0.06	0.02 ± 0.008
Heart	0.17 ± 0.02	0.08 ± 0.02	0.06 ± 0.01	0.04 ± 0.02	0.02 ± 0.008	0.01 ± 0.005
Blood	3.42 ± 1.56	4.10 ± 0.52	0.98 ± 0.12	0.38 ± 0.24	0.23 ± 0.07	0.12 ± 0.04
Testes	0.14 ± 0.01	0.09 ± 0.04	0.09 ± 0.04	0.06 ± 0.03	0.07 ± 0.04	0.06 ± 0.03
Stomach	0.44 ± 0.09	0.30 ± 0.07	0.29 ± 0.10	0.17 ± 0.04	0.31 ± 0.14	0.18 ± 0.09

a. Expressed as % dose per whole tissue dry weight.

b. Expressed as % dose per gram dry weight.

c. Each value is the mean ± standard deviation of 6 animals.

* GIT - gastrointestinal tract; BM - bone marrow.
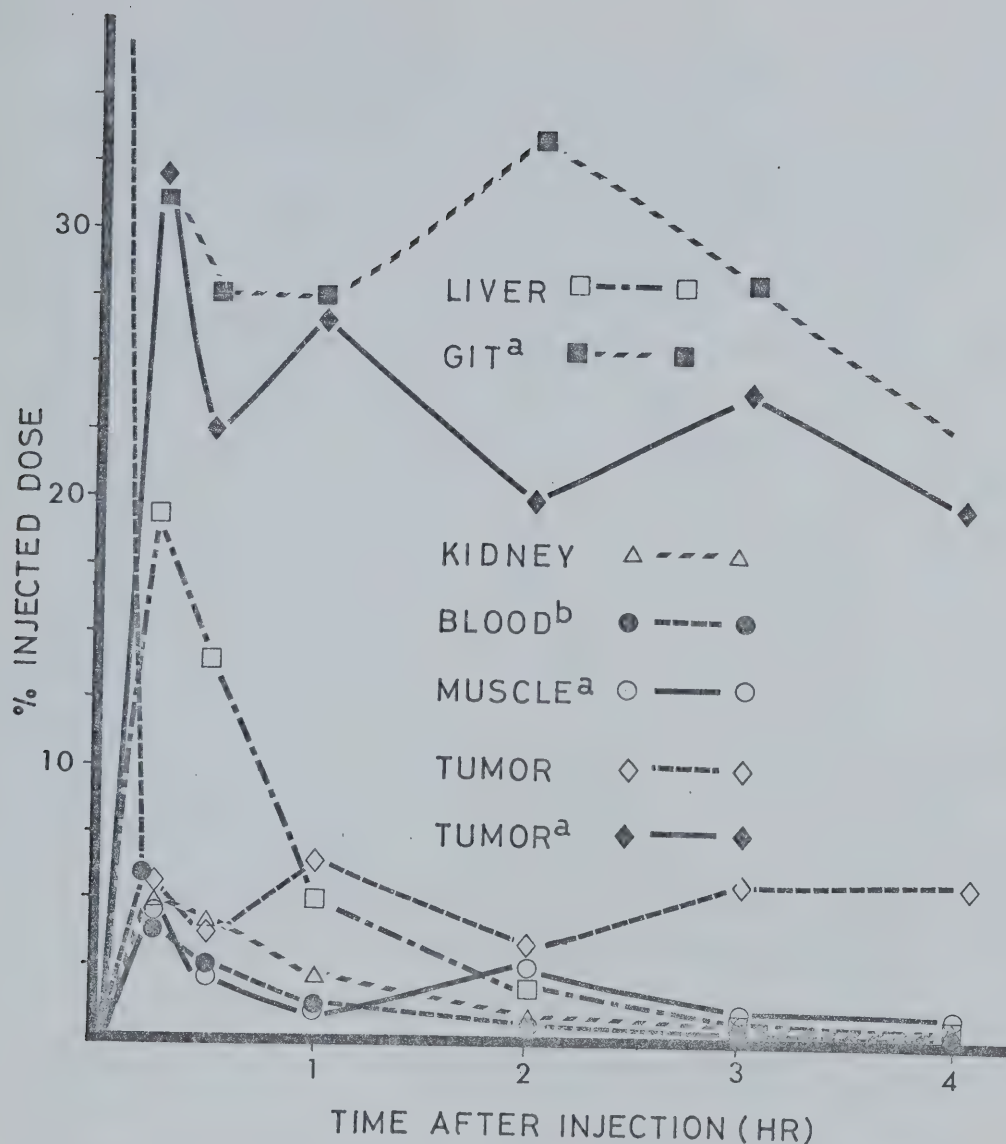
FIGURE 20

Tissue incorporation after injection of 5-fluoro-2'-deoxyuridine-6-^{3}H in Lewis lung carcinoma. Expressed as % of injected dose per whole organ dry weight. Each determination is the mean of 6 animals.

a. Expressed as % of injected dose per gram tissue dry weight.

b. Expressed as % of injected dose per estimated total blood volume (1.5 ml) per mouse.

The bone marrow, gastrointestinal tract and tumor to blood ratios exhibited steadily increasing values suggesting, as expected, incorporation of the radioactivity proportional to the proliferation rate of the tissues (Table 13). The relatively constant ratios found in the liver and kidney suggested that the activity found in these tissues was proportional to the blood concentration. After injection of FU-6-^{3}H, the kidney and liver to blood ratios were found to peak and decline rapidly. The difference in distribution patterns may be attributed to the more complex metabolism of FUdR relative to FU.

The more rapidly growing tissues, such as the gastrointestinal tract, bone marrow and tumor, were found to concentrate the radioactivity after the injection of FUdR-6-^{3}H to a greater extent than the muscle (Table 14). The tissue to muscle ratios for these tissues peaked between 2.5 and 3.0 hours after injection and then levelled off. The liver and kidney to muscle ratios reached a maximum at 1 hour which was followed by rapid loss of radioactivity, a pattern similar to the Ehrlich ascites model. The blood to muscle and muscle to blood ratios were almost constant suggesting that little active uptake of radioactivity by the muscle occurred and that the activity present may have been due primarily to blood circulating in the muscle tissue. This conjecture is supported by the observation that the muscle to blood ratio is a fraction of 1.

4.   Tissue Distribution of 5-Fluorouracil-6-^{3}H in the Lewis
     Lung Carcinoma Model

The fraction of the total radioactive dose of FU-6-^{3}H incorporated by the liver was approximately 30% at 15 minutes (Tables 15, 16;

94

TABLE 13

Tissue to Blood Ratios After Injection of 5-Fluoro-2'-Deoxyuridine-6-^{3}H in Lewis Lung Carcinoma[a,b]

| | Time (minutes) after administration | | | | | |
	15	30	60	120	180	240
Spleen	2.0 ± 0.4	3.7 ± 0.6	10.2 ± 5.0	21.6 ± 11.9	35.8 ± 12.4	61.7 ± 14.1
Liver	7.5 ± 2.6	7.6 ± 1.3	7.4 ± 2.7	7.5 ± 2.8	7.6 ± 2.2	10.2 ± 3.0
GIT*	3.0 ± 1.2	4.3 ± 2.8	11.4 ± 5.9	44.3 ± 21.9	64.0 ± 30.5	61.4 ± 40.8
Muscle	0.5 ± 0.1	0.3 ± 0.1	0.3 ± 0.1	3.7 ± 5.5	1.5 ± 0.6	1.6 ± 1.0
Kidney	9.1 ± 3.2	10.1 ± 2.9	13.5 ± 4.6	12.9 ± 4.4	13.1 ± 3.0	12.8 ± 3.7
BM*	3.9 ± 1.3	3.4 ± 2.2	13.9 ± 1.8	43.9 ± 20.3	62.6 ± 30.8	95.0 ± 43.6
Lung	0.9 ± 0.4	0.9 ± 0.2	1.2 ± 0.2	2.3 ± 0.8	3.3 ± 1.0	4.0 ± 1.6
Heart	0.6 ± 0.2	0.5 ± 0.1	0.6 ± 0.2	1.3 ± 0.5	1.6 ± 0.6	1.2 ± 0.5
Blood	1.0 ± 0.0	1.0 ± 0.0	1.0 ± 0.0	1.0 ± 0.0	1.0 ± 0.0	1.0 ± 0.0
Testes	0.8 ± 0.2	1.0 ± 0.2	2.0 ± 0.8	11.8 ± 17.4	————	7.7 ± 4.0
Tumor	3.4 ± 2.5	3.6 ± 0.8	8.3 ± 4.2	28.0 ± 20.2	52.5 ± 8.8	50.2 ± 22.5
Stomach	1.0 ± 0.4	1.2 ± 0.3	4.1 ± 4.4	8.4 ± 4.9	22.6 ± 18.6	12.8 ± 4.7

a. Ratios calculated on a dry tissue weight basis.

b. Each value is the mean ± standard deviation of 6 animals.

* GIT – gastrointestinal tract; BM – bone marrow.

TABLE 14

Tissue to Muscle Ratios After Injection of 5-Fluoro-2'-Deoxyuridine-6-^{3}H in Lewis Lung Carcinoma[a,b]

Time (minutes) after administration

	15	30	60	120	180	240
Spleen	4.0 ± 1.0	12.5 ± 3.9	32.8 ± 16.9	20.0 ± 14.4	26.7 ± 10.4	43.7 ± 15.2
Liver	14.8 ± 3.7	24.5 ± 1.3	22.3 ± 6.9	6.6 ± 5.0	5.6 ± 2.0	7.2 ± 3.2
GIT*	6.0 ± 1.9	13.5 ± 7.6	31.1 ± 7.6	34.5 ± 21.8	44.2 ± 15.5	36.8 ± 18.9
Muscle	1.0 ± 0.0	1.0 ± 0.0	1.0 ± 0.0	1.0 ± 0.0	1.0 ± 0.0	1.0 ± 0.0
Kidney	17.9 ± 4.0	30.7 ± 6.6	40.3 ± 10.2	11.4 ± 7.3	10.0 ± 4.0	8.9 ± 2.7
BM*	6.5 ± 2.2	8.9 ± 6.3	23.9 ± 2.0	30.2 ± 7.0	37.2 ± 6.6	33.0 ± 14.7
Lung	1.9 ± 1.1	2.7 ± 0.6	3.9 ± 1.4	2.1 ± 1.4	2.5 ± 1.0	2.6 ± 0.5
Heart	1.2 ± 0.2	1.7 ± 0.4	1.8 ± 0.4	1.6 ± 1.9	1.2 ± 0.7	0.8 ± 0.2
Blood	2.0 ± 0.4	3.3 ± 1.3	3.3 ± 1.6	1.1 ± 0.9	0.8 ± 0.3	0.8 ± 0.3
Testes	1.5 ± 0.4	3.0 ± 1.0	6.7 ± 5.6	3.6 ± 1.6	—	4.9 ± 2.5
Tumor	6.6 ± 4.0	11.3 ± 2.9	27.8 ± 3.0	22.4 ± 21.1	40.1 ± 14.3	33.3 ± 15.4
Stomach	2.1 ± 0.7	3.6 ± 0.7	13.0 ± 12.3	6.4 ± 4.6	14.5 ± 9.1	8.5 ± 2.0

a. Ratios calculated on a dry tissue weight basis.

b. Each value is the mean ± standard deviation of 6 animals.

* GIT – gastrointestinal tract;   BM – bone marrow.

figure 21). The following rapid loss of radioactivity may have been a function of the rapid metabolism of the drug. Little of the radio-activity was incorporated by the tumor mass at any time after injection. However, at 4 hours, it was found to have accumulated 0.2% of the injected dose, second only to the liver.

The tissue to blood ratios indicated that the bone marrow, gastrointestinal tract and tumor concentrated the radioactivity injected as FU-6-^{3}H from the blood more slowly than the activity injected as FUdR-6-^{3}H (Table 17). The kidney accumulated the radio-activity quickly reaching a maximum ratio within 30 minutes, which then rapidly decreased in value. The liver similarly reached a maximum ratio, levelled off and then showed a loss of radioactivity at a rate slower than the kidney. At 4 hours the tumor had a tissue to blood ratio of 11, which was not significantly different from either the kidney or the liver to blood ratios.

The tissue to muscle ratios of the liver and kidney, as expected, peaked quickly followed by a rapid decrease (Table 18). However the gastrointestinal tract and bone marrow to muscle ratios levelled off after 15 minutes and remained constant for the remainder of the study suggesting little active incorporation of the drug after the initial surge. The tumor reached a maximum at a slower rate than the bone marrow or gastrointestinal tract and indicated that an increase in tumor to muscle ratio may occur at longer time intervals after injection.

The results from the tissue distribution using FUdR-6-^{3}H and FU-6-^{3}H correlated quite well with the results obtained by Harbers

TABLE 15

Tissue Incorporation After Injection of 5-Fluorouracil-6-^{3}H in Lewis Lung Carcinoma[a,c]

Time (minutes) after administration

	15	30	60	120	180	240
Spleen	0.11 ± 0.02	0.12 ± 0.04	0.07 ± 0.02	0.04 ± 0.02	0.04 ± 0.02	0.02 ± 0.001
Liver	30.18 ± 5.62	16.03 ± 7.03	7.90 ± 1.50	2.29 ± 1.21	1.08 ± 0.65	0.63 ± 0.56
GIT[b]*	5.49 ± 0.71	4.47 ± 0.41	2.39 ± 0.22	1.15 ± 0.60	1.57 ± 1.96	0.56 ± 0.26
Muscle[b]	2.80 ± 0.72	2.03 ± 0.30	1.43 ± 0.12	1.16 ± 0.47	0.98 ± 0.69	0.42 ± 0.06
Kidney	5.25 ± 0.61	4.48 ± 0.75	1.54 ± 0.36	0.41 ± 0.13	0.20 ± 0.10	0.10 ± 0.05
BM*	0.09 ± 0.02	0.07 ± 0.01	0.04 ± 0.01	0.02 ± 0.004	0.02 ± 0.01	0.01 ± 0.001
Lung	0.26 ± 0.04	0.20 ± 0.03	0.12 ± 0.02	0.06 ± 0.04	0.04 ± 0.02	0.025 ± 0.005
Heart	0.13 ± 0.01	0.12 ± 0.06	0.04 ± 0.004	0.03 ± 0.01	0.02 ± 0.01	0.01 ± 0.004
Blood	2.73 ± 0.55	1.63 ± 0.45	0.63 ± 0.14	0.21 ± 0.08	0.21 ± 0.16	0.07 ± 0.02
Testes	0.05 ± 0.01	0.06 ± 0.03	0.03 ± 0.01	0.02 ± 0.01	0.02 ± 0.009	0.02 ± 0.005
Tumor	0.46 ± 0.34	1.00 ± 0.50	0.64 ± 0.41	0.48 ± 0.53	0.49 ± 0.53	0.19 ± 0.13
Tumor[b]	6.35 ± 1.79	6.38 ± 1.53	5.14 ± 0.85	3.85 ± 2.01	2.12 ± 1.39	1.75 ± 0.34
Stomach	0.17 ± 0.02	0.18 ± 0.05	0.09 ± 0.04	0.05 ± 0.01	0.04 ± 0.02	0.02 ± 0.005

a. Expressed as % dose per whole tissue dry weight.

b. Expressed as % dose per gram of tissue dry weight.

c. Each value is the mean ± standard deviation of 6 animals.

* GIT - gastrointestinal animals; BM - bone marrow.

TABLE 16

Tissue Incorporation After Injection of 5-Fluorouracil-6-^{3}H in BDF, Controls[a,c]

Time (minutes) after administration

	15	30	60	120	180	240
Spleen	0.08 ± 0.02	0.06 ± 0.01	0.05 ± 0.02	0.03 ± 0.004	0.02 ± 0.004	0.015 ± 0.005
Liver	31.52 ± 4.58	21.18 ± 5.02	10.57 ± 3.10	3.40 ± 2.67	0.82 ± 0.39	0.51 ± 0.18
GIT *	5.98 ± 0.44	4.98 ± 1.49	2.34 ± 0.57	1.04 ± 0.28	1.24 ± 0.80	0.51 ± 0.11
Muscle[b]	2.81 ± 0.28	2.36 ± 0.65	1.66 ± 0.54	0.88 ± 0.24	0.68 ± 0.23	0.81 ± 0.72
Kidney	6.14 ± 1.07	3.95 ± 0.49	2.02 ± 0.71	0.48 ± 0.21	0.14 ± 0.05	0.09 ± 0.04
BM *	0.09 ± 0.03	0.06 ± 0.005	0.06 ± 0.04	0.02 ± 0.004	0.015± 0.005	0.015 ± 0.008
Lung	0.28 ± 0.03	0.21 ± 0.02	0.13 ± 0.03	0.05 ± 0.01	0.03 ± 0.008	0.02 ± 0.005
Heart	0.15 ± 0.02	0.10 ± 0.02	0.05 ± 0.01	0.02 ± 0.008	0.02 ± 0.005	0.01 ± 0.004
Blood	2.44 ± 0.35	1.39 ± 0.13	0.61 ± 0.19	0.20 ± 0.06	0.12 ± 0.07	0.07 ± 0.02
Testes	0.06 ± 0.01	0.04 ± 0.006	0.06 ± 0.05	0.02 ± 0.004	0.02 ± 0.008	0.014 ± 0.005
Stomach	0.18 ± 0.03	0.15 ± 0.04	0.10 ± 0.02	0.05 ± 0.02	0.03 ± 0.008	0.02 ± 0.01

a. Expressed as % dose per whole tissue dry weight.

b. Expressed as % dose per gram tissue dry weight.

c. Each value is the mean ± standard deviation of 6 animals.

* GIT – gastrointestinal tract; BM – bone marrow.
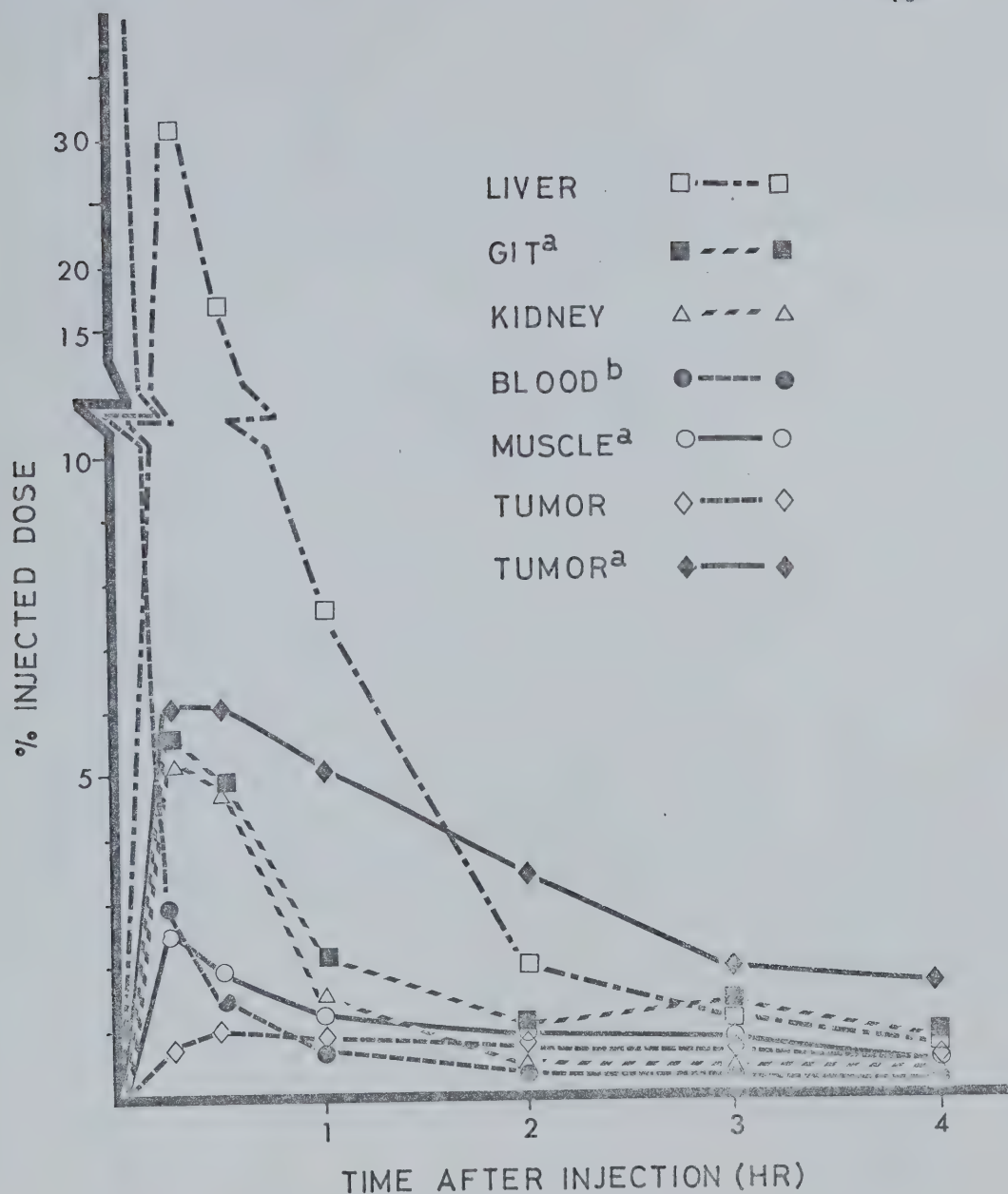
FIGURE 21

Tissue incorporation after injection of 5-fluorouracil-6-^{3}H in Lewis lung carcinoma. Expressed as % of injected dose per whole organ dry weight. Each determination is the mean of 6 animals.

a. Expressed as % of injected dose per gram tissue dry weight.

b. Expressed as % of injected dose per estimated total blood volume (1.5 ml) per mouse.

TABLE 17

Tissue to Blood Ratios After Injection of 5-Fluorouracil-6-^{3}H in Lewis Lung Carcinoma[a,b]

Time (minutes) after administration

	15	30	60	120	180	240
Spleen	0.5 ± 0.1	0.9 ± 0.2	1.2 ± 0.1	2.6 ± 0.9	2.6 ± 1.3	4.4 ± 1.6
Liver	9.9 ± 2.8	10.0 ± 5.1	11.2 ± 1.4	10.2 ± 3.9	6.2 ± 4.7	8.9 ± 4.4
GIT*	0.7 ± 0.1	1.0 ± 0.3	1.4 ± 0.2	2.1 ± 1.4	1.9 ± 0.9	3.5 ± 1.8
Muscle	0.4 ± 0.1	0.5 ± 0.1	0.8 ± 0.2	2.2 ± 1.0	2.1 ± 0.3	2.5 ± 0.6
Kidney	13.5 ± 3.1	21.3 ± 5.8	17.2 ± 2.5	16.4 ± 6.1	11.2 ± 5.4	12.4 ± 3.2
BM*	1.1 ± 0.2	1.7 ± 0.5	2.5 ± 0.8	3.4 ± 1.1	3.7 ± 1.3	5.6 ± 2.2
Lung	0.8 ± 0.1	1.2 ± 0.4	1.6 ± 0.5	2.9 ± 2.2	2.8 ± 1.5	3.3 ± 0.8
Heart	0.6 ± 0.1	0.8 ± 0.2	0.8 ± 0.2	1.5 ± 0.9	1.2 ± 0.5	2.0 ± 0.7
Blood	1.0 ± 0.0	1.0 ± 0.0	1.0 ± 0.0	1.0 ± 0.0	1.0 ± 0.0	1.0 ± 0.0
Testes	0.4 ± 0.0	0.6 ± 0.1	0.8 ± 0.2	2.4 ± 1.5	1.9 ± 0.8	3.7 ± 1.5
Tumor	0.8 ± 0.2	1.5 ± 0.5	3.0 ± 0.7	7.8 ± 4.8	5.7 ± 3.0	11.4 ± 3.6
Stomach	0.6 ± 0.1	0.9 ± 0.3	1.2 ± 0.3	2.0 ± 0.8	2.2 ± 1.0	

a. Ratios calculated on a dry weight basis.

b. Each value is the mean ± standard deviation of 6 animals.

* GIT - gastrointestinal tract; BM - bone marrow.

TABLE 18

Tissue to Muscle Ratios After Injection of 5-Fluorouracil-6-^{3}H in Lewis Lung Carcinoma[a,b]

Time (minutes) after administration

	15	30	60	120	180	240
Spleen	1.5 ± 0.3	1.9 ± 0.3	1.6 ± 0.4	1.3 ± 0.6	1.2 ± 0.6	1.7 ± 0.4
Liver	27.0 ± 5.8	21.1 ± 9.2	14.3 ± 2.9	5.5 ± 3.4	2.9 ± 2.2	3.6 ± 2.0
GIT*	2.0 ± 0.4	2.3 ± 0.3	1.7 ± 0.2	1.0 ± 0.4	0.9 ± 0.4	1.4 ± 0.5
Muscle	1.0 ± 0.0	1.0 ± 0.0	1.0 ± 0.0	1.0 ± 0.0	1.0 ± 0.0	1.0 ± 0.0
Kidney	38.0 ± 9.9	46.8 ± 11.5	22.3 ± 6.9	8.9 ± 5.4	5.2 ± 2.5	5.1 ± 1.5
BM*	3.2 ± 0.6	3.6 ± 0.6	3.0 ± 0.3	1.8 ± 0.9	1.7 ± 0.6	2.3 ± 0.6
Lung	2.3 ± 0.5	2.6 ± 0.3	2.0 ± 0.7	1.3 ± 0.6	1.3 ± 0.8	1.4 ± 0.2
Heart	1.6 ± 0.3	1.8 ± 0.5	1.0 ± 0.2	0.7 ± 0.4	0.6 ± 0.2	0.8 ± 0.2
Blood	2.9 ± 1.0	2.3 ± 0.5	1.3 ± 0.3	0.5 ± 0.2	0.5 ± 0.1	0.4 ± 0.1
Testes	0.9 ± 0.1	1.3 ± 0.6	1.1 ± 0.4	1.1 ± 0.5	0.9 ± 0.8	1.0 ± 0.0
Tumor	2.3 ± 0.5	3.2 ± 0.8	3.7 ± 0.8	3.6 ± 1.6	2.8 ± 1.3	2.3 ± 2.0
Stomach	1.7 ± 0.4	2.0 ± 0.4	1.5 ± 0.2	1.1 ± 0.7	1.0 ± 0.4	4.6 ± 0.9

a. Ratios calculated on a dry weight basis.

b. Each value is the mean ± standard deviation of 6 animals.

* GIT - gastrointestinal tract; BM - bone marrow.

et al.[26] and Chaudhuri et al.[39] using FUdR-2-^{14}C and FU-2-^{14}C. These workers demonstrated that FUdR-2-^{14}C gave higher tumor to tissue ratios than FU-2-^{14}C at each time period. In addition, they found that both of these drugs exhibited the highest concentration of radioactivity in the tumor compared to all the tissues studied at 24 hours post injection. Our results confirmed the superior incorporation of radioactivity injected as FUdR-6-^{3}H. However, at 4 hours the tumor did not have the highest concentration of radioactivity of all the tissues studied. In general, the liver and gastrointestinal tract had incorporated levels of radioactivity similar to the tumor 4 hours after injection of either compound. It is possible that at 24 hours the tumor would have exhibited the highest concentration of radioactivity of all the tissues, but if ^{18}F is to be used as the tracer, 4 hours would probably represent the maximum time available for practical purposes.

It should also be noted that significantly different experimental conditions were employed for the study using tritium as a tracer than the work using carbon-14. The specific activity of the ^{14}C labeled drugs was 4.1 μCi/mg for FU-2-^{14}C and 5.9 x 10^6 cpm/1.5 mg for FUdR-2-^{14}C which is much lower than the tritiated compounds which had specific activities of 9.4 mCi/mg of FUdR-6-^{3}H and 7.7 mCi/mg of FU-6-^{3}H. Therefore, the actual quantities in terms of drug mass injected for the ^{14}C tracer studies were much greater than the quantities used in the tritiated tracer experiments. The tumor models used in the two experiments were different with the ^{14}C labeled compounds studied in the Sarcoma 180 model and the ^{3}H labeled drugs examined in the Ehrlich ascites and Lewis lung

carcinoma models. The routes of injection were also different in that the FU-6-^{3}H and FUdR-6-^{3}H were injected intravenously and the FU-2-^{14}C and FUdR-2-^{14}C were administered by intraperitoneal injection. Therefore, direct comparison of the different experimental results must be made with caution, keeping the above variables in mind.

Specifically, the results indicated rapid uptake of a large quantity of radioactivity in the liver in the four models studied, an observation readily explained by the fact that the liver is the main site of metabolism of both FU and FUdR. The high concentrations in the kidney found in all four models was expected and can be explained by the rapid excretion of both compounds via the renal system as demonstrated in the excretion studies.

The radioactivity due to injection of FUdR-6-^{3}H was generally incorporated into the more rapidly proliferating tissues, such as the gastrointestinal tract, bone marrow and tumor, to a greater degree than was found after injection of FU-6-^{3}H. This may be explained through examination of the anabolic and catabolic pathways of the two fluorinated pyrimidines. FUdR is catabolized more slowly than FU as it must be freed of the deoxyribose sugar moiety before it can undergo enzymatic reduction of the pyrimidine nucleus. There-fore, even after the first catabolic step, FUdR is still available as FU while FU has been reduced to 5,6-dihydro-5-fluorouracil after its first catabolic step and is not available to the enzymes as a substrate for FdUMP synthesis. The anabolic pathway for the conver-sion of FUdR to FdUMP is a one step phosphorylation by Thymidine Kinase[43], while FU must be converted to FUMP by Phosphoribosyl

Transferase and then to FdUMP by a Ribonucleotide Reductase via the dinucleotide, FUDP, intermediate. Therefore, FUdR is available longer as a substrate and more readily converted to the active monophosphate FdUMP, than is FU.

In order for any radiopharmaceutical to be of use in the evaluation of malignant cell viability, it must be incorporated to a significant extent by the tumor cells and preferably exhibit a high tissue to background ratio. However, because the location of the tumor will be known, this ratio does not need to be as great as the ratio necessary for an imaging agent. The high uptake of FU-6-^{3}H and FUdR-6-^{3}H by the liver and gastrointestinal tract precludes the use of either compound for working with tumors in the abdominal region. The use of FUdR-5-^{18}F may be feasible for malignancies located in the chest region as indicated by the tumor to lung and heart ratios of 11 and 38 respectively and the tumor to blood and muscle ratios of 50 and 33 respectively, found in the Lewis lung carcinoma model 4 hours after injection of FUdR-6-^{3}H. Tumor to blood and muscle ratios of 17 and respective ratios of 5 and 12 for the tumor to lung and heart ratios, 4 hours after injection of FUdR-6-^{3}H in the Ehrlich ascites tumor model are less encouraging. The ratios after injection of FU-6-^{3}H into the Lewis lung model were 3, 6, 11 and 5 for the tumor to lung, heart, blood and muscle respectively and were 2, 3, 7 and 4 in the Ehrlich ascites carcinoma model.

These results would suggest that the use of FUdR-5-^{18}F may be preferential to FU-5-^{18}F as an alternative or adjuvant to the IUdR-5-^{131}I currently being considered for use in the evaluation of tumor

therapy. Further work must be considered to determine if a correlation between the uptake of FUdR-5-^{18}F and cell viability exists and is exploitable for this purpose.

5. Subcellular Distribution

The data in Table 19 illustrates the results of preliminary studies on the subcellular distribution of the radioactivity in the liver after injection of FUdR-6-^{3}H and FU-6-^{3}H in Swiss albino mice. The liver was chosen since previous work by Chaudhuri[35] demonstrated that this organ was the major site of catabolism of the fluorinated pyrimidines. This metabolic process is carried out by the enzymes present in the 105,000 g supernatant. Our data indicated that the major portion of the radioactivity was associated with the soluble enzyme fraction. This suggested the possibility that the rapid uptake of radioactivity by the liver was due to rapid metabolism of the FU-6-^{3}H and FUdR-6-^{3}H and the subsequent decline in radioactivity due to clearance of the metabolites by the blood and their urinary excretion. It would be interesting to determine the cellular distribution of the radioactivity of the gastrointestinal tract and tumor mass as it has been reported that some tumors cannot metabolize the fluorinated pyrimidines[26,35]. This, however, was beyond the scope of the present project.

F. URINARY AND FECAL EXCRETION OF 5-FLUORO-2'-DEOXYURIDINE-6-^{3}H

The excretion rate of FU and FUdR was evaluated using the tritiated analogs, FU-6-^{3}H and FUdR-6-^{3}H in two different tumor

TABLE 19

Subcellular Distribution of Radioactivity in the Liver[a,b]

	FU-6-^{3}H		FUdR-6-^{3}H	
	$\overline{X}$	SD	$\overline{X}$	SD
105,000 g supernatant	6077.7 ±	1932.5	5854.7 ±	981.7
105,000 g pellet	428.0 ±	93.8	477.7 ±	45.6
10,000 g pellet	433.7 ±	118.7	389.3 ±	39.9
700 g pellet	1268.0 ±	149.0	1160.3 ±	303.0

a. Three ICR mice at each data point.

b. Expressed as dpm per mg protein, one hour after intravenous injection.

models, viz; the Lewis lung carcinoma in male BDF_1 hybrid mice and
solid Ehrlich ascites carcinoma in male Swiss albino mice. Six mice
in each group were administered, via intravenous injection, 0.64 µCi
FU-6-^{3}H or 0.83 µCi FUdR-6-^{3}H in 0.1 ml normal saline. The excreted
matter, both urine and feces, was prepared for analysis by oxidation
of each sample to H_2O-^{3}H with a Packard Tricarb 306 tissue sample
oxidizer and counted on a Searle Mark III liquid scintillation
spectrometer. The results were expressed as the per cent of the
administered dose, excreted cumulatively, during each time period
up to 84 hours after injection (Table 20).

The radioactivity injected as either FU-6-^{3}H or FUdR-6-^{3}H was
rapidly excreted in the urine. The feces contained very little of
the recovered radioactivity, confirming a similar observation made by
Chaudhuri[39]. Within 24 hours, 75 to 85% of the radioactivity injected
as FU-6-^{3}H and approximately 70% of the radioactivity injected as
FUdR-6-^{3}H had been found in the excreted samples. This data corre-
lates well with Chaudhuri[39] who reported that 88% of the radioactivity
injected as FU-2-^{14}C had been recovered in 24 hours and Harbers et al.[26]
who observed an excretion of 70% of the radioactivity injected as
FUdR-2-^{14}C within 24 hours. Both authors derived their results from
female Swiss albino mice. An examination of the tissue distribution
data indicates that the radioactivity injected as FUdR-6-^{3}H was
concentrated in the gastrointestinal tract of each of the four animal
models to a greater extent than the FU-6-^{3}H and seemed to remain
relatively stable at that level during the four hour time interval
examined. The other tissues incorporated similar levels of

radioactivity after injection of either compound. This observation may partially account for the lesser amount of radioactivity excreted upon injection of FUdR-6-^{3}H than was accumulated after injection of FU-6-^{3}H during the first 24 hours.

The excretion curves (figures 22 to 25) revealed two components for both compounds, a rapid excretion of radioactivity within the first 6 hours after injection, followed by a gradual decline to a slow elimination component which appeared to be linear after 24 hours. Visual comparison of the curves suggested a slower rate of elimination of radioactivity from the Ehrlich models than from the controls. These curves were drawn using the mean values of six animals at each data point as found in Table 19.

The biological half-lives tabulated in Table 21 were calculated from the slope of each of the two components of the excretion curve of each individual mouse. These were then quoted as the mean ± the standard deviation of 6 animals for each group. The individual half-life values for the rapid component of the curve were also subjected to a completely random designed analysis of variance test to determine the variability within and between each treatment group. The error mean square derived from this test was used to compare the eight treatment groups by means of the Duncan's Multiple Range Test. This analysis suggested that at the 1% level of confidence, the excretion rate of the radioactivity from the Ehrlich model injected with either FU-6-^{3}H or FUdR-6-^{3}H was significantly slower than the excretion rate from the other six treatment groups. The other six treatment groups were not significantly different from each other and neither were the

TABLE 20

Cumulative Urinary and Fecal Excretion After Intravenous Injection of
5-Fluoro-2'-Deoxyuridine-6-^{3}H and 5-Fluorouracil-6-^{3}H[a,b]

Time (Hrs)	5-FUdR-6-^{3}H				5-FU-6-^{3}H			
	BDF_1	LLCa	ICR	EAC	BDF_1	LLCa	ICR	EAC[c]
1	28.3 ± 23.8	20.6 ± 22.1	10.9 ± 16.7	6.9 ± 15.6	34.4 ± 20.7	49.3 ± 6.6	6.0 ± 14.7	0.07 ± 0.03
3	42.3 ± 22.0	52.5 ± 5.8	44.1 ± 24.1	6.9 ± 15.6	54.1 ± 7.8	56.7 ± 12.4	36.9 ± 40.8	0.1 ± 0.1
6	60.3 ± 7.7	60.0 ± 7.1	63.3 ± 5.7	16.3 ± 25.6	62.0 ± 9.8	70.4 ± 9.7	77.2 ± 12.7	17.3 ± 38.0
12	64.2 ± 6.9	62.1 ± 7.5	68.2 ± 7.8	56.6 ± 10.4	70.5 ± 9.9	76.3 ± 5.1	81.1 ± 12.8	81.0 ± 9.5
24	69.6 ± 4.4	70.4 ± 3.4	72.7 ± 6.1	70.8 ± 4.9	73.9 ± 5.4	79.0 ± 3.8	85.8 ± 10.1	87.6 ± 7.2
36	71.6 ± 4.4	72.2 ± 3.6	75.3 ± 6.4	74.4 ± 5.1	74.4 ± 5.3	79.2 ± 3.7	86.3 ± 9.8	88.4 ± 7.1
48	75.8 ± 3.9	76.3 ± 3.4	78.5 ± 6.0	78.2 ± 5.1	76.1 ± 4.5	79.8 ± 3.5	86.6 ± 9.9	88.8 ± 7.2
60	77.6 ± 3.8	77.7 ± 3.7	80.2 ± 5.9	80.2 ± 5.6	76.4 ± 4.5	79.9 ± 3.5	86.8 ± 9.8	89.1 ± 7.1
72	80.1 ± 3.0	80.0 ± 3.5	81.7 ± 5.4	82.3 ± 5.6	76.8 ± 4.6	80.4 ± 3.3	87.2 ± 9.5	89.3 ± 7.1
84	80.9 ± 3.0	80.8 ± 3.5			76.9 ± 4.6	80.5 ± 3.3		

a. Data expressed as % of total injected dose ± standard deviation.

b. Six animals per data point.

c. Five animals per data point.
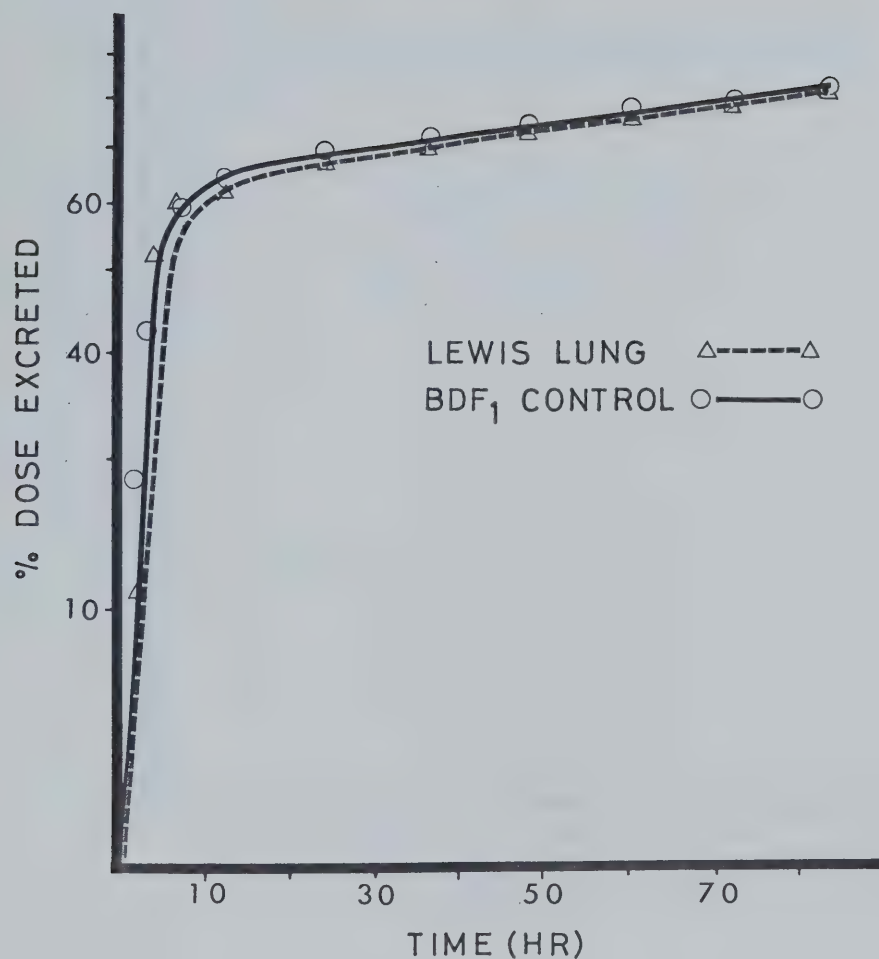
FIGURE 22

Excretion of 5-fluoro-2'-deoxyuridine-6-^{3}H from Lewis lung carcinoma and BDF$_1$ control animals. Each determination is the mean of 6 animals. The FUdR-6-^{3}H was injected intravenously via the dorsal vein.
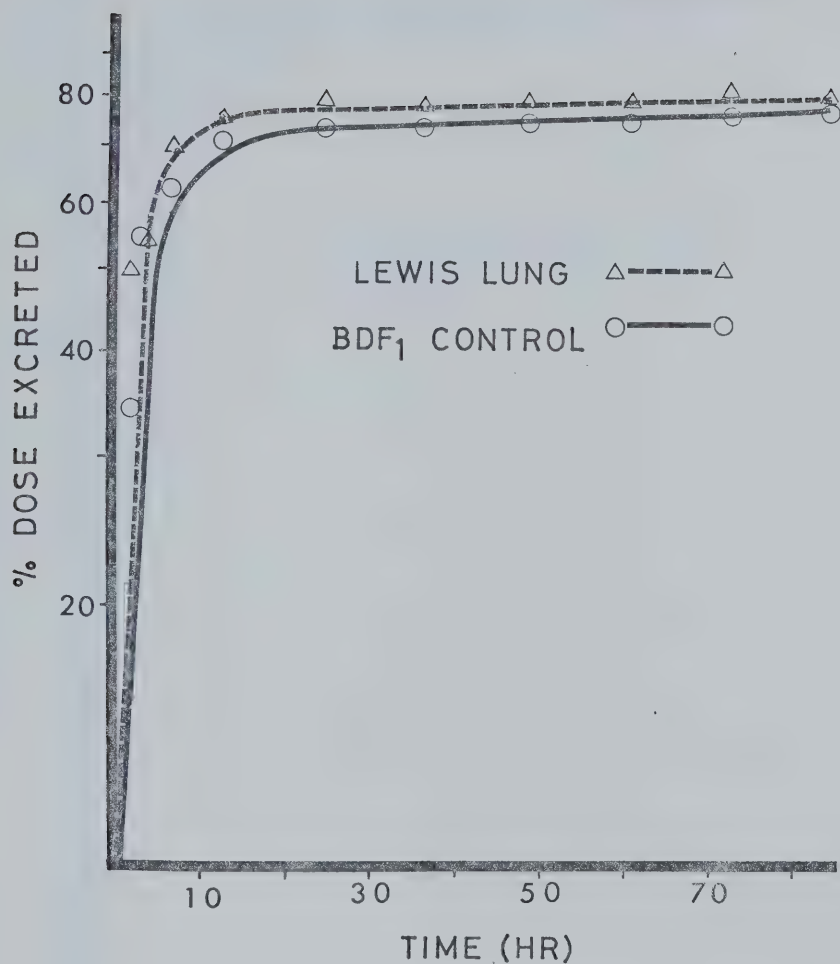
FIGURE 23

Excretion of 5-fluorouracil-6-^{3}H from Lewis lung carcinoma and BDF$_1$ control animals. Each determination is the mean of 6 animals. The FU-6-^{3}H was injected intravenously via the dorsal vein.
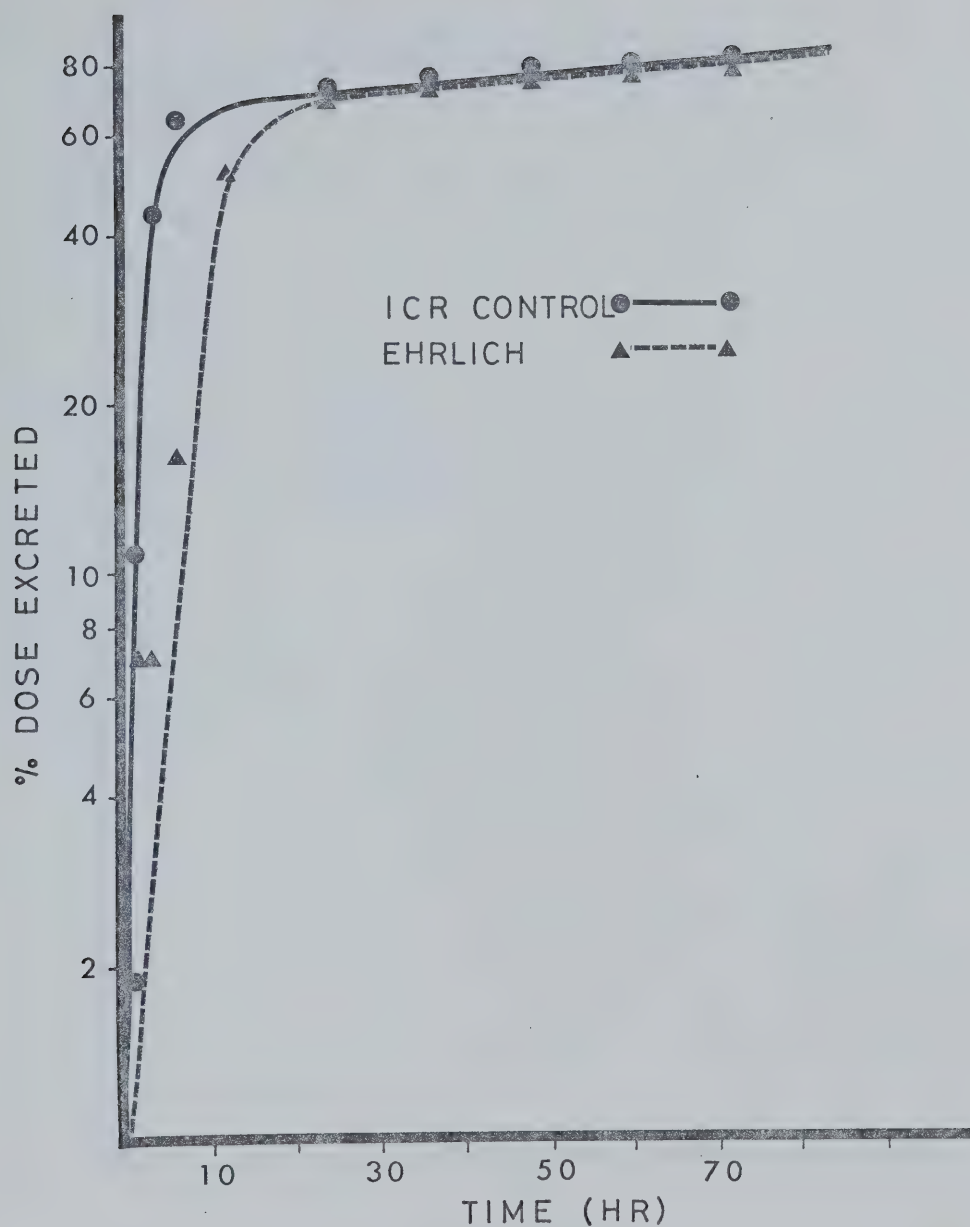
FIGURE 24

Excretion of 5-fluoro-2'-deoxyuridine-6-^{3}H from Ehrlich ascites
carcinoma and ICR control animals. Each determination is the mean
of 6 animals. The FUdR-6-^{3}H was injected intravenously via the
dorsal vein.
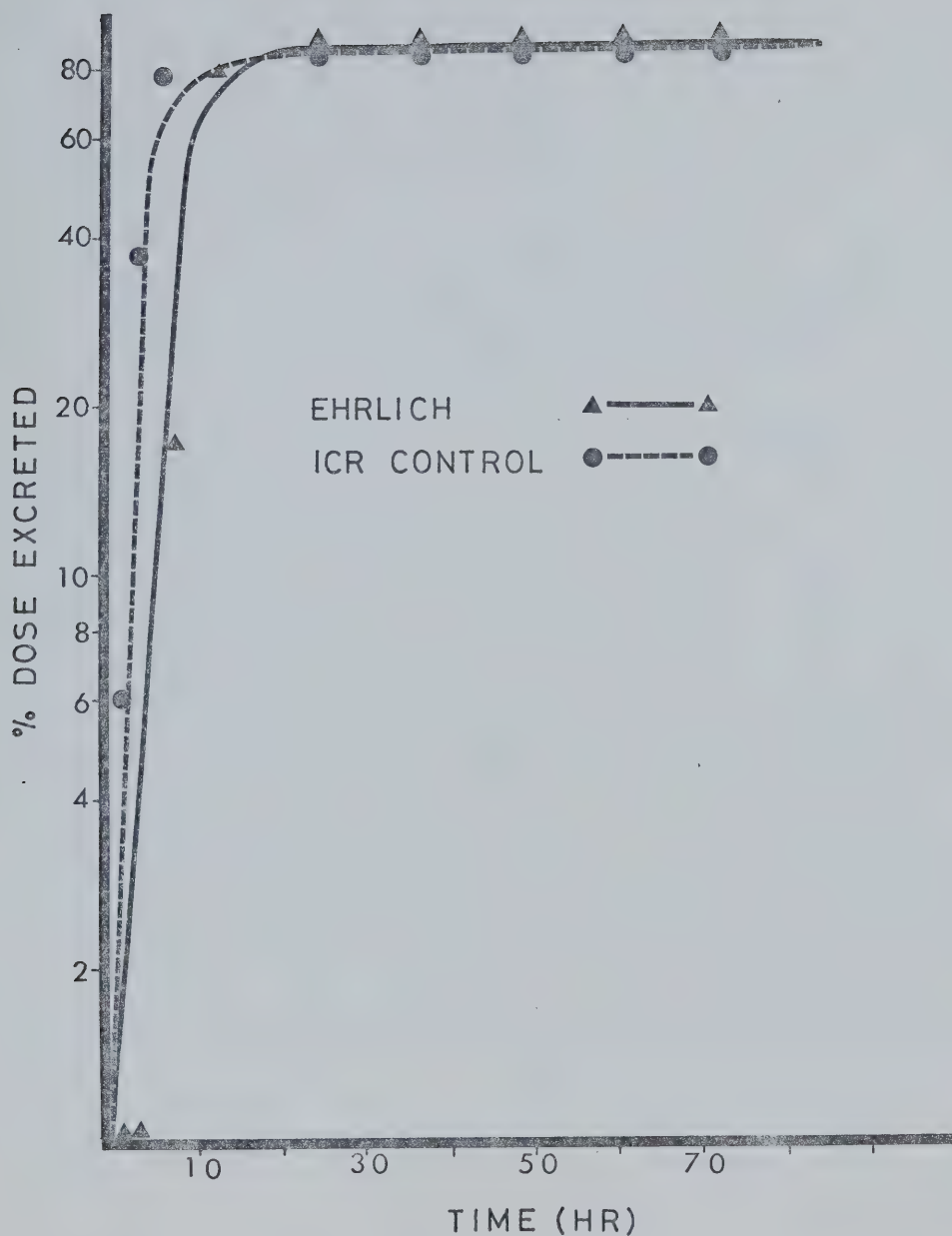
FIGURE 25

Excretion of 5-fluorouracil-6-^{3}H from Ehrlich ascites carcinoma and ICR control animals. Each determination is the mean of 6 animals. The FU-6-^{3}H was injected intravenously via the dorsal vein.

TABLE 21

5-Fluoro-2'-Deoxyuridine-6-^{3}H and 5-Fluorouracil-6-^{3}H
Biological Half-Lives[a,b]

Tumor Model	Short Component[d]		Long Component	
	FUdR-6-^{3}H	FU-6-^{3}H	FUdR-6-^{3}H	FU-6-^{3}H[c]
ICR	1.3 ± 0.4	1.3 ± 0.5	73.2 ± 4.5	127.8 ± 44.2
EAC	3.8 ± 1.6	2.9 ± 0.5	49.4 ± 7.9	288.6 ± 57.7
BDF,	1.2 ± 0.3	1.6 ± 0.7	79.7 ± 5.1	260.0 ± 54.4
LLCa	1.1 ± 0.3	1.5 ± 0.7	80.1 ± 8.4	337.0 ± 83.6

a. Values in hours

b. Six values per data point

c. Five values per data point

d. Manually calculated from computer data

two Ehrlich models different from each other. The observation that Ehrlich ascites carcinoma cells cannot appreciably metabolize FU-2-^{14}C or FUdR-2-^{14}C [40] may be reflected in the slower excretion rates found for the tritiated analogs from the Ehrlich model.

Similar analysis of the slow excretion component of the curve suggested that after injection of FU-6-^{3}H, the excretion rate of radioactivity is slower from each model than the excretion rate of the radioactivity associated with FUdR-6-^{3}H from the same models. This may be a reflection of the more complex metabolism of FUdR with respect to FU. It was explained previously that FUdR may be utilized by cells to a greater degree than FU since it is more readily converted to FdUMP and is available as a useful substrate for a longer period of time[43].

Another factor contributing to this difference in excretion rates may be associated with the enhanced concentration of radioactivity in the gastrointestinal tract after injection of FUdR-6-^{3}H when compared with that found for FU-6-^{3}H. Since more activity remained to be excreted during the longer time intervals, the slope of the long lived component of the excretion curve for FUdR-6-^{3}H was steeper than the slope observed for FU-6-^{3}H. This may have been reflected as a shorter long term excretion component for FUdR-6-^{3}H.

The radiation dose to a patient due to the administration of ^{18}F labeled FU or FUdR is a function of the effective half-life (T_E) of the radioactive compound. This term includes both the physical half-life (T_P) and the biological half-life (T_B) of the radiopharmaceutical, expressed as:

$$T_E = \frac{(T_p)(T_B)}{T_p + T_B} \qquad (2)$$

Considering the short physical half-life of ^{18}F (109.7 minutes), excretion during the first 12 hours after administration of FU-5-^{18}F or FUdR-5-^{18}F would be the most important as the radioactivity present at the end of that time, due to physical decay alone, would be only 1/64 of the initial dose. The effective half-life, calculated using the mean biological half-life from Table 21 for the short lived component of the curve, was found to be approximately 0.92 hours for both FUdR-5-^{18}F and FU-5-^{18}F.

The urinary metabolites of FU-2-^{14}C and FUdR-2-^{14}C have been studied extensively[26,35-40,44,105,106]. Chaudhuri reported that 50% of the total activity in the urine 4 hours after intraperitoneal injection of FUdR-2-^{14}C into Swiss mice, was present as the unmetabolized parent species and 38% of the activity was present in the original chemical form 12 hours after intraperitoneal injection of FU-2-^{14}C. The results of thin layer chromatographic analysis of the urine excreted after intravenous injection of FUdR-6-^{3}H and FU-6-^{3}H into Swiss albino mice are given in Table 22. After 1 hour 15% of the FUdR-6-^{3}H and 10% of the FU-6-^{3}H remained unmetabolized. Partial explanation for the differences in the rates of metabolism may be found in a comparison of the specific activities and actual quantities of the compound injected, as well as the different routes of administration used in the two experiments. The ^{14}C labeled compounds were injected intraperitoneally in doses of 1.5 mg of FUdR-2-^{14}C (3.9×10^6 cpm/mg) and 4.5 mg of FU-2-^{14}C (4.1 μCi/mg)

TABLE 22

Chromatographic Excretion Analysis[a,b,c]

Drug Admin.	Solvent System	Origin	FUdR	5FU	Residual
5-Fluoro-2'-deoxyuridine-6-[3]H	Ethyl Acetate : Water (100/3 v/v)	77.0	14.8	3.6	4.6
	Ethyl Acetate : Acetone (2/3 v/v)	77.4	10.5	2.9	9.2
	nButanol : Water (saturated)	83.2	5.4	3.6	7.8
5-Fluorouracil-6-[3]H	Ethyl Acetate : Water (100/3 v/v)	88.6	1.3	8.4	1.7
	Ethyl Acetate : Acetone (2/3 v/v)	81.7	2.1	11.9	4.3
	nButanol : Water (saturated)	87.2	5.2	5.8	1.8

a. Silica gel thin layer chromatography

b. Pooled data of 3 male ICR mice

c. Expressed as % of recovered radioactivity per entire chromatogram

per mouse. The tritiated analogs were injected intravenously in substantially lower doses, using 1.8×10^{-4} mg of FUdR-6-^{3}H (9.4 mCi/mg) and 1.6×10^{-4} mg of FU-6-^{3}H (7.7 mCi/mg) per animal These observations suggest that the larger dose of ^{14}C labeled compounds may have been metabolized at a slower rate due to a mass effect and possible saturation of the enzyme sites. In addition, the tritiated analogs would reach the liver and enter the metabolic pathway more quickly via intravenous injection than the ^{14}C labeled compounds which were injected intraperitoneally.

No attempt was made to isolate or identify the metabolites of either FUdR-6-^{3}H or FU-6-^{3}H. The identity of the recovered unmetabolized substrate was based on the chromatographic mobilities of the urine components compared with known standards in three different solvent systems. The concentration of the metabolites recovered was too low to allow chemical analysis by conventional means.

V. SUMMARY

1. a. A fast and efficient method for the synthesis of FUdR-5-^{19}F
        and FU-5-^{19}F, in respective chemical yields of 56 and 58%,
        was developed utilizing elemental fluorine.

    b. Rapid separation of the desired product from the crude
        reaction mixture was accomplished via a modified high pressure
        liquid chromatographic (HPLC) technique, allowing collection
        of FU within 15 minutes and FUdR within 35 minutes.

2. Recoil synthesis of FUdR-5-^{18}F was found to be unsuitable, due
    to the production of a large percentage of thermal degradation
    and radiolysis products. Some components of this mixture were
    tentatively identified chromatographically as uracil, 2'-UdR,
    FUdR-5-^{18}F and possibly some FU-5-^{18}F. In addition, the radio-
    chemical yields of FUdR-5-^{18}F were low, averaging 0.5% of the
    theoretical expectation.

3. a. The continuous flow reaction proved to be unsuitable for
        labeling 2'-UdR with ^{18}F. When deuteron irradiated F_2/Ne
        (1% v/v) gas was slowly purged through a solution of 2'-UdR
        in glacial acetic acid, a low chemical yield of FUdR-5-^{19}F
        (23%) was observed but no FUdR-5-^{18}F was detected.

    b. When a constant static volume of F_2/Ne (1% v/v) was
        bombarded with deuterons followed by elution of the
        adsorbed F_2-^{18} from the irradiation chamber with 2'-UdR
        in glacial acetic acid, a low yield of FUdR-5-^{18}F (1%
        radiochemical) was observed via HPLC.

    c. Chemical analysis of the reaction mixture in b, prior to
        HPLC analysis, indicated that 92.1% of the ^{18}F in solution

was present in a chemical form which would react with $CaCl_2$
to precipitate as $CaF_2-^{18}F$.

d. Initial attempts to determine the recovery of $F_2-^{18}F$ with
a continuous flow of F_2/Ne (1% v/v) resulted in yields of
$10 \pm 5\%$.

e. Elution of the target vessel with aqueous KF (20% w/v) or
$LiBF_4$ (20% w/v) gave recoveries of $70 \pm 10\%$ and $50 \pm 10\%$
of the fluoride ion respectively.

These observations, a through e, suggested that the ^{18}F was not
available as $F_2-^{18}F$ in sufficient concentration for efficient
radiofluorination of 2'-UdR. This was attributed to adsorption
of the $F_2-^{18}F$ produced, onto the large inner surface area of the
irradiation vessel-reaction chamber system. This is supported
by the observation that no FUdR-5-^{18}F was detected upon reaction
of a continuous flow of irradiated F_2/Ne (1% v/v) gas with
2'-UdR, however a radiochemical yield of approximately 1% was
observed when the adsorbed $F_2-^{18}F$ was eluted with the reaction
solution. The low concentration of scavenger $F_2-^{19}F$ gas in the
neon target gas may have been too low to promote efficient
production of $F_2-^{18}F$. This is supported by the low radiochemical
yield obtained upon elution of the adsorbed $F_2-^{18}F$.

4. a. The tumor and gastrointestinal tract of both tumor models
incorporated a greater concentration of radioactivity
injected as FUdR-6-^3H when compared with FU-6-^3H.

b. The tumor to blood, muscle, lung, and heart ratios for the
Lewis lung carcinoma model were 50, 33, 11 and 38 respec-
tively 4 hours after intravenous injection of FUdR-6-^3H.

c. The tumor to blood, muscle, lung and heart ratios for the
    Lewis lung carcinoma model were 11, 5, 3 and 6 respectively
    4 hours after intravenous injection of FU-6-^{3}H.

d. The tumor to blood, muscle, lung and heart ratios for the
    Ehrlich ascites carcinoma model were 17, 17, 5 and 12 res-
    pectively 4 hours after intravenous injection of FUdR-6-^{3}H.

e. The tumor to blood, muscle, lung and heart ratios for the
    Ehrlich ascites carcinoma model were 7, 4, 2 and 3 respec-
    tively 4 hours after intravenous injection of FU-6-^{3}H.

f. In general the tumor, gastrointestinal tract and liver
    were found to have incorporated similar levels of radio-
    activity injected as FUdR-6-^{3}H within 4 hours in both tumor
    models. The data for FU-6-^{3}H was essentially the same.

These observations indicated that FUdR-5-^{18}F may be more useful
than FU-5-^{18}F for determining tumor viability. This is supported
by the larger tumor to tissue ratios obtained after injection of
FUdR-6-^{3}H and the greater incorporation, as per cent of injected
dose, of FUdR-6-^{3}H by the tumor with respect to FU-6-^{3}H. The
high liver and gastrointestinal tract incorporation of FUdR-6-^{3}H
suggested that tumors in the chest cavity region would be most
suitable for this radiopharmaceutical.

5. a. During the initial excretion phase, FUdR-6-^{3}H and FU-6-^{3}H
        were found to be excreted at a significantly slower rate
        from the Ehrlich ascites tumor than the other three models.
        This was thought to be due to the inability of Ehrlich
        ascites cells to metabolize either FU or FUdR.

b. During the second excretion component, FUdR-6-^{3}H was shown
    to be excreted at a faster rate than FU-6-^{3}H. This may be
    attributed to the more complex metabolism and enhanced
    incorporation by the gastrointestinal tract, of FUdR with
    respect to FU.

c. The effective half-lives for FUdR-5-^{18}F and FU-5-^{18}F were
    calculated from the biological half-lives found for the
    tritiated analogs in mice. Only the initial phase of
    excretion was considered in the calculation. A value of
    approximately 0.92 hours was found for both ^{18}F labeled
    compounds.

d. One hour after injection of FUdR-6-^{3}H, 15% of the radio-
    activity in the urine was identified chromatographically
    as the unmetabolized parent compound and 10% of the
    radioactivity in the urine, 1 hour after injection of
    FU-6-^{3}H was present as non-metabolized substrate.

6. Use of the Ehrlich ascites carcinoma model will be discon-
tinued in favor of tumors with more favorable biochemical and physical
properties.

VI. BIBLIOGRAPHY

1. Hofer, K.G., Prensky, W. and Hughes, W.L.: Death and Metastatic Distribution of Tumor Cells in Mice Monitored with ^{125}I-Iododeoxyuridine. J. Nat. Cancer Inst. <u>163</u>: 13, 1969.

2. Hofer, K.G.: Tumor Cell Death In Vivo After Administration of Chemotherapeutic Agents. Cancer Chemotherapy Repts. <u>273</u>: 53, 1969.

3. Hofer, K.G. and Hughes, W.L.: Incorporation of Iododeoxyuridine-^{125}I into the DNA of L1210 Leukemia Cells During Tumor Development. Cancer Res. <u>236</u>: 30, 1970.

4. Hughes, W.L., Commerford, S.L., Gitlin, D., Krueger, R.C., Schultze, B., Shah, U. and Reilly, P.: Deoxyribonucleic acid Metabolism <u>In Vivo</u>: I. Cell Proliferation and Death as Measured by Incorporation and Elimination of Iododeoxyuridine. Federation Proc. <u>23</u>: 640, 1964.

5. Feinendegen, L.E., Bond, V.P., and Hughes, W.L.: ^{125}I-DU (5-Iodo-2'-Deoxyuridine) in Autoradiographic Studies of Cell Proliferation. Exp. Cell Res. <u>43</u>: 107, 1966.

6. Jenkinson, I.S., Shuter, B.J. and Wright, P.N.M.: Cell Kinetics Methods for Clinical Use: Assessment of Autoradiography and ^{125}I-Iodo-Deoxyuridine with Mouse Ehrlich Tumors. Cell Tissue Kinet. <u>8</u>: 307, 1975.

7. Begg, A.C. and Fowler, J.F.: A Rapid Method for the Determination of Tumor RBE. Brit. J. Radiol. <u>47</u>: 154, 1974.

8. Rotenberg, A.D., Bruce, W.R. and Baker, R.G.: Incorporation of 5-Iododeoxyuridine-^{131}I in Spontaneous C3H Mouse Mammary Tumors. Brit. J. Radiol. <u>35</u>: 337, 1962.

9. Schuhmacher, J., Kampmann, H., Mattern, J., Volm, M., Wayss, K. and Zimmerer, J.: Incorporation of ^{131}Iododeoxyuridine into the DNA of Tumour-bearing Rats after Partial Synchronization as a Tool in Scintigraphic Tumour Localization. Nucl. Med. <u>12</u>: 309, 1974.

10. Hampton, E.G. and Eidenoff, M.L.: Administration of 5-Iodo-deoxyuridine-I^{131} in the Mouse and Rat. Cancer Res. <u>21</u>: 345, 1961.

11. Fidler, I.J.: Metastasis: Quantitative Analysis of Distribution and Fate of Tumour Emboli Labeled with ^{125}I-5-Iodo-2'-Deoxyuridine. J. Nat. Cancer Inst. <u>45</u>: 773, 1970.

12. Merits, I. and Cain, J.C.: DNA Labeled with 5-[^{131}I]Iodo-2'-Deoxyuridine and 5-[^{82}Br]bromo-2'-Deoxyuridine. Biochim. Biophys. Acta. <u>209</u>: 327, 1970.

13. Fossati, G., Holden, H. and Herberman, R.: Evaluation of the Cell-mediated Immune Response to Murine Sarcoma Virus by [^{125}I]Iododeoxyuridine Assay and Comparison with Chromium 51 and Microcytotoxicity Assays. Cancer Res. 35: 2600, 1975.

14. Porteous, D.D. and Munro, T.R.: The Kinetics of the Killing of Mouse Tumor Cells In Vivo by Immune Responses. Intern. J. Cancer 10: 112, 1972.

15. Stirrat, G.M.: A Terminal-labelling Microcytotoxicity Assay with ^{125}I-Iododeoxyuridine as a Label for Target Cells. J. Immunol. Methods 12: 201, 1976.

16. Vogel, H.H., Zaldiver, R.: Cocarcinogenesis: The Interaction of Chemical and Physical Agents. Radiation Res. 47, 644, 1971.

17. Green, J.A. and Baron, S.: 5-Iododeoxyuridine Potentiation of the Replication In Vitro of Several Unrelated RNA and DNA Viruses. Science 180: 1099, 1975.

18. Szybalski, W.: X-Ray Sensitization by Halopyrimidines. Cancer Chemotherapy Rept. 58: 539, 1974.

19. Penman, B.W., Wong, M. and Thilly, W.G.: Mutagenicity of 5-Halodeoxyuridines to Diploid Human Lymphoblasts. Life Sci. 19: 563, 1976.

20. Bloomer, W.D. and Adelstein, S.J.: Antineoplastic Activity of Iodine-125 Labeled Iododeoxyuridine. J. Nucl. Med. 16, 516, 1975.

21. Prusoff, W.H., Holmes, W.L. and Welch, A.D.: Nonutilization of Radioactive Iodinated Uracil, Uridine, and Orotic Acid by Animal Tissues In Vivo. Cancer Res. 13: 221, 1953.

22. Welch, A.D. and Prusoff, W.H.: Synopsis of Recent Investigations of 5-Iodo-2'-Deoxyuridine. Cancer Chemotherapy Rept. 6: 29, 1961.

23. Heidelberger, C., Griesbach, L., Montag, B., Mooren, D., Cruz, O., Schnitzer, R.J. and Grunberg, E.: Studies on Fluorinated Pyrimidines. II. Effects on Transplanted Tumors. Cancer Res. 18, 305, 1958.

24. Duschinsky, R., Pleven, E. and Heidelberger, C.: The Synthesis of 5-Fluoropyrimidines. J. Am. Chem. Soc. 79: 4559, 1957.

25. Henderson, J.F. and Paterson, A.R.P.: "Nucleotide Metabolism. An Introduction." Academic Press, New York and London, 1973, Chapter 11.

26. Harbers, E., Chaudhuri, N.K. and Heidelberger, C.: Studies of Fluorinated Pyrimidines. VIII. Further Biochemical and Metabolic Investigations. J. Biol. Chem. 234: 1255, 1958.

27. Hartmann, K.U. and Heidelberger, C.: Studies on Fluorinated Pyrimidines. XIII. Inhibition of Thymidylate Synthetase. J. Biol. Chem. 236: 3006, 1961.

28. Santi, D.V., Pena, V.A. and Lam, S.S.M.: On the Structure of the Cofactor in the Complex formed with Thymidylate Synthetase, 5,10-Methylenetetrahydrofolate and 5-Fluoro-2'-Deoxyuridylate. Biochim. Biophys. Acta 438: 324, 1976.

29. Leary, R.P., Beaudette, N. and Kisliuk, R.L.: Interaction of Deoxyuridylate with Thymidylate Synthetase. J. Biol. Chem. 250: 4864, 1975.

30. Heidelberger, C., Birnie, G.D., Boohar, J. and Wentland, D.: Fluorinated Pyrimidines. XX. Inhibition of the Nucleoside Phosphorylase Cleavage of 5-Fluoro-2'-Deoxyuridine by 5-Trifluoromethyl-2'-Deoxyuridine. Biochim. Biophys. Acta 76: 315, 1963.

31. Heidelberger, C. and Ansfield, F.S.: Experimental and Clinical Use of Fluorinated Pyrimidines in Cancer Chemotherapy. Cancer Res. 23: 1226, 1963.

32. Heidelberger, C., Sunthankar, A.V., Griesbach, L. and Randerson, S.: Fluorinated Pyrimidines. XII. Effects of Simple Nucleotides on Transplanted Tumors. Proc. Soc. Exp. Biol. Med. 104: 127, 1960.

33. Mukherjee, K.L. and Heidelberger, C.: Inhibition of the Incorporation of Formate-C^{14} into DNA Thymine of Ehrlich Ascites Carcinoma Cells by 5-Fluoro-2'-Deoxyuridine-5'-Monophosphate and Related Compounds. Cancer Res. 22: 815, 1962.

34. Mukherjee, K.L., Curreri, A.R., Jauid, M. and Heidelberger, C.: Tissue Distribution of 5-Fluorouracil-2-C^{14} and 5-Fluoro-2'-Deoxyuridine in Cancer Patients. Cancer Res. 23: 67, 1963.

35. Chaudhuri, N.K., Mukherjee, K.L. and Heidelberger, C.: Studies on Fluorinated Pyrimidines. VII. The Degradative Pathway. Biochem. Pharmacol. 1: 328, 1958.

36. Heidelberger, C., Ghobar, A., Baker, R. and Mukherjee, K.L.: Studies on Fluorinated Pyrimidines. X. In Vivo Studies on Tumor Resistance. Cancer Res. 20: 897, 1960.

37. Heidelberger, C., Kaldor, G., Mukherjee, K.L. and Danneberg, P.: Studies on Fluorinated Pyrimidines. XI. In Vitro Studies on Tumor Resistance. Cancer Res. 20: 903, 1960.

38. Mukherjee, K.L., Boohar, J., Wentland, D., Ansfield, F.J. and Heidelberger, C.: Studies on Fluorinated Pyrimidines. XVI. Metabolism of 5-Fluorouracil-2-C^{14} and 5-Fluoro-2'-Deoxyuridine-2-C^{14} in Cancer Patients. Cancer Res. 23: 49, 1963.

39. Chaudhuri, N.K., Montag, B. and Heidelberger, C.: Studies on Fluorinated Pyrimidines. III. The Metabolism of 5-Fluorouracil-2-C^{14} and 5-Fluoroorotic-2-C^{14} Acid in Vivo. Cancer Res. 18: 318, 1958.

40. Mukherjee, K.L. and Heidelberger, C.: Studies on Fluorinated Pyrimidines. IX. The Degradation of 5-Fluorouracil-6-C^{14}. J. Biol. Chem. 235: 433, 1960.

41. Chabner, B.A., Myers, C.E., Coleman, N. and Johns, D.G.: The Clinical Pharmacology of Antineoplastic Agents. New Engl. J. Med. 292: 1107, 1975.

42. Sartorelli, A.C. and Johns, D.G.: "Antineoplastic and Immuno-suppressive Agents". Hand. Exp. Pharm. XXXVIII/2, Springer-Verlag Berlin-Heidelberg, New York, 1975, Chapter 41.

43. Myers, C.E., Diasio, R., Eliot, H. and Chabner, B.A.: Pharmaco-kinetics of the Fluoropyrimidines: Implications for their Clinical Use. Cancer Treatment Reviews 3: 175, 1976.

44. Heidelberger, C., Griesbach, L., Cruz, O., Schnitzer, R.J. and Grunberg, E.: Fluorinated Pyrimidines. VI. Effects of 5-Fluorouridine and 5-Fluoro-2'-Deoxyuridine on Transplanted Tumors. Proc. Soc. Exp. Biol. Med. 97: 470, 1958.

45. Portier, J.: Solid State Chemistry of Ionic Fluorides. Angew. Chem. Intern. Ed. Engl. 15: 475, 1976.

46. Cotton, F.A. and Wilkinson, G.: "Advanced Inorganic Chemistry", Interscience Publishers, United States, 1962, Chapter 14.

47. Gottschling, H. and Heidelberger, C.: Fluorinated Pyrimidines. XIX. Some Biological Effects of 5-Trifluoromethyluracil and 5-Trifluoromethyl-2'-Deoxyuridine on Escherichia coli and Bacteriophage T4B. J. Mol. Biol. 7: 541, 1963.

48. Lederer, C.M., Hollander, J.M., Perlman, I.: "Table of Isotopes", Sixth Edition, John Wiley and Sons, Inc., New York, 1967.

49. Technical Reports Series No. 128: "Radioisotope Production and Quality Control." International Atomic Energy Agency, Vienna, 1971, p. 589.

50. Lambrecht, R.M., Montescu, C., Fowler, J. and Wolf, A.P.:
    Novel [18]F Intermediates for the Synthesis of Radiopharma-
    ceuticals. J. Nucl. Med. 13: 785, 1972.

51. Fowler, J.S., Finn, R.D., Lambrecht, R.M. and Wolf, A.P.:
    The Synthesis of ^{18}F-5-Fluorouracil. J. Nucl. Med. 14: 63,
    1973.

52. Wolf, W., Berman, J.A. and Shani, J.: Radiopharmacokinetics
    of 5-Fluorouracil. J. Nucl. Med. 16: 582, 1975.

53. Frascino, J.A., Freed, B.R. and Woodard, H.Q.: Fluorine-18
    Metabolism in the Acutely Uremic Rat. Health Phys. 29: 279,
    1975.

54. Wallace-Durbin, P.: The Metabolism of Fluorine in the Rat
    Using ^{18}F as a Tracer. J. Dental Res. 33: 789, 1954.

55. Hoskins, D.J. and Chamberlain, M.J.: Studies in Man with [18]F.
    Clin. Sci. 42: 153, 1972.

56. Carlson, C.H., Armstron, W.D. and Singer, L.: Distribution
    and Excretion of Radiofluoride in the Human. Proc. Soc. Exp.
    Biol. Med. 104: 235, 1960.

57. Ericsson, Y. and Ullberg, S.: Autoradiographic Investigations
    of the Distribution of ^{18}F in Mice and Rats. Acta Odontol.
    Scand. 16, 363, 1958.

58. Volker, J.F., Sognnaes, R. and Bibby, B.G.: Studies on the
    Distribution of Radioactive Fluoride in the Bones and Teeth
    of Experimental Animals. Am. J. Physiol. 132: 707, 1941.

59. Blau, M., Nagler, W. and Bender, M.A.: Fluorine-18: A New
    Isotope for Bone Scanning. J. Nucl. Med. 3: 332, 1962.

60. Riggins, R.S., De Nardo, G.L., D'Ambrosia, R. and Goldman, M.:
    Assessment of Circulation in the Femoral Head by [18]F Scinti-
    graphy. J. Nucl. Med. 15: 183, 1974.

61. Bonte, F.J., Parkey, R.W., Graham, K.D. and Moore, J.G.:
    Distributions of Several Agents Useful in Imaging Myocardial
    Infarcts. J. Nucl. Med. 16: 132, 1975.

62. Anbar, M. and Guttman, S.: The Accumulation of Fluoroborate
    Ions in Thyroid Glands of Rats. Endocrinology 66: 888, 1960.

63. Entzian, W., Aronow, S., Soloway, H. and Sweet, W.H.: A Pre-
    liminary Evaluation of F[18]-Labeled Tetrafluoroborate As a
    Scanning Agent for Intracranial Tumors. J. Nucl. Med. 5: 542,
    1964.

64. Askenasy, H.M., Anbar, M., Laor, Y., Lewitus, Z., Kosary, I.Z. and Guttman, S.: The Localization of Intracranial Space Occupying Lesions by Fluoroborate Ions Labelled with Fluorine-18. Am. J. Roentgenol. 88: 350, 1962.

65. Camner, P., Philipson, K. and Svedberg, J.: Production of 7 μ Monodisperse Fluorocarbon Resin Particles Tagged with [18]F. Intern. J. Appl. Radiation Isotopes 22: 349, 1971.

66. Hoyte, R.M., Lin, S.S., Christman, D.R., Atkins, H.L., Hauser, W. and Wolf, A.P.: Organic Radiopharmaceuticals Labeled with Short-lived Nuclides: ^{18}F-Labeled Phenylalanines. J. Nucl. Med. 12: 280, 1971.

67. Goulding, R.W. and Gunasekera, S.W.: Fluorine-18 Labelled L-p-Fluorophenylalanine. Intern. J. Appl. Radiation Isotopes 26: 561, 1975.

68. Goulding, R.W. and Palmer, A.J.: The Preparation of Fluorine-18 Labelled p-Fluorophenylalanine for Clinical Use. Intern. J. Appl. Radiation Isotopes 23: 133, 1972.

69. Cottrall, M.F., Taylor, D.M. and McElwain, T.J.: Investigations of ^{18}F-p-Fluorophenylalanine for Pancreas Scanning. Brit. J. Radiol. 46: 277, 1973.

70. Hoyte, R.M., Lin, S.S., Atkins, H.L., Christman, D.R., Hauser, W., Klopper, J.F. and Wolf, A.P.: Organ Distribution Studies with ^{18}F-6-Fluorotryptophan. J. Nucl. Med. 12: 367, 1971.

71. Atkins, H.L., Christman, D.R., Fowler, J.S., Hauser, W., Hoyte, R.M., Klopper, J.F., Lin, S.S. and Wolf, A.P.: Organic Radio-pharmaceuticals Labeled with Isotopes of Short Half-life. V. ^{18}F-Labeled 5- and 6-Fluorotryptophan. J. Nucl. Med. 13: 713, 1972.

72. Firnau, G., Nahmias, C. and Garnett, S.: The Preparation of [^{18}F]5-Fluoro-DOPA with Reactor-Produced Fluorine-18. Intern. J. Appl. Radiation Isotopes 24: 182, 1973.

73. Chan, P., Firnau, G. and Garnett, E.S.: F-18 Fluoro-DOPA As A New Brain Scanning Agent. J. Nucl. Med. 16: 518, 1975.

74. Nagai, T.: Programs Aimed at the Development of a Radiopharmaceutical for Adrenal Scanning. J. Nucl. Med. 11: 217, 1970.

75. Robinson Jr., G.D.: Rapid Synthesis of High-Specific-Activity, Biologically Active ^{18}F-Fluoroaliphatic Analog Compounds. J. Nucl. Med. 14: 446, 1973.

76. Robinson Jr., G.D.: 2-Fluoroethanol: High Specific Activity, Fluorine-18 Labeling in a Flow System. J. Nucl. Med. 16: 561, 1975.

77. Kook, C.S., Reed, M.F. and Digenis, G.A.: Preparation of [18F] Haloperidol. J. Med. Chem. 18: 533, 1975.

78. March, J.: "Advanced Organic Chemistry: Reactions, Mechanisms and Structure." McGraw-Hill Book Company, 1968.

79. Nozaki, T. and Tanaka, Y.: The Preparation of 18F-Labelled Aryl Fluorides. Intern. J. Appl. Radiation Isotopes 18: 111, 1967.

80. Digenis, G.A., Kook, C.S. and Reed, M.F.: The Synthesis of F-18-Haloperidol. J. Nucl. Med. 16: 525, 1975.

81. Reactions of Elemental Fluorine Reappraised. Chem. and Eng. News, April 26, 1976, p. 23.

82. Pischel, H., Holy, A., Wagner, G. and Cech, D.: Carboxymethylated Uracil, 2'-Deoxyuridine and Their 5-Fluoro, 5-Bromo and 5-Iodo Derivatives. Collection Czech. Chem. Commun. 40: 2689, 1975.

83. Cech, D. and Meinert, H.: Uber die Reaktion von Uracil und seinen Nucleosiden mit Elementarem Fluor. J. Prakt. Chem. 315: 149, 1973.

84. Cech, D. and Holy, A.: Preparation of Some 2'-Deoxy-5-Fluoro-uridine Derivatives by a Direct Fluorination. Collection Czech. Chem. Commun. 41: 3335, 1976.

85. Barton, D.H.R., Hesse, R.H., Markmell, R.E., Pechet, M.M. and Rozen, S.: Fluorination at Saturated Carbon. 2. Direct Fluorination of Steroids. J. Am. Chem. Soc. 98: 3036, 1976.

86. Maraschin, N.J., Catsikis, B.D., Davis, L.H., Jarvinen, G. and Lagow, R.J.: Synthesis of Structurally Unusual Fluorocarbons by Direct Fluorination. J. Am. Chem. Soc. 97: 513, 1975.

87. Lebowitz, E., Richards, P. and Baranosky, J.: 18F Recoil Labeling. Intern. J. Appl. Radiation Isotopes 23: 392, 1972.

88. Anbar, M. and Neta, P.: Formation of 18F-Labeled Fluoro-Organic Compounds by the 19F(n,2n) Reaction. J. Chem. Phys. 37: 2757, 1962.

89. Anbar, M. and Neta, P.: The Production and Use of 18F-Labeled Organic Compounds. Intern. J. Appl. Radiation Isotopes 14: 119, 1963.

90. Hoover, J.E.: "Remington's Pharmaceutical Sciences". Mack
     Publishing Company, Easton, Pennsylvania, 1970.

91. Miller, G.L.: Protein Determination for Large Numbers of
     Samples. Anal. Chem. 31: 964, 1959.

92. Horwitz, J.P. and Tomson, A.J.: Some 6-Substituted Uracils.
     J. Org. Chem. 26: 3392, 1961.

93. Krchňák, V. and Arnold, Z.: Diazotization of the Amino Group
     on the Pyrimidine Nucleus. Collection Czech. Chem. Commun.
     40: 1390, 1975.

94. Barton, D.H.R., Hesse, R.H., Toh, H.T. and Pechet, M.M.: A
     Convenient Synthesis of 5-Fluorouracil. J. Org. Chem. 37: 329,
     1972.

95. Robins, M.J. and Naik, S.R.: Nucleic Acid Related Compounds.
     III. A Facile Synthesis of 5-Fluorouracil Bases and Nucleosides
     by Direct Fluorination. J. Am. Chem. Soc. 93: 5277, 1971.

96. Robins, M.J. and Naik, S.R.: A Direct Synthesis of 5-Fluoro-
     cytosine and its Nucleosides Using Trifluoromethyl Hypofluorite.
     J. Chem. Soc. Chem. Commun. 18, 1972.

97. Robins, M.J., MacCoss, M., Naik, A.R. and Ramani, G.: Nucleic
     Acid Related Compounds. 21. Direct Fluorination of Uracil and
     Cytosine Bases and Nucleosides Using Trifluoromethyl Hypofluorite.
     Mechanism, Stereochemistry and Synthetic Applications. J. Am.
     Chem. Soc. 98, 7381, 1976.

98. Earl, R.A. and Townsend, L.B.: The Synthesis of 1-(Tetrahydro-
     2-furanyl)-5-Fluorouracil (Ftorafur) via Direct Fluorination
     (1). J. Heterocyclic Chem. 9: 1141, 1972.

99. Enge, H.A.: "Introduction to Nuclear Physics", Addison-Wesley
     (Canada) Limited, Don Mills, Ontario, 1966, Chapter 12.

100. Chase, G.D. and Rabinowitz, J.L.: Principles of Radioisotope
     Methodology. Burgess Publishing Company, Third Edition, 1971.

101. French, R.J. and McCready, V.R.: The Use of ^{18}F for Bone
     Scanning. Brit. J. Radiol. 40: 655, 1967.

102. Creutzig, H.: Vergleichende Untersuchungen mit Osteotropen
     Radiopharmaka II. Plasmaclearance von ^{18}F und ^{99m}Tc-EHDP.
     Fortschr. Rontgenstr. 123: 313, 1975.

103. Shane, L.L. and Winchell, H.S.: Fluorine-18 Labeling of
     Steroids: Method and Results. J. Nucl. Med. 8: 336, 1967.

104. Nozaki, T., Tanaka, Y., Shimamura, A. and Karasawa, T.: The Preparation of Anhydrous $H^{18}F$. Intern. J. Appl. Radiation Isotopes 19: 27, 1968.

105. Lebowitz, E., Richard, P. and Baranosky, J.: ^{18}F Recoil Labeling. J. Nucl. Med. 12: 377, 1971.

106. Danneberg, P.B., Montag, B.J. and Heidelberger, C.: Studies on Fluorinated Pyrimidines. IV. Effects on Nucleic Acid Metabolism in Vivo. Cancer Res. 18: 330, 1958.

107. Bosch, L., Harbers, E. and Heidelberger, C.: Studies on Fluorinated Pyrimidines. V. Effects on Nucleic Acid Metabolism in Vitro. Cancer Res. 18: 335, 1958.

108. McQuarrie, S.A.: "The Production of Positron Emitting Nuclides by a Van de Graaff for Use in Nuclear Medicine", University of Alberta, 1975.

VII. APPENDICES

APPENDIX 1

Tissue to Blood Ratios After Injection of 5-Fluoro-2'-Deoxyuridine-6-^{3}H in Swiss Albino Controls[a,b]

Time (minutes) after administration

	15	30	60	120	180	240
Spleen	2.7 ± 1.6	3.7 ± 1.7	10.9 ± 4.8	35.8 ± 24.3	108.2 ± 98.7	99.1 ± 80.8
Liver	4.4 ± 3.5	8.7 ± 1.9	8.0 ± 4.1	8.8 ± 1.7	9.8 ± 4.6	5.3 ± 1.6
GIT *	2.3 ± 1.3	6.0 ± 2.0	11.0 ± 6.8	53.6 ± 37.5	102.5 ± 85.6	134.0 ± 67.3
Muscle	0.4 ± 0.07	0.4 ± 0.1	0.6 ± 0.3	1.3 ± 0.6	3.11 ± 2.9	1.6 ± 0.2
Kidney	7.3 ± 2.3	10.6 ± 0.8	15.3 ± 6.6	14.3 ± 4.2	15.7 ± 7.7	14.5 ± 4.9
BM *	1.6 ± 0.3	3.5 ± 1.3	7.2 ± 3.0	32.3 ± 29.2	64.7 ± 56.0	60.8 ± 46.4
Lung	0.7 ± 0.1	1.0 ± 0.1	1.6 ± 0.7	2.7 ± 1.3	4.1 ± 3.0	5.0 ± 2.9
Heart	0.6 ± 0.1	0.6 ± 0.2	0.8 ± 0.2	1.1 ± 0.3	1.6 ± 0.7	1.4 ± 0.4
Blood	1.0 ± 0.0	1.0 ± 0.0	1.0 ± 0.0	1.0 ± 0.0	1.0 ± 0.0	1.0 ± 0.0
Testes	0.7 ± 0.2	1.2 ± 0.3	2.1 ± 1.4	6.0 ± 3.3		
Stomach	1.1 ± 0.3	1.9 ± 0.5	4.6 ± 1.7	10.5 ± 5.6		31.0 ± 15.3
Tail	5.2 ± 3.4	2.3 ± 1.4	12.4 ± 12.7	10.1 ± 5.5	23.0 ± 12.6	12.2 ± 3.9

a. Ratios calculated on dry tissue weight basis.

b. Each value is the mean ± standard deviation of 6 animals.

* GIT - gastrointestinal tract; BM - bone marrow.

APPENDIX 2

Tissue to Muscle Ratios After Injection of 5-Fluoro-2'-Deoxyuridine-6-^{3}H in Swiss Albino Controls[a,b]

Time (minutes) after administration

	15	30	60	120	180	240
Spleen	7.4 ± 4.2	9.8 ± 6.1	20.3 ± 9.3	26.9 ± 11.3	40.2 ± 39.4	60.7 ± 45.6
Liver	12.3 ± 11.0	22.2 ± 8.6	13.4 ± 3.4	8.2 ± 3.6	4.6 ± 2.1	3.4 ± 0.9
GIT*	6.7 ± 4.8	15.1 ± 7.6	13.6 ± 6.4	38.8 ± 16.3	42.6 ± 32.4	84.4 ± 38.3
Muscle	1.0 ± 0.01	1.0 ± 0.1	1.0 ± 0.0	1.0 ± 0.0	1.0 ± 0.0	1.0 ± 0.0
Kidney	19.9 ± 5.9	26.4 ± 7.1	26.6 ± 7.2	12.5 ± 4.0	7.0 ± 3.1	9.2 ± 2.3
BM*	4.3 ± 0.6	10.9 ± 8.6	13.1 ± 5.6	23.5 ± 17.8	15.8 ± 5.8	37.7 ± 27.3
Lung	1.8 ± 0.3	2.6 ± 0.7	2.7 ± 0.3	2.1 ± 0.3	1.7 ± 1.0	3.1 ± 1.7
Heart	1.6 ± 0.2	1.6 ± 0.6	1.6 ± 0.4	1.0 ± 0.3	0.7 ± 0.3	0.9 ± 0.3
Blood	2.8 ± 0.5	2.5 ± 0.5	2.0 ± 0.8	1.0 ± 0.5	0.5 ± 0.3	0.6 ± 0.1
Testes	1.8 ± 0.8	2.8 ± 0.9	3.8 ± 2.3	5.0 ± 2.3		
Stomach	3.1 ± 1.2	5.0 ± 2.1	8.1 ± 1.8	8.6 ± 2.7		19.4 ± 7.0

a. Ratios calculated on a dry tissue weight basis.

b. Each value is the mean ± standard deviation of 6 animals.

* GIT - gastrointestinal tract; BM - bone marrow.

APPENDIX 3

Tissue to Muscle Ratios After Injection of 5-Fluorouracil-6-^{3}H in Swiss Albino Controls[a,b]

Time (minutes) after administration

	15	30	60	120	180	240
Spleen	1.8 ± 0.4	1.9 ± 0.5	2.0 ± 0.7	1.9 ± 0.3	2.3 ± 0.5	3.1 ± 0.8
Liver	21.9 ± 7.9	25.7 ± 5.4	15.9 ± 5.4	10.3 ± 4.8	5.4 ± 1.7	3.9 ± 0.9
GIT *	1.9 ± 0.4	2.6 ± 0.7	2.5 ± 1.0	1.6 ± 0.3	2.0 ± 0.4	2.4 ± 1.0
Muscle	1.0 ± 0.0	1.0 ± 0.0	1.0 ± 0.0	1.0 ± 0.0	1.0 ± 0.0	1.0 ± 0.0
Kidney	24.3 ± 6.0	31.3 ± 8.4	24.5 ± 13.0	12.3 ± 3.2	7.4 ± 1.6	6.2 ± 2.2
BM *	2.6 ± 0.5	3.2 ± 0.9	2.9 ± 1.1	2.4 ± 0.3	2.8 ± 1.0	3.8 ± 0.4
Lung	2.2 ± 0.6	2.6 ± 0.8	2.1 ± 0.7	1.6 ± 0.4	1.7 ± 0.2	2.0 ± 0.5
Heart	1.6 ± 0.3	1.7 ± 0.5	1.2 ± 0.4	0.8 ± 0.2	0.9 ± 0.1	1.0 ± 0.2
Blood	2.8 ± 0.6	2.6 ± 0.8	2.2 ± 1.9	0.7 ± 0.2	2.0 ± 2.6	0.4 ± 0.1
Testes	1.5 ± 0.6	1.9 ± 0.4	1.3 ± 0.8	1.2 ± 0.1	1.7 ± 1.1	2.1 ± 0.9
Stomach	1.6 ± 0.4	1.9 ± 0.6	1.8 ± 0.6	1.6 ± 0.3	1.7 ± 0.4	2.1 ± 0.2

a. Ratio calculated on a dry tissue weight basis.

b. Each value is the mean ± standard deviation of 6 animals.

* GIT - gastrointestinal tract; BM - bone marrow.

APPENDIX 4

Tissue to Blood Ratios After Injection of 5-Fluorouracil-6-^{3}H in Swiss Albino Controls[a,b]

Time (minutes) after administration

	15	30	60	120	180	240
Spleen	0.7 ± 0.3	0.8 ± 0.1	1.2 ± 0.6	2.9 ± 0.6	3.3 ± 2.3	7.3 ± 2.3
Liver	8.0 ± 2.7	10.3 ± 1.9	10.3 ± 5.0	14.7 ± 4.6	8.9 ± 6.8	9.1 ± 2.3
GIT*	0.7 ± 0.0	1.0 ± 0.1	1.7 ± 1.2	2.4 ± 0.6	2.8 ± 2.0	5.5 ± 2.8
Muscle	0.4 ± 0.1	0.4 ± 0.2	0.8 ± 0.7	1.7 ± 0.5	1.5 ± 1.0	2.4 ± 0.8
Kidney	8.6 ± 1.0	12.3 ± 1.7	14.9 ± 8.8	18.3 ± 3.4	11.4 ± 8.3	14.1 ± 3.1
BM*	1.0 ± 0.1	1.4 ± 0.2	1.9 ± 1.0	3.8 ± 0.9	3.6 ± 2.3	8.8 ± 3.7
Lung	0.8 ± 0.1	1.0 ± 0.2	1.3 ± 0.6	2.5 ± 0.5	2.5 ± 1.7	4.7 ± 1.8
Heart	0.6 ± 0.1	0.7 ± 0.0	0.7 ± 0.3	1.3 ± 0.2	1.3 ± 0.9	2.4 ± 0.6
Blood	1.0 ± 0.0	1.0 ± 0.0	1.0 ± 0.0	1.0 ± 0.0	1.0 ± 0.0	1.0 ± 0.0
Testes	0.6 ± 0.4	0.9 ± 0.6	0.9 ± 0.8	2.0 ± 1.0	1.8 ± 1.0	5.6 ± 4.3
Stomach	0.6 ± 0.0	0.7 ± 0.1	1.1 ± 0.5	2.4 ± 0.7	2.6 ± 1.8	4.9 ± 1.4

a. Ratios calculated on a dry tissue weight basis.

b. Each value is the mean ± standard deviation of 6 animals.

* GIT - gastrointestinal tract; BM - bone marrow.

APPENDIX 5

Tissue to Blood Ratios After Injection of 5-Fluoro-2'-Deoxyuridine-6-^{3}H in BDF, Controls[a,b]

Time (minutes) after administration

	15	30	60	120	180	240
Spleen	2.3 ± 1.4	1.8 ± 1.0	5.2 ± 2.5	20.6 ± 12.1	20.8 ± 5.7	40.3 ± 16.0
Liver	11.6 ± 6.4	6.7 ± 2.7	9.9 ± 1.6	12.4 ± 5.8	8.2 ± 1.6	9.4 ± 2.3
GIT*	4.8 ± 3.2	4.2 ± 0.3	15.8 ± 1.1	51.3 ± 20.7	78.6 ± 43.9	161.5 ± 64.7
Muscle	0.7 ± 0.4	0.5 ± 0.3	0.6 ± 0.1	1.6 ± 1.2	6.8 ± 8.8	3.2 ± 2.1
Kidney	12.2 ± 6.3	9.0 ± 1.7	19.1 ± 6.0	22.1 ± 10.3	14.3 ± 3.6	17.8 ± 4.2
BM*	3.08 ± 0.61	4.80 ± 1.70	9.87 ± 3.42	33.27 ± 19.54	45.92 ± 11.01	64.38 ± 22.22
Lung	1.0 ± 0.6	0.4 ± 0.3	1.6 ± 0.3	2.7 ± 1.6	4.2 ± 2.6	4.8 ± 1.0
Heart	0.7 ± 0.3	0.4 ± 0.1	0.8 ± 0.2	2.0 ± 1.6	1.2 ± 0.2	1.9 ± 0.6
Blood	1.0 ± 0.0	1.0 ± 0.0	1.0 ± 0.0	1.0 ± 0.0	1.0 ± 0.0	1.0 ± 0.0
Testes	0.9 ± 0.1	0.9 ± 0.2	5.9 ± 7.2	4.2 ± 0.7	9.5 ± 10.7	15.8 ± 8.2
Stomach	0.9 ± 0.1	1.0 ± 0.1	3.0 ± 0.5	7.6 ± 3.6	21.2 ± 13.1	24.2 ± 12.9

a. Ratios calculated on a dry tissue weight basis.

b. Each value is the mean ± standard deviation of 6 animals.

* GIT - gastrointestinal tract; BM - bone marrow.

APPENDIX 6

Tissue to Muscle Ratio After Injection of 5-Fluoro-2'-Deoxyuridine-6-^{3}H in BDF$_1$ Controls[a,b]

Time (minutes) after administration

	15	30	60	120	180	240
Spleen	3.4 ± 0.6	4.2 ± 2.5	8.6 ± 3.2	13.3 ± 4.2	10.0 ± 8.1	15.9 ± 8.4
Liver	17.9 ± 3.5	15.5 ± 7.1	17.1 ± 2.9	8.8 ± 3.2	3.8 ± 2.9	3.8 ± 1.8
GIT*	7.2 ± 1.7	10.5 ± 4.2	27.5 ± 4.0	36.2 ± 11.8	34.8 ± 30.3	59.7 ± 24.2
Muscle	1.0 ± 0.0	1.0 ± 0.0	1.0 ± 0.0	1.0 ± 0.0	1.0 ± 0.0	1.0 ± 0.0
Kidney	18.8 ± 1.5	22.0 ± 8.8	33.8 ± 12.2	15.4 ± 4.8	8.1 ± 5.1	7.1 ± 3.2
BM*	6.34 ± 1.58	14.45 ± 3.56	30.87 ± 11.15	25.13 ± 19.71	33.12 ± 6.06	48.72 ± 16.08
Lung	1.6 ± 0.2	0.9 ± 0.6	2.8 ± 0.5	1.7 ± 0.8	2.2 ± 2.3	1.8 ± 0.6
Heart	1.2 ± 0.2	0.9 ± 0.4	1.4 ± 0.0	1.4 ± 1.0	0.7 ± 0.4	0.7 ± 0.3
Blood	1.8 ± 0.7	2.5 ± 1.3	1.8 ± 0.4	0.9 ± 0.5	0.5 ± 0.4	0.4 ± 0.2
Testes	1.9 ± 0.2	2.1 ± 0.6	9.2 ± 10.1	3.4 ± 1.6	2.5 ± 1.4	5.6 ± 3.0
Stomach	2.0 ± 0.6	2.5 ± 1.5	5.4 ± 2.0	5.3 ± 2.1	7.4 ± 6.0	8.9 ± 5.2

a. Ratios calculated on a dry tissue weight basis.

b. Each value is the mean ± standard deviation of 6 animals.

* GIT - gastrointestinal animals; BM - bone marrow.

APPENDIX 7

Tissue to Blood Ratios After Injection of 5-Fluorouracil-6-[3H] in BDF, Controls[a,b]

Time (minutes) after administration

	15	30	60	120	180	240
Spleen	0.6 ± 0.1	0.7 ± 0.1	1.5 ± 0.2	2.4 ± 0.4	2.7 ± 1.0	4.0 ± 0.9
Liver	11.5 ± 1.3	12.7 ± 1.4	14.7 ± 1.2	13.7 ± 3.3	7.6 ± 2.8	8.0 ± 2.0
GIT*	0.9 ± 0.1	1.2 ± 0.2	1.4 ± 0.2	2.1 ± 0.6	4.5 ± 2.8	3.0 ± 0.7
Muscle	0.4 ± 0.0	0.6 ± 0.2	1.0 ± 0.4	1.7 ± 0.5	2.5 ± 1.1	4.2 ± 2.5
Kidney	17.5 ± 3.8	18.2 ± 2.2	22.9 ± 4.7	18.0 ± 1.8	10.7 ± 5.0	10.9 ± 1.9
BM*	1.3 ± 0.1	1.6 ± 0.3	3.2 ± 1.7	3.4 ± 0.4	4.5 ± 2.3	5.8 ± 2.9
Lung	1.1 ± 0.2	1.2 ± 0.1	1.8 ± 0.4	2.6 ± 0.4	2.7 ± 1.0	3.2 ± 0.6
Heart	0.7 ± 0.1	0.7 ± 0.1	0.8 ± 0.1	1.2 ± 0.1	1.3 ± 0.3	1.7 ± 0.6
Blood	1.0 ± 0.0	1.0 ± 0.0	1.0 ± 0.0	1.0 ± 0.0	1.0 ± 0.0	1.0 ± 0.0
Testes	0.4 ± 0.1	0.5 ± 0.1	2.2 ± 2.4	1.4 ± 0.3	2.8 ± 1.3	9.5 ± 11.7
Stomach	0.7 ± 0.1	0.8 ± 0.2	1.4 ± 0.3	2.2 ± 0.3	3.0 ± 1.6	3.2 ± 0.7

a. Ratios calculated on a dry weight basis.

b. Each value is the mean ± standard deviation of 6 animals.

* GIT – gastrointestinal tract; BM – bone marrow.

APPENDIX 8

Tissue to Muscle Ratios After Injection of 5-Fluorouracil-6-^{3}H in BDF, Controls[a,b]

Time (minutes) after administration

	15	30	60	120	180	240
Spleen	1.5 ± 0.2	1.4 ± 0.4	1.5 ± 0.2	1.5 ± 0.3	1.1 ± 0.3	1.3 ± 0.5
Liver	28.1 ± 1.8	23.3 ± 6.9	16.4 ± 6.0	9.3 ± 6.4	3.2 ± 1.0	2.5 ± 1.3
GIT*	2.2 ± 0.3	2.2 ± 0.8	1.5 ± 0.4	1.3 ± 0.3	1.8 ± 0.8	1.0 ± 0.5
Muscle	1.0 ± 0.0	1.0 ± 0.0	1.0 ± 0.0	1.0 ± 0.0	1.0 ± 0.0	1.0 ± 0.0
Kidney	43.3 ± 10.9	33.0 ± 7.8	24.8 ± 7.0	11.4 ± 4.4	4.4 ± 1.8	3.3 ± 1.5
BM*	3.1 ± 0.3	2.9 ± 0.4	3.3 ± 1.8	2.1 ± 0.5	1.8 ± 0.4	1.9 ± 1.1
Lung	2.6 ± 0.4	2.3 ± 0.6	1.9 ± 0.5	0.4 ± 0.1	1.1 ± 0.2	1.0 ± 0.5
Heart	1.8 ± 0.1	1.3 ± 0.3	0.9 ± 0.4	0.8 ± 0.3	0.6 ± 0.2	0.5 ± 0.3
Blood	2.4 ± 0.2	1.8 ± 0.5	1.1 ± 0.4	0.6 ± 0.2	0.5 ± 0.4	0.3 ± 0.2
Testes	0.9 ± 0.2	0.9 ± 0.2	1.8 ± 1.2	0.9 ± 0.3	1.1 ± 0.2	4.1 ± 6.8
Stomach	1.8 ± 0.2	1.6 ± 0.3	1.4 ± 0.4	1.4 ± 0.5	1.2 ± 0.4	1.0 ± 0.6

a. Ratios calculated on a dry weight basis.

b. Each value is the mean ± standard deviation of 6 animals.

* GIT - gastrointestinal animals; BM - bone marrow.